Golden perch (*Macquaria ambigua*) otolith microchemistry: modern validations and ancient applications

Kelsie Long

A thesis submitted for the degree of Doctor of Philosophy of The Australian National University

Declaration

Hereby I declare and confirm that this thesis represents my own work, except where otherwise acknowledged.

Kelsie Long

Word Count: ~ 50 289

Acknowledgements

This PhD has been one of the hardest and most rewarding things I have ever done. It would not have been possible without the encouragement, assistance and support of a large number of people. In particular, I would like to acknowledge and thank the following:

I would firstly like to acknowledge and thank my supervisory panel. Thanks to Rainer Grün for starting me on this archaeogeochemistry journey, for driving me to Narrandera to collect modern golden perch otolith samples, for encouraging me to push on when I hit the mid-PhD slump, and for providing feedback and corrections on the final thesis draft.

A special thank you to Ian Williams for guiding me through and assisting me with the workings of the SHRIMP, from mount preparation to data reduction, no matter how many questions I had or how many times I came to you for help you were always happy to talk me through it. Especially in the last few months, your support encouragement and guidance is the reason I have been able to produce and submit a completed thesis.

Thanks also to Stephen Eggins for providing key advice and assistance at the beginning of the project and during the mid-term review. Thanks to John Kalish for providing otoliths samples, coming along to all my major talks and providing necessary input on the biological aspects of the project as well as comments and corrections on the draft Long et al., (2018) paper.

The technical and analytical aspects of this project were supported by a large number of people and I would like to take this opportunity to acknowledge and thank them for their invaluable assistance. Stewart Fallon for providing the radiocarbon dating and micro milling facilities; thanks also to Les Kinsley for providing facilities and assistance with all LA-ICPMS trace element analyses; Harri Kokkonen and John Chivers for assisting with the development of improved otolith preparation procedures; Simon Robertson for ageing the fish otoliths; Joe Cali for assistance with the powdered otolith $\delta^{18}O$ analyses on the Dual Inlet Mass Spectrometer; Hilary Stuart-Williams for analysing the tank water samples and finally Rachel Wood for guiding me through the radiocarbon processes, providing input on multiple draft papers and being wonderful and supportive throughout my PhD. The lake level modelling chapter would not have been possible without the

assistance and guidance of Eelco Rohling and Dave Heslop. All the figures and coding were created by Dave; Eelco provided direction for the modelling and feedback on the interpretation. I thank them both for all their work and assistance at a very late stage of my PhD.

Clayton Sharpe and colleagues from the Narrandera Fisheries Centre provided water samples, otolith samples, temperature records and fish length and weight histories. I thank them for this and for still providing me with more information about the tanks and fish 4 years after I originally collected them. I would also like to thank Karina Meredith and colleagues from ANSTO for providing me with water $\delta^{18}O$, temperature and composition information for the Barwon-Darling River system. My thanks also goes to Wilfred Shawcross for allowing me to work on the otoliths he collected in the 1970s and for providing helpful feedback on early paper drafts, especially regarding the site chronology/sedimentology.

Thanks to the archaeogeochemistry crew, Malte Willmes, Hannah James, Mathieu Duval and Fang. You were all so supportive, friendly and always up for a coffee and chat. Special thanks to Hannah for putting up with me as an officemate and filling our room with plants. To Inger Mewburn and Victoria Firth-Smith, thank you for the various opportunities for supported writing (Thesis boot camp, veterans' days academic writing month etc.). You provide the care that we know the university feels for PhD students but which we don't always see. I wrote most of my thesis at your boot camps and learnt the core value of my thesis doing 3MT. Keep up the good work! Thank you to Nicola Stern and colleagues of the Mungo Archaeology Project for all your advice, feedback, support and for the wonderful work you are doing in the Willandra.

I would like to acknowledge and thank the traditional owners of Lake Mungo and the Willandra Lakes; the Elders from the Traditional Tribal Groups, the Barkindji/Paakintji, Mutthi Mutthi and Ngyiampaa, for their interest in and support of this work.

Funding was provided by an Australian Research Council Discovery Grant DP150100487 *Landscape Archaeology at Lake Mungo* (Dr Nicola Stern Dr Zenobia Jacobs, Dr Simon McClusky, Prof. Ian S Williams, Prof. Colin V Murray-Wallace, Prof Rainer Grün, Dr Timothy P Denham). Additional funding support for radiocarbon dating was provided by the Australian Archaeology Association. An ANU Vice

Chancellor travel grant (2015) supported me to attend and present my work at the International Union for Quaternary Research (INQUA) congress in Nagoya, Japan. A National Science Foundation Travel Grant (2014) supported me to attend the stable isotope short course (Isocamp) at the University of Utah, USA. An Australian Quaternary Association (AQUA) travel grant (2014) supported me to attend and present my research at the AQUA biennial conference in Mildura.

A big thank you to my family who have supported me through 12 years of primary and secondary school and 4 years of undergraduate studies only to have me commit to another 5 years of post-graduate study! You cheered for me through graduation and the 3-minute thesis competition and drove me to visit Grandma mid-way through the PhD when it all got too much. I love you and hope you know that you have helped to make me the person I am today, and I am so happy and lucky because of that.

The final and biggest thank you I have is for my partner Elijah Jones for believing in me and providing me with food, love and coffee throughout my PhD. The only way I can think to repay you is to finish my thesis and stop stressing about it.

Abstract

Inland archaeological sites in the Australian arid zone contain few records of past environments. For those archives that do exist, such as sedimentary records, it can be difficult to associate the environmental conditions that they record directly with the time scales of human occupation. At the world heritage site of Lake Mungo, in north western New South Wales, lake shore dunes preserve a record of human occupation, and of alternating phases of wet and dry conditions in the adjacent lake. These two records provide a promising opportunity to generate commensurate behavioural and palaeoenvironmental information. As further surveying of the lunettes is completed and a more detailed and robust chronology using direct Optically Stimulated Luminescence (OSL) dating of the lunettes is constructed, a fuller more nuanced picture of changes in lake level, human occupation and climate will emerge. By finding new samples, new materials and new methods of analysis the chronology of human occupation and lake level changes at Lake Mungo and other Quaternary sites will become more detailed.

This study investigates the potential of golden perch otoliths, which are found throughout the shoreline dunes of Lake Mungo, for providing additional detail about lake level fluctuations and general environmental conditions. Fish otoliths are bone-like structures that form in the inner ears of bony fish. They develop by the incremental deposition of calcium carbonate onto an organic matrix, forming annual growth rings. As otolith grow they take up and preserve a record of the trace element and isotopic composition of the ambient water. Some of these chemical markers are affected by changes in water level and temperature.

This study analyses the $\delta^{18}O_{CaCO3}$ values and trace element (Sr/Ca and Ba/Ca ratios) composition across the age increments of golden perch otoliths. The $\delta^{18}O_{CaCO3}$ values of modern golden perch from tanks of known $\delta^{18}O_{H2O}$ values and temperature conditions were used to validate the assumption that golden perch otoliths form in isotopic equilibrium with the ambient water. Further analyses of modern otoliths from river populations of golden perch and from populations who died in an evaporating lake were examined to determine if known flooding and drying events were preserved in their microchemistry. The same analytical methods were applied to a collection of ancient otoliths excavated from the shorelines of Lake Mungo in the 1970s to investigate changes in water conditions (flooding and drying events)

through time. These ancient otoliths were also radiocarbon dated to establish a more detailed chronology of the site. This study also investigates how mass balance models and ancient otolith $\delta^{18}O_{CaCO3}$ values can be used to test scenarios of lake level change at Lake Mungo.

Table of contents

List of Figures

List of Tables

1. Introduction

The studies that make up this thesis used cutting edge technologies to examine the effect of ambient conditions on golden perch otolith (ear stone) microchemical and isotopic records, and to further develop their application to understanding the ancient archaeological sites at Lake Mungo.

Otoliths can be remarkably well preserved in the archaeological record due to their dense monomineralic composition (aragonite) and are found throughout the shoreline dunes of Lake Mungo, a Pleistocene evaporative lake in western New South Wales. Excavations and surface collections along the lakeshore in the 1960s and 70s identified over 2500 fish otoliths. In recent years surveying and excavation of the central Mungo lunettes as part of the LaTrobe University's Mungo Archaeology Project (MAP) have turned up clusters of otoliths within fish bone hearths (fireplaces), as well as individual otoliths eroded onto the surface of the lunette. The morphology of these otoliths allows identification of the fish species that were living in Lake Mungo tens of thousands of years ago, namely golden perch (*Macquaria ambigua*), silver perch (*Bidyanus bidyanus*), Murray cod (*Maccullochella peelii*) and Macquarie perch (*Macquaria australasica*) (Kefous, 1977).

Initial feasibility studies (Boljkovac, 2009; Long et al., 2014) indicated possible seasonal fluctuations and evidence of evaporation preserved in the $\delta^{18}O_{CaCO3}$ values of hearth- and surface-collected otoliths dated to ~20 ka, around the time of the Last Glacial Maximum (LGM). Similar fluctuations in trace element ratios (Sr/Ca and Ba/Ca) potentially related to changes in ambient salinity and water composition associated with fish entry into the lakes and evaporation. Otoliths provide the opportunity to build up a record of lake level and climate change on timescales relevant to human lives—years rather than millennia. There is a range of internal and external conditions that affect the trace element ratios preserved in otoliths, many of which are species specific. The relative influence of these needs to be assessed before they can be applied to archaeological interpretations.

1.1 Scope of the Project

This thesis has two main aims: 1) validation of the use of $\delta^{18}O_{CaCO3}$ values and trace element chemistry (Ba and Sr) in modern golden perch otoliths for reconstructing

evaporation and flooding events and 2) the application of these techniques to interpretation of the archaeological and environmental history of Lake Mungo.

Under these two main aims are several sub-aims: (i) to improve on current preparation and analytical techniques of modern and ancient golden perch otoliths the better to associate age increments with microchemical analyses, (ii) to validate/assess the relationship between temperature, ambient $\delta^{18}O_{H2O}$ values and the $\delta^{18}O_{CaCO3}$ values of golden perch otoliths using tank-raised and wild fish, (iii) to validate/assess the influence of evaporation and flooding on the microchemistry of golden perch otoliths (iv) to apply $\delta^{18}O_{CaCO3}$ and trace element analysis to otoliths related to the earliest period of human occupation of Lake Mungo, (v) to construct a model to test the lake desiccation scenario suggested by the hearth otolith records (Long et al., 2014) and to more broadly understand how changes in the Mungo lake level would have been reflected in water $\delta^{18}O_{H2O}$ values and hence the otolith $\delta^{18}O_{CaCO3}$ values.

The chemical composition of fish otoliths is widely employed for tracking modern fish migration (Dufour et al., 1998; Wells et al., 2003; Clarke et al., 2015), recording environmental histories (Radtke et al., 1996; Wurster et al., 2005; Dorval et al., 2011) and delineating stock structures (Edmonds and Fletcher, 1997; Pangle et al., 2010). Otoliths can provide a range of information relevant to stock management including; season of birth, age at death and growth rate among others (Secor et al., 1995). The unique properties of fish otoliths have also been applied at archaeological sites to study past water temperatures and salinities (Patterson et al., 1993; Knudson, 2009; Disspain et al., 2011) but the potential of these structures as archives of lake level fluctuations is still being investigated. In a feasibility study of golden perch otolith microchemistry from hearth sites at Lake Mungo (Long et al., 2014), it was demonstrated that otoliths have the potential to link human occupation events with evaporation of the Lake. The link between otolith microchemistry and lake level changes needed to be tested under modern conditions, however, before further interpretation of the flooding and drying history of Lake Mungo can be attempted.

1.2 Signposting

Chapter 2 provides a background to archaeological research at Lake Mungo and introduces otoliths: their structure, composition and applications at modern and

ancient sites. It summarises what is currently understood about the relationship between $\delta^{18}O_{CaCO3}$ values , Sr/Ca and Ba/Ca ratios in otoliths and external vs internal variables and provides an overview of their application at Lake Mungo as recorders of ancient lake conditions.

Chapter 3 presents an account of all collection, preparation and analytical procedures employed. It also presents a revised otolith preparation methodology that improves the registration of laser ablation inductively coupled plasma mass spectrometry (LA-ICPMS) and sensitive high-resolution ion microprobe (SHRIMP) microanalyses with age increments.

Chapters 4 to 6 have been written as self-contained texts suitable for publication, aside from the collection, preparation and analytical procedures, which have been removed from the individual chapters and consolidated in Chapter 3.

Chapter 4 presents a study focused on validating the relationship between the $\delta^{18}O_{CaCO3}$ values of golden perch otoliths and ambient $\delta^{18}O_{H2O}$ values, whilst also providing an opportunity for examining the seasonality of otolith increment formation.

Chapter 5 presents a study which tests the relationship between water $\delta^{18}O_{H2O}$ values, temperature and golden perch (*Macquaria ambigua*) otolith $\delta^{18}O_{CaCO3}$ values in wild river populations caught near the Menindee lakes.

Chapter 6 provides an alternative explanation for the commonly-observed ~4‰ increase in the $\delta^{18}O_{CaCO3}$ values of LGM otoliths by modelling Willandra lake levels and $\delta^{18}O_{H2O}$ values under different ambient conditions.

Chapter 7 summarises the key findings of this project and provides some suggestions for future directions for otolith microchemical research and its application to archaeological and modern research areas/sites.

Attached to the back of this thesis is the paper: "Long et al., (2018), Fish otolith microchemistry: Snapshots of lake conditions during early human occupation of Lake Mungo, Australia" which was produced as part of this thesis and published in Quaternary International, Volume 463, Part A, pg 29-43. This paper presents another validation study that uses otoliths from an evaporative lake in South Australia, Lake Hope, to verify expected trends in otolith $\delta^{18}O_{CaCO3}$ values, Sr/Ca and

Ba/Ca ratios with evaporation, salinity increase and fish stress. This paper also examines the $\delta^{18}O_{CaCO3}$ values, Sr/Ca and Ba/Ca records and radiocarbon dates of otoliths from an archaeological excavation at Lake Mungo related to an earlier period of human occupation (37–42 cal kBP).

2. Background

This thesis investigates the utility of golden perch otolith microchemistry for preserving signals of evaporation and flooding events and the application of this record to tracking lake level fluctuations at the archaeological site of Lake Mungo. This chapter firstly presents a summary of archaeological research at Lake Mungo, establishing the current understanding of the timing of broad lake level fluctuations and human occupation as recorded in the lakeshore sediments, then summarises the current understanding of the relationships between otolith microchemistry ($\delta^{18}O_{CaCO3}$ values, Sr/Ca and Ba/Ca ratios) and environmental conditions, and finally presents an overview of archaeological applications of these microchemical techniques, including the influence of cooking and waste disposal methods and potential diagenetic effects.

Oxygen isotopes in carbonates are commonly employed for reconstructing past temperatures. In marine systems this is straightforward as the $\delta^{18}O_{H2O}$ value of ocean water is known or can be estimated. For freshwater systems, however, the past water composition is usually unknown. At Lake Mungo an otolith temperature record remains out of reach (except possibly by the analysis of CO_2 isotopologues—see Ghosh et al., 2007), but there is the potential to create a record of lake level change that can be directly related to the timescales of human lives. This thesis investigates the possibilities and limitations of using $\delta^{18}O_{CaCO3}$ values and trace elements in otoliths to track short term lake level changes.

2.1 The Willandra Lakes: Lake Mungo

The story of the Willandra lakes begins at about 26 Ma when sea water flooded into the Murray Basin from the south. At about 6.5 Ma the water began a slow and halting retreat, the coastline nearing its modern position at about 3 Ma. Damming of the Murray River by the uplift of the Pinnaroo Block at about 2.5 Ma led to the formation of the vast freshwater Lake Bungunnia, which at its maximum extent covered more than 50,000km^2 (Stephenson, 1986; Zhisheng et al., 1986; McLaren et al., 2011). The climate at this time was wetter, with rainfall levels much higher than the present. The Lake Bungunnia barrier was breached at about 0.8 Ma and the lake drained (Page et al., 2009). The Willandra Lakes formed in the low-lying basins left behind by Lake Bungunnia. They were filled by water from the mountains to the east and were profoundly affected by global glacial and interglacial cycles of climate change,

a record of which is preserved in lake side dunes (Bowler, 1976, 1998; Bowler et al., 2012; Fitzsimmons et al., 2014).

Lake Mungo is one of 13 large basins and numerous smaller now-dry basins in south-western NSW that make up the Willandra Lakes World Heritage Area (Fig. 2.1). In the 1970s human remains discovered in the shoreline lunettes of Lake Mungo pushed dates for human occupation of Australia to beyond 20,000 years BP (Bowler et al., 1970), radically changing the contemporary understanding of Australian pre-history. The development of new dating technologies and further discoveries of human remains at Lake Mungo pushed back the timing of human occupation to beyond 40,000 years BP (Bell, 1991; Bowler and Price, 1998; Bowler et al., 2003).

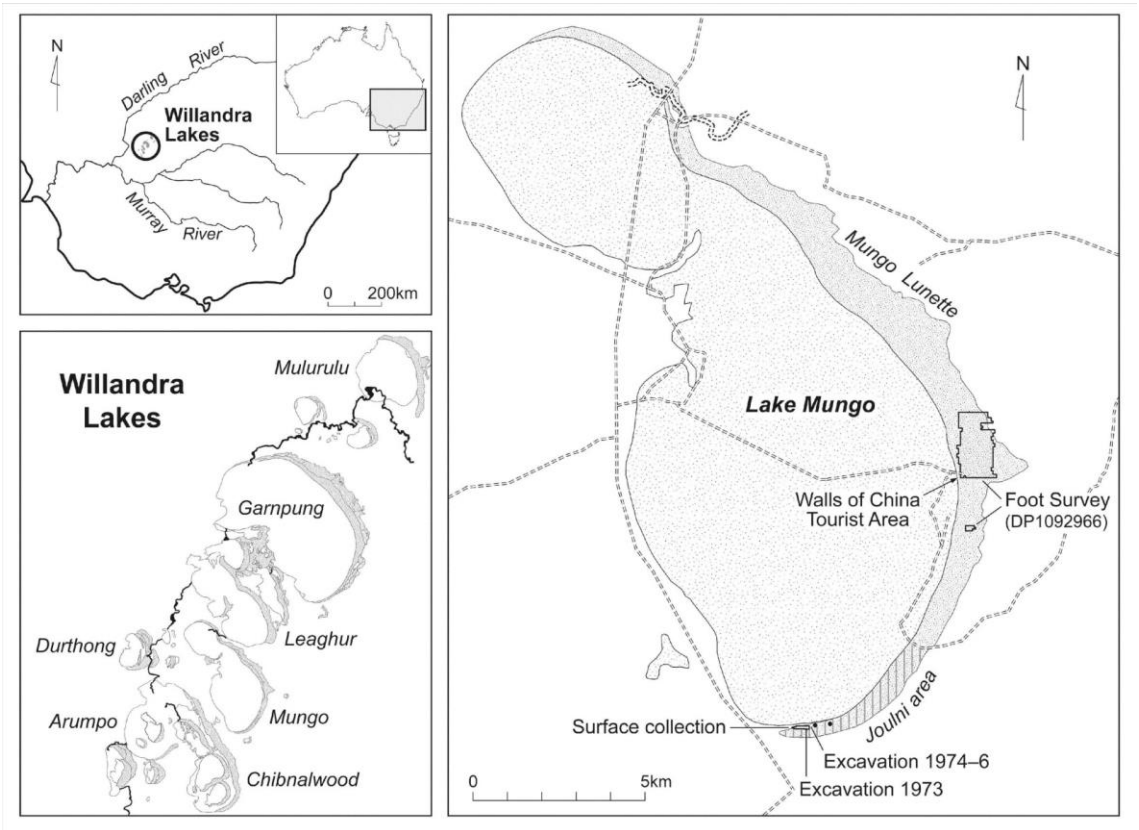

Figure 2.1: Maps showing the location of the Willandra Lakes in south eastern Australia and the location of current and past archaeological excavation and surveying. Image kindly provided by Rudy Frank (Mungo Archaeology Project) adapted from satellite images of the area.

The Willandra Lakes existed intermittently in cycles of wet and dry conditions throughout the Quaternary until approximately 14.5 ka when they dried out completely (Bowler 1998; Bowler et al. 2012; Fitzsimmons et al. 2014, Fitzsimmons et al. 2015). These cycles are evident in the lunettes as alternating layers of quartz

sand dunes (QSD) indicating full lake conditions, pelletal clay dunes (PCD) indicating drying trends, and soil formation indicating intervals of stable lake conditions (Bowler, 1998). When the lake waters were high, waves eroded quartz beaches and sand blew onto the eastern shorelines (Bowler, 1971, 1976). Seasonal exposure of saline mudflats on the lake floor permitted the efflorescence of salts, breaking up clays into pellets which were blown by high velocity winds onto the shorelines (Bowler, 1971, 1976).

The Lake Mungo lunettes are more eroded than others in the system and so have the greatest exposure of archaeology. The shorelines of other lakes may contain just as much archaeology but due to less erosion this remains concealed beneath the surface. Lake Mungo filled via an overflow outlet with Lake Leaghur, so once water entered Lake Mungo the only way it could leave was by evaporation. This made the Lake particularly sensitive to hydrologic changes and its lunettes contain a record lake level fluctuations stretching back at least 300 ka (Bowler et al., 2012; Stern et al., 2013; Fitzsimmons et al., 2014). Bowler et al. (1970) identified at least three periods of alternating stability and instability, soil-forming and dune-building cycles within the Quaternary: Golgol, Mungo and Zanci (Bowler et al., 1970). Original radiocarbon dating for these layers established a chronology of 40,000 to 15,000 BP with Golgol older than the limits of radiocarbon dating. Following further surveying of the lunettes the Mungo unit was divided into the Upper Mungo and Lower Mungo units and an additional unit named Arumpo was distinguished between Upper Mungo and Zanci to accommodate the large and complex package of aeolian materials between sediments of the Mungo and those of the Zanci laminar sands depositional stages (Bowler, 1998). Bowler's stratigraphy was based on only a few key sections of the lunette. Present work at the site is focused on extending mapping of the lunette geomorphology to the central and northern sections of the dunes.

Fitzsimmons et al. (2014) studied the stratigraphy of the central portion of the Lake Mungo lunettes north east of where human remains (Mungo Man and Mungo Lady) were uncovered and the original surveys took place. Their study established a separate classification of discreet stratigraphic units from A to I (oldest to youngest), which is comparable to the stratigraphic units established by Bowler (1998) and Bowler et al. (2003) from the southern toe of the lunette. A summary of these units in relation to those of Bowler is as follows, illustrated in Figure 2.2).

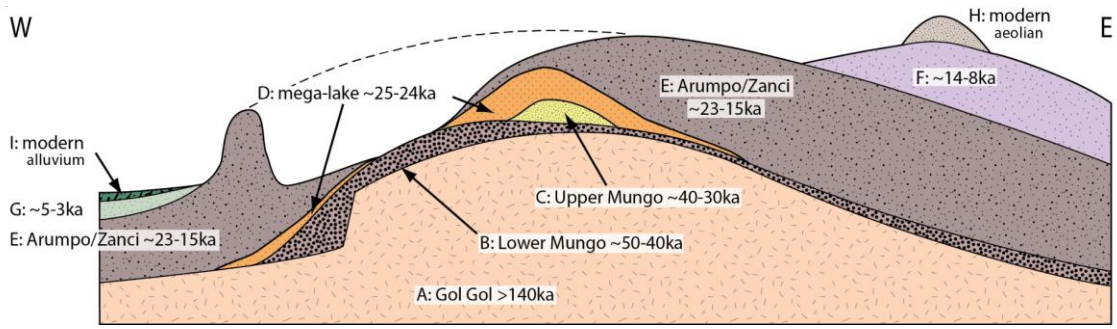

Figure 2.2: A schematic cross-section summarising the stratigraphic sequence in the central Mungo lunette with reference to units from the southern lunettes described by Bowler (1998) adapted from Fitzsimmons, K. E., Stern, N., Spry, C. (submitted) Holocene and Anthropocene aeolian reactivation of the Willandra Lakes lunettes, semi-arid south-eastern Australia. The Holocene.

At the core of the lunettes is the Golgol (Unit A), a pale pink carbonate horizon that formed during a prolonged period of lake inactivity. It contains no archaeological traces and predates the last interglacial, at > 141 ka based on OSL dating (Fitzsimmons et al., 2014). This is followed by the Lower Mungo layer (Unit B), which is comprised of red beach sands, weak discontinuous soils and no clay, overall indicating high lake levels (Bowler, 1998; Fitzsimmons et al., 2014). In 1969 burnt human remains (Mungo I) were uncovered from this layer and in 1974 a fully articulated skeleton (Mungo III) was found only 450m away in the same southern lunette unit (Bowler et al., 2003). This layer was dated by OSL in the central Mungo lunettes to ~ 50–40 ka (Fitzsimmons et al., 2014). Overlying Unit B is the Upper Mungo layer (Unit C), which is comprised of a thin layer of pale alternating sands and clay representing oscillating water levels in the lake. This layer contains a high density of archaeological traces in the central Mungo lunettes and was dated to ~ 40–30 ka (Fitzsimmons et al., 2014). The Arumpo/Zanci (Unit E) makes up the greatest volume of sediment in the lunette, representing oscillating lake conditions over Marine Isotope Stage (MIS) 2 and the Last Glacial Maximum (LGM, ~ 24–14 ka). A previously unidentified steeply dipping red sandy unit containing beach pebbles and no clay was recorded by Fitzsimmons et al. (2014). This was thought to be a discrete high lake level period that is discussed further in a more recent paper (Fitzsimmons et al., 2015) as a mega lake phase. This current chronology of lakeshore sediment and water conditions is being updated as new geological surveys are undertaken and further dates obtained.

The greatest density of archaeological remains in the Lake Mungo lunettes comes from times when the lake levels were fluctuating (Stern, 2015). One explanation for this is that while the lakes were full, fish and shellfish would have been hard to locate. The other possibility being that fish and shellfish were not abundant during these conditions. In contrast, during oscillating lake conditions, flood pulses would have recharged the system, bringing in large amounts of food and enhancing the biological productivity of the lake (Stern, 2015). Radiocarbon dating of large numbers of otoliths and shellfish from various surface exposures and excavations at Lake Mungo has resulted in dates that cluster around the time of last glacial maximum (LGM) (Bowler et al., 2012). The stratigraphy is currently being updated and reassessed based on further surveying of the lower and central lunettes.

Current work by the Mungo Archaeology Project (MAP) involves generating tightly integrated archaeological and geological data in order to reduce the possibility of chronological mismatches between the two. Dr Nicola Stern as part of MAP has developed a methodology for landscape archaeology in the Willandra that considers the empirical characteristic of the archaeological and depositional records and which is designed to generate commensurate behavioural and palaeoenvironmental information. This methodology is documented in further detail in Stern et al, (2013) and Stern (2015), but in brief involves:

1. the systematic location and documentation of archaeological sites or feature that are being exposed on the surface of the lunette, this documentation includes information about the contents and context of the feature, including the type of sediments in which it lies, an image of the feature and its 3D coordinates as recorded using the GDA (Geocentric Datum Australia - Australian mapping grid);

2. cross sections designed to provide detailed micromorphological data and geochronological data for documenting depositional history; identification of mappable units

3. mapping of geological boundaries exposed on the surface of the lunette (on georectifiied air photos, so that site locations and stratigraphic boundaries and sample locations are all on the GDA and can be related to each other)

4. analysis of the number and type of feature preserved in sediments representing different hydrological conditions

5. analysis of the density and types of archaeological features preserved in different stratigraphic units and corresponding palaeoenvironmental conditions

Only by carefully and methodically surveying, marking and examining the archaeological remains and the sediments, with which they are associated, as described above, can a comprehensive picture of the Lake's past be constructed (Stern, et al., 2013; Stern, 2015). As further surveying of the lunettes is completed and a more detailed and robust chronology using direct OSL dating of the lunettes is constructed, a fuller more nuanced picture of changes in lake level, human occupation and climate will emerge. By finding new samples, new materials and new methods of analysis the chronology of human occupation and lake level changes at Lake Mungo and other Quaternary sites will become more detailed.

This thesis examines one possible source of new information, fish otoliths. Otoliths can provide information about fish species present at archaeological sites as well as an indication of the size and age of the fish. They also preserve in their trace element and $\delta^{18}O_{CaCO3}$ values a record of individual fish movement between water of different elemental composition or environmental conditions. Fish otoliths can be dated using radiocarbon and, as demonstrated in the studies presented here, provide an opportunity to validate the evidence for changes in lake level that are preserved in the stratigraphy and assist in correlating those changes across the lunettes. They can also add more detail to the record of lake level conditions occurring on timescales comparable to human lives (10–40 years). Overall, otoliths make an important contribution to MAP's goal of generating commensurate behavioural and palaeoenvironmental information.

2.2 Initial work on Lake Mungo otolith geochemistry

A systematic foot survey of the central Mungo lunettes was initiated in 2009 to establish the types of activity traces preserved in the lunette and their sedimentary and stratigraphic context (Stern, 2015). The foot survey team identified a series of fish bone hearths containing golden perch otoliths. This presented an opportunity

to examine the usefulness of fish otolith microchemistry for documenting changes in ambient lake conditions over timescales directly comparable to human lives.

The geochemical records preserved in fish otoliths remain a largely untapped resource for understanding lake level changes, chronology and aquatic exploitation by humans. When found in a hearth, otoliths provide a direct link between human occupation and environmental conditions, as well as chronological information. The otoliths provided radiocarbon dates for the hearth sites and placed humans at the lakeshore between 19,400 and 19,700 years cal BP, around the end of the Last Glacial Maximum (Long et al., 2014). Analyses of the trace elements and $\delta^{18}O_{CaCO3}$ values across the age rings of these hearth otoliths and others from the Willandra lakes area provided, in addition, a record of environmental conditions at the time (Long et al. 2014). Increases in the $\delta^{18}O_{CaCO3}$ values in the immediate lead up to fish death were interpreted as evidence for a drying trend in the Lake. This could be interpreted as supporting the Easy Prey Hypothesis, which states that fish were trapped in Lake Mungo after drying conditions cut the lake off from the rest of the system. As the lake continued to evaporate, poor water conditions and increasing salinity caused the fish to become sluggish and easy prey for humans. However, given the low numbers of fish (~ 2 to 26) present in the hearth sites it is more likely that these resulted from human activity such as spearing or netting rather than the high numbers suggested by the Easy Prey Hypothesis. The increasing trend of $\delta^{18}O_{CaCO3}$ values in the otoliths does not directly offer information about how the fish were caught, only that the water $\delta^{18}O_{H2O}$ value was increasing which typically occurs during evaporation (but see Chapter 6 of this thesis).

Nevertheless, this initial otolith study provided an example of how geochemical techniques, when applied to archaeological material (otoliths), could provide an improved understanding of past lake conditions and link these to past human occupants. This current project aims to expand and further develop our understanding of how fish otolith geochemistry can be used to determine past environmental conditions in association with human occupation.

2.3 Otoliths

Otoliths are paired calcium carbonate structures that grow within the endolymph sack in the inner ears of bony fish (Fig. 2.3). They develop by the incremental deposition of calcium carbonate onto an organic matrix, forming annual growth

rings. These rings are thought to be seasonal, with slow growth in winter producing thin, dark bands and fast growth in summer producing thicker lighter bands (Pannella, 1971). There are three main types of otolith; sagitta, lapillus and asteraci. In most fish species the sagitta is the largest otolith and is thus the most commonly studied. All otoliths referred to in this thesis are sagittae from golden perch (*Macquaria ambigua*) or a closely related subspecies, Lake Eyre golden perch (*Macquaria ambigua sp.*).

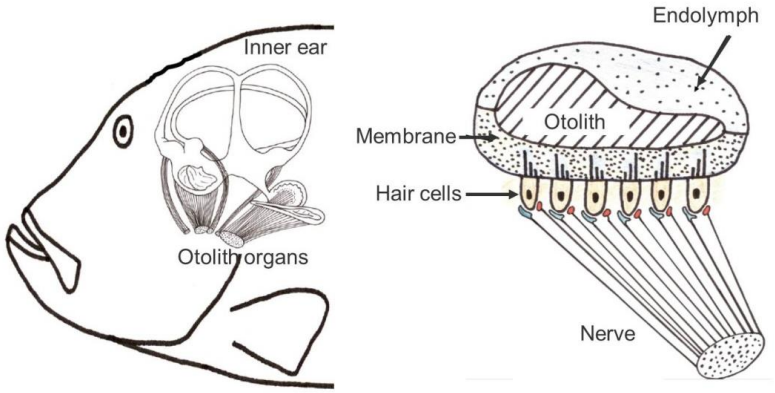

Figure 2.3: Diagram showing the position of the otolith in the inner ear of teleost fish.

There are several key features of otoliths that make them useful for studying past environmental conditions. Otolith growth is continuous and occurs even when somatic growth has ceased (Blacker, 1974; Boehlert, 1985; Anderson et al., 1992b). Also, unlike bones, otoliths are not subject to resorption, except under extreme stress (Mugiya and Uchimura, 1989). Otoliths survive for a long time in archaeological records and are commonly found associated with archaeological remains or within hearths and middens. They have even been found preserved in sediments from the Jurassic (Patterson, 1999) and Cretaceous period (Carpenter et al., 2003). Most importantly, during otolith formation elements and isotopes are taken up from the surrounding water. Some of these elements and isotopes reflect the ambient conditions experienced over the course of the fish's life, including temperature, salinity and water $\delta^{18}O_{H2O}$ values (Campana, 1999).

2.3.1 Golden perch (Macquaria ambigua)

The golden perch is a long-lived species that is found predominately in lowland, warmer, turbid, slow flowing rivers (Lintermans, 2007). The oldest recorded modern golden perch was 26 years old (Mallen-Cooper and Stuart, 2003), but the

average modern life expectancy is 10–12 years. Otoliths from archaeological sites show that this fish species had a much longer lifespan in the past, with the oldest reaching 43 years (Prichard, 2005). The age of maturation is 2 years for males and 4 years for females.

Golden perch can migrate more than 1000 km prior to spawning, which in most cases coincides with a rise in water levels (Reynolds, 1983; Ye et al., 2008; King et al., 2009; Faulks et al., 2010; Koster et al., 2017). Until recently, golden perch were thought to spawn exclusively in response to flood pulses. However, there is increasing evidence that the unpredictable conditions of Australian freshwater environments require a more opportunistic spawning strategy, and golden perch have been observed to spawn during low/no flow events (Humphries et al., 1999; Mallen-Cooper et al., 2003; Ebner et al., 2009; King et al., 2009). A two-year radio tagging study to investigate the movements of 51 golden perch in the Murray River, Victoria, showed that during winter golden perch did not undertake movements > 5 km and displayed strong home range fidelity (O'Connor et al., 2005). Outside the breeding season, adults can occupy areas of 100 m^2 for weeks or months before relocating (Lintermans, 2007).

Golden perch can grow up to 740 mm in length and 23 kg in weight, but commonly weigh less than 5 kg. They are opportunistic carnivores. Juvenile fish feed on aquatic insect larvae and microcrustaceans, whilst adults eat mainly shrimp, yabbies, small fish and benthic aquatic insect larvae (Lintermans, 2007). Golden perch can tolerate a wide range of salinities (0–33 ppt) and temperatures (4–37°C), and both juveniles and sub-adults can survive in seawater (Langdon, 1987).

2.3.2 Otolith growth and seasonal increment formation

Otolith growth is linked to endogenous and exogenous factors and is regulated by fish physiology (Morales-Nin, 2000). Variation in the amount of $CaCO_3$ relative to protein content results in the different incremental layers, which form within the otolith and are used for fish aging (Morales-nin, 1987). Biomineralisation of otoliths is primarily controlled by organic compounds in the endolymph (Allemand et al., 2007; Fablet et al., 2011). When fish of the same age are compared it is the faster growers (the larger fish) that have heavier otoliths (Francis and Campana, 2004), suggesting that the rate of fish somatic growth affects the amount of otolith material deposited. As noted above, however, otoliths continue to grow even after somatic

growth has ceased (Blacker, 1974; Boehlert, 1985; Anderson et al., 1992b). In practice, otolith size tends to relate more to fish age than fish length (Francis and Campana, 2004).

Seasonal age increments generally appear as two zones; a wide translucent zone that appears bright under transmitted light, and a narrow opaque zone that appears dark. Under reflected light the opposite is true (Wright et al., 2002). According to Nolf (1985) "In temperate species, the formation of the opaque and translucent zones (under reflected light) has been generally shown to correspond to high growth in spring and low growth in winter, respectively (Beckman and Wilson, 1995)". However, as pointed out by Fablet et al. (2011), this statement is often not valid. Opposite patterns have been reported, as well as additional non-periodical zones that may lead to erroneous age and growth estimates (e.g. de Pontual et al., 2006). This may also be a descriptive issue, with published reports not clearly identifying whether the otolith increments were viewed under reflected or transmitted light.

In some fish species daily resolved increments have also been observed. Daily structures, referred to as L-zones and D-zones, are thought to be produced by the endogenous circadian rhythm and form over a 24 h period (Pannella, 1971; Campana, 1984; Wright, 1991).

It is generally assumed that seasonal zones are related to changes in seasonal somatic growth and environmental factors such as temperature, which has been shown to influence otolith growth in several species (Brothers et al., 1983; Mosegaard et al., 1988). The relationship between the incremental zones and the seasons is different for different fish species. The formation of opaque zones in the otoliths of *Acanthurid* fishes in eastern Australia, for example, corresponds to the rise in water temperature in summer (Choat and Axe, 1996). Otolith opaque zone formation in North Sea cod (*Gadus morhua*), in contrast, is related to winter and early spring (Millner et al., 2011).

It is important to establish the relationship between the growth of otolith zones and seasonal conditions because in archaeology the last growth zones are often used to determine the season of death and the seasonality of fishing practices (Higham and Horn, 2000). Zone formation can be disrupted by certain environmental conditions, leading to the formation of additional translucent or opaque zones of non-annual

periodicity (Neat et al., 2008). The incremental growth of otoliths has also been used to recreate fish growth chronologies and to relate interannual growth variation to landscape-scale changes in temperature and supraseasonal drought (Morrongiello et al., 2011).

Oxygen isotopes can be used to test the relationship between the formation of otolith zones and seasonal temperature change. Using a high-resolution ion microprobe Matta et al. (2013) measured $\delta^{18}O_{CaCO3}$ values in 10 µm spots across and within opaque and translucent increments of yellowfin sole (*Limanda aspera*) otoliths. Fluctuations were found to relate to seasonal changes in temperature and water composition, with fish movement between fresher near shore waters and deeper saline ocean waters. Narrow translucent bands were related to the slowing or stopping of growth in winter (December to May) and thicker opaque bands reflected faster growth during the warmer seasons of June–November (Mary Elizabeth Matta et al., 2013). Høie et al. (2006) micromilled carbonate from the growth zones of Atlantic cod (*Gadus morhua*) otoliths and compared $\delta^{18}O_{CaCO3}$ values to relative light intensities. No consistent relationship was found. In some otoliths increased translucency coincided with higher temperatures (as predicted), but in others increased translucency coincided with low temperatures. Stress linked to gonad development or starvation was cited as a possible cause for this mismatch (Høie and Folkvord, 2006). Otolith growth and the relationship between increments and seasons is not always straight forward. Oxygen isotopes offer an opportunity to test the periodic deposition of different zones in relation to seasons for each species studied.

2.4 Golden perch seasonal zone formation and aging

Golden perch otoliths form continuously and deposit annual marks even after the fish stop growing longer (Anderson et al., 1992b). When thin sections of golden perch otoliths are viewed under transmitted light a concentric pattern of light (translucent) and darker brown (opaque) bands is clearly visible (Anderson et al., 1992b). Fish age is estimated by counting the opaque growth bands. These bands become visible in modern golden perch otoliths in October and the aging of fish from thin sections has been validated up to 22 years of age (Anderson et al., 1992b; Stuart, 2006). The thin opaque bands are thought to relate to slow winter growth and the thick translucent bands to fast growth during summer (Anderson et al., 1992b).

Daily increments have also been observed and validated up to the age of 15 days, although the first increment did not form until days 1-2 (Brown and Wooden, 2007). These daily increments are not easily observable and were found to be too fine and diffuse within golden perch opaque increments under 1000x magnification to provide accurate daily age information during a spawning investigation (Ebner et al., 2009). No daily structures were observed in golden perch otoliths in the studies reported in this thesis. There have been no previous studies to investigate the relationship between golden perch increment type and seasonal temperature changes recorded in otolith $\delta^{18}O_{CaCO3}$ values. Chapter 4 of this thesis will examine this relationship in golden perch otoliths from modern tanks.

Simon Robertson from Fish Ageing Services (FAS)$^{PTY\ LTD}$ aged all the otoliths in this study. In order to account for different otolith growth rates between the fish it is standard practice in otolith (and hence fish) aging to adjust ages around a designated birth date. This ensures that fish spawned in the same brood are allocated to the same age group (Anderson et al., 1992b). The opaque increments are deposited annually, as described above, but the timing of this deposition may vary by a few months between fish of the same age group. For example, in the same age group one fish might form the annual mark in October whilst another fish forms the annual mark in January. If both these fish are caught in late November one fish will be aged as one year older than the other because the final opaque zone is visible on the outer edge, but the fish are the same age.

To attempt to take this into account and match up fish that were spawned in the same cohort, each fish is assigned the same birthday of January 1st. This means that if a fish is captured in December, or generally before the assigned birth date of January 1st, and an opaque zone has just become visible on the edge of the otolith then one is subtracted from the zone count (age = zone count -1). If a fish is captured before the assigned birth date and the edge is wide then age = zone count. If a fish is captured after the assigned birth date and the edge type is a wide translucent zone, the opaque zone is expected to have formed but is not yet visible and so age = zone count +1. If the fish is captured after the assigned birth date and the edge type is a narrow translucent band then the age = zone count. This method provides an age that when subtracted from the year of capture, will place the fish into the year it was spawned.

2.5 Oxygen isotopes (O isotopes)

2.5.1 Basic principles

Oxygen has three natural stable isotopes (^{18}O, ^{17}O and ^{16}O) with different natural abundances (~ 0.205%, 0.038%, 99.757%) and atomic masses (17.9992, 16.9991, 15.9949). $\delta^{18}O_{H2O}$ values can change with the water source or fractionate due to processes such as evaporation. For palaeoenvironmental research the focus is on the $^{18}O/^{16}O$ ratio. When water is evaporating the lighter isotope (^{16}O) enters the vapour phase more readily than the heavier isotope (^{18}O), leaving behind a water body that is enriched in ^{18}O. These fractionations are affected by temperature, with the concentration of ^{18}O in precipitation decreasing as temperature falls (Epstein and Mayeda, 1953; Dansgaard, 1954; Dansgaard, 1964; Koch, 1998). By convention, $\delta^{18}O_{CaCO3}$ values are calculated relative to the composition of the Vienna Pee Dee Belemnite (VPDB) standard as a delta value (δ):

$$\delta = \left(\frac{R_{sample} - R_{standard}}{R_{standard}}\right) \times 1000\ (‰) \qquad (2.1)$$

where R represents the $^{18}O/^{16}O$ in the sample or standard (VPDB). The $\delta^{18}O$ values are expressed as per mil units (‰). The $\delta^{18}O_{H2O}$ values, in contrast, are calculated relative to the $\delta^{18}O_{H2O}$ value of Vienna Standard Mean Ocean Water (VSMOW). The following equation, originally from Friedmann and O'Neil (1977) but updated based on the work of Coplen, (1996), can be used to convert $\delta^{18}O_{H2O}$ values from VSMOW to VPDB:

$$\delta^{18}O_{(VPDB)} = \left(0.97001 * (\delta^{18}O_{VSMOW})\right) - 29.29 \qquad (2.2)$$

2.5.2 Temperature dependent fractionation of O isotopes in carbonates

The fractionation of O isotopes between aragonite (or calcite) and water is well studied and the equations for determining temperature from carbonate $\delta^{18}O$ has been refined progressively over time (Epstein et al., 1951, 1953; Friedman and O'Neil, 1977; Kim and O'Neil, 1997; Kim et al., 2007).

Carbonate materials precipitated from an aqueous solution take up ^{18}O in preference to ^{16}O, so the ratio $^{18}O/^{16}O$ in the carbonate is higher than that in the water. The effect is larger at lower temperatures. This is illustrated in Figure 2.4, where the $\delta^{18}O_{CaCO3}$ values of calcite is plotted as a function of temperature and water composition (NB. the $\delta^{18}O$ values of calcite and water are referenced to

different standards). Any given calcite $\delta^{18}O_{CaCO3}$ value can be the result of many combinations of water temperature and ambient water composition, as well as biological or kinetic effects, which occur in some biological carbonates.

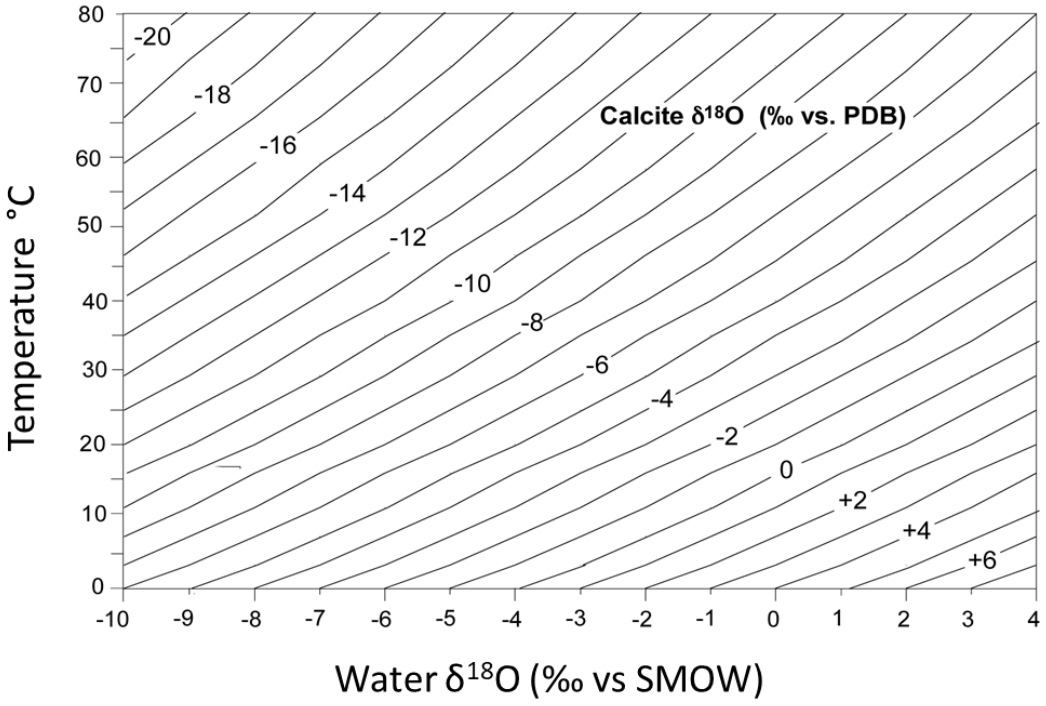

Figure 2.4: Plot showing the $\delta^{18}O$ values of calcite precipitated at isotopic equilibrium for given water $\delta^{18}O$ values (X-axis) and temperatures (Y-axis). Adapted from Railsback (2006) using the equation from Friedman and O'Neill (1977):
$10^3 \ln\alpha = (2.78 \times 10^6)/(T^2) - 2.89$ with T in Kelvin.

Calcium carbonate can crystallise as calcite, aragonite or vaterite (Campana, 1999). The polymorphs that form affects the O isotope fractionation factor (Kim et al., 2007). Aragonite, for example, is enriched in ^{18}O by 0.6‰ compared to calcite formed at the same temperature from a solution of the same $\delta^{18}O_{H2O}$ values (Kim et al., 2007). Multiple polymorphs are found in the inner ear of fish; Sagittae and lapilli are formed of aragonite, whilst asterascii are made of vaterite (Campana, 1999). Calcitic regions in otoliths can occur but are much rarer (Davies et al., 1988).

The original $\delta^{18}O$–$CaCO_3$ –palaeotemperature scale was developed by Epstein et al. (1953) and used the equation:

$$T = 16.5 - 4.3\,(c - w) + 0.14(c - w)^2 \qquad (2.3)$$

Where 'T' is temperature, 'c' is the $\delta^{18}O_{VPDB}$ value of the calcite and 'w' is the $\delta^{18}O_{VSMOW}$ value of the water. Subsequent studies have built on this equation using

different carbonate generating organisms. For example foraminiferal studies use two major equations for calculating palaeotemperatures:

1) Shackleton (1974), based on O'Neil et al. (1969):

$$T = 16.9 - 4.38(\delta_c - \delta_w) + 0.12\ (\delta_c - \delta_w)^2 \quad (2.4)$$

2) Hays and Grossman (1991), based on O'Neil et al. (1969):

$$T = 15.7 - 4.36(\delta_c - \delta_w) + 0.12\ (\delta_c - \delta_w)^2 \quad (2.5)$$

where 'T' is the temperature estimate in ˚C; 'δ_c' is the $\delta^{18}O_{VPDB}$ value of the calcite; 'δ_w' is the $\delta^{18}O_{VSMOW}$ value of the water. For every 1‰ change in the $\delta^{18}O_{CaCO3}$ value of foraminifera a change of ~4.3°C in water temperature can be inferred, assuming there is no change in water composition. Similar temperature equations have been developed for coral and diatoms (Leclerc and Labeyrie, 1987; Smith et al., 2000; Hill et al., 2011).

As with other carbonates, the two main effects on the $\delta^{18}O_{CaCO3}$ value of fish otoliths are the ambient water composition and temperature. Otolith O isotope equilibration with seawater has been demonstrated for a number of marine fish species, but slightly different temperature fractionation equations have been developed. Thorrold et al., (1997) developed a temperature equation using Atlantic croaker (*Micropogonias undulatus*):

$$1000\ \ln\alpha = 18.56\ (10^3 {T_K}^{-1}) - 32.54 \quad (2.6)$$

Where $\alpha_{otolith\text{-}water}$ is the fractionation factor between the otolith and the water

$$\alpha = \frac{\delta^{18}O_{aragonite}+1000}{\delta^{18}O_{water}+1000} \quad (2.7)$$

and T is temperature in Kelvin (K = T°C + 273). This can also be expressed as follows:

$$\delta c - \delta w = 4.64 - 0.21\ T_C \quad (2.8)$$

where $\delta_c - \delta_w$ is reported relative to PDB. Kalish (1991) generated the following relationship between $\delta^{18}O_{CaCO3}$ values measured in the otolith aragonite of tank and wild salmon (*Arripis trutta*) and temperature:

$$\delta^{18}O = 6.69 - 0.326\ T_C \quad (2.9)$$

Høie et al., (2003) investigated metabolic and kinetic effects in cod otoliths. Prey levels were manipulated in tanks maintained at two different temperatures containing juveniles, sub adults and adults. The difference between the $\delta^{18}O_{CaCO3}$ values of the otoliths and the $\delta^{18}O_{H2O}$ values was significantly influenced by temperature, but not by feeding level. These effects are less well studied in freshwater fish such as golden perch.

A study by Patterson et al., (1993) is the only one to develop a palaeotemperature equation for freshwater fish. By analysing the otolith $\delta^{18}O_{CaCO3}$ values of freshwater fish species within a single lake system that occupied different thermal ranges, Patterson et al., (1993) were able to characterise the influence of ambient water values on the final otolith $\delta^{18}O_{CaCO3}$ values for a temperature range of 3.2 to 30.3°C. Their final equation:

$$10^3 ln\alpha_{otolith-water} = 18.56\,(10^3/T) - 33.49 \qquad (2.10)$$

where α is defined as above (Equation 2.7), is similar to those for inorganic aragonite between 0 to 40°C (Kim et al., 2007) and marine fish, valid from 6 to 20°C (Høie, 2004).

The $\delta^{18}O_{CaCO3}$ values of otoliths can be used to reconstruct past temperature fluctuations when the $\delta^{18}O_{H2O}$ value is known or can be estimated. For the investigation of Australian freshwater fish otoliths there is the added problem of fish migration between different waters and evaporation or flooding occurring. These will affect the $\delta^{18}O_{H2O}$ values and hence the $\delta^{18}O_{CaCO3}$ values of precipitated otolith carbonate.

2.6 Trace elements: Sr and Ba

Sr/Ca and Ba/Ca ratios in otoliths are affected by a range of exogenous and endogenous factors. Temperature, salinity, fish growth and reproduction have all been cited as key influences (Kalish, 1989; Townsend et al., 1992; Campana, 1999; Bath et al., 2000; Zimmerman, 2005; Diouf et al., 2006; Walther et al., 2010; Sturrock et al., 2015; Grammer et al., 2017). The existence, relative proportion, and direction of these influences, as well as interactions between them (Elsdon and Gillanders, 2002; de Vries et al., 2005), are inconsistent between experiments and appear to be species specific. The only consistent result is that there is a strong link between Ba/Ca and Sr/Ca ratios in the water and those in the otoliths, and this can be used

broadly to track fish migration between fresh, brackish and marine waters. However, there are still inconsistencies in the direction of this relationship with some supporting a positive (e.g. Elsdon and Gillanders, 2005a, 2005b) and others a negative (e.g. Bath et al., 2000) relationship.

2.6.1 Sr and Ba in freshwater

Sr and Ba are alkaline-earth elements chemically similar to Ca and Mg. They occur in trace quantities in all-natural water sources (Skougstad and Albert, 1963; Sinclair and McCulloch, 2004). The Sr content of marine waters is relatively constant at 7600–8000 μg l^{-1} (Martin and Whitfield, 1983; Capo et al., 1998), whilst in freshwater environments dissolved Sr concentrations range from as low as 2.9 μg l^{-1} in the Caroni River Venezuela (Gaillardet et al., 2003) up to 2940 μg l^{-1} in the Avon River, Australia (Goldstein and Jacobsen, 1987). Terrestrial water and sediment sources tend to have elevated Ba concentrations compared to seawater (Shaw et al., 1998; Gaillardet et al., 2003).

2.6.2 Sr/Ca and Ba/Ca ratios in otoliths—effects of ambient conditions

Sr is found in relatively high concentrations in both water and otoliths compared with other trace elements. Its concentration is fairly stable within any given aquatic habitat, but can vary greatly between them (Campana, 1999; Secor and Rooker, 2000; Woodcock and Walther, 2014). Sr randomly substitutes for Ca in the otolith $CaCO_3$ of golden perch (Doubleday et al., 2013) and is mainly sourced from the water the fish is living in rather than the food it eats (Doubleday et al., 2013; Izzo et al., 2015). Similarly, Ba is readily incorporated into aragonitic hard parts (corals, otoliths, shells), substituting for Ca in the aragonite lattice at concentrations, which reflect the Ba/Ca in the ambient environment (Sinclair and McCulloch, 2004; Gonneea et al., 2017). Water is the main source for Ba and Ca, but food contributes up to 25% of otolith Ba in marine settings (Webb et al., 2012; Izzo et al., 2015).

Sr/Ca ratios in fish otoliths have commonly been used in modern studies to track the migration of fish through different water bodies (McCulloch et al., 2005) and determine the origins of fish stocks (Bastow et al., 2002). This is based on high Sr/Ca ratios being observed in otoliths and water during marine residency and lower ratios during time in freshwater—the opposite has been found for Ba/Ca ratios (Elsdon and Gillanders, 2004, 2005a, 2005b). Some studies have shown that

temperature has a greater effect on Sr/Ca and Ba/Ca ratios than does salinity, but that overall the greatest effect is changes in ambient concentrations (Fowler et al., 1995; Collingsworth et al., 2010). This means that Sr/Ca ratios in otoliths can be broadly used to distinguish between habitats with vastly different ambient Sr/Ca, such as marine vs estuarine vs freshwater.

It has been observed that the otoliths of fish moving between fresh and marine waters record changes in ambient water Ba/Ca (Milton and Chenery, 2001; Elsdon and Gillanders, 2004, 2005a, 2005b), which tends to be higher in fresh water than in marine. Analyses across otoliths of Spotted Algae-eating Goby (*Sicydium punctatum*) by Tabouret et al., (2011) show higher Sr/Ca values and lower Ba/Ca ratios relating to larval marine residency. That study concluded that the variations in Ba/Ca are related to changes in the ambient environment during freshwater residency rather than physiological effects. Hamer et al., (2006) found that Ba incorporation into the otoliths of tank-reared snapper was positively correlated with ambient concentrations, but independent of seasonal temperature or growth cycles. In contrast, Sturrock et al., (2015) found that otolith Ba/Ca was negatively correlated with ambient concentrations, salinity and temperature. Neither temperature nor the interaction between temperature and ambient Ba concentration had any significant effects on the Ba/Ca ratio of tank-reared yellow perch (*Perca flavescens*) otoliths (Collingsworth et al., 2010). There is a broad consensus that Ba/Ca in otoliths relates closely to the ambient Ba/Ca ratio of the water (Bath et al., 2000; de Vries et al., 2005; Elsdon and Gillanders, 2005b; Walther and Thorrold, 2006; Dorval et al., 2007; Clarke et al., 2015). However, the sense of this relationship appears to differ between species.

Interactive and species-specific effects cannot be discounted, and there are few studies examining influences of environmental and physiological variables on freshwater fish. General differences between the influences on freshwater and marine fish have also been observed. For example, water Sr/Ca ratios were shown to have the greatest influence on the Sr/Ca ratios in the otoliths of freshwater and diadromous species, but not so for marine fish (Brown and Severin, 2009).

2.6.3 Sr/Ca and Ba/Ca ratios in otoliths—effects of salinity

Sr/Ca and Ba/Ca ratios in otoliths are generally assumed to be linked to salinity. Many studies use them as markers for fish migration between fresh, estuarine and

marine waters. Zimmerman (2005) found that within the otoliths of a variety of fish species Sr/Ca ratios increased significantly with ambient salinity, although there were some differences in the degree of increase between species. The degree of difference was just sufficient to distinguish movement between marine and freshwater, but not more subtle changes in ambient conditions or salinity. Other studies concur that increased salinity results in higher Sr/Ca ratios in otoliths (e.g. Diouf et al., 2006). Those changes in the otolith Sr/Ca ratios, however, were not necessarily due to salinity changes, but more likely to changes in the ambient water values. In the study by Zimmerman (2005), ambient water Sr/Ca was found to increase with salinity. This link is further supported by the results of an experiment by Kraus et al., (2004) which showed that, when water had constant salinity and Ca levels, there were significant increases in otolith Sr/Ca when the water Sr concentrations were increased. The effect of salinity was insignificant. Chang et al., (2004), in a similar test of the relationships between water Sr/Ca, salinity and otolith Sr/Ca, found that a salinity change from 5‰ to 35‰ had no effect on otolith Sr/Ca ratios.

There are, however, studies that show negative correlations between otolith Sr/Ca ratios and salinity (e.g. Sturrock et al., 2015) as well as those finding no obvious relationship between ambient water composition or salinity (e.g. Dorval et al., 2007). This further suggests, as noted in section 2.6.2 above, that the factors of influence are species specific.

2.6.4 Sr/Ca and Ba/Ca ratios in otoliths—effects of temperature

Studies of the effect of temperature on the Sr/Ca ratios in fish otoliths have returned inconsistent results. Some studies have found a negative correlation between Sr/Ca ratios and temperature (Radtke, 1989; Townsend et al., 1992; Secor et al., 1995; Sturrock et al., 2015) whilst others have found a positive or insignificant relationship (Kalish, 1989; Fowler et al., 1995; Tzeng, 1996; Chesney et al., 1998; Dorval et al., 2007). A strong positive interaction between temperature and ambient chemistry for both Sr/Ca and Ba/Ca was found in the study by Elsdon and Gillanders (2002). Chesney et al., (1998) found no significant relationships between Sr concentrations or Sr/Ca ratios and temperature, salinity or growth rate. The main reasons cited for these discrepancies between results are that relationships are species specific and that ontogenetic growth factors may have affected the results.

Less is known about the relationship between otolith Ba/Ca ratios and environmental and physiological variables. Hamer et al., (2006) found Ba incorporation into the otoliths of tank-reared snapper was positively correlated with ambient concentrations, but independent of seasonal temperature or growth cycles. In contrast, Sturrock et al., (2015) found that otolith Ba/Ca was negatively correlated with ambient concentrations, salinity and temperature. Neither temperature nor the interaction between temperature and ambient Ba concentration had any significant effects on the Ba/Ca ratio of tank-reared yellow perch otoliths (Collingsworth et al., 2010). Experiments have determined that the partitioning of Ba between inorganic aragonite and fluid is temperature dependent (Dietzel et al., 2004; Gaetani and Cohen, 2006) but in biological aragonite there tends to be variability in Ba/Ca ratios that cannot be explained by temperature alone, suggesting that there are other contributing factors.

2.6.5 Sr/Ca and Ba/Ca ratios in otoliths—other influences

The precipitation rate of fish otoliths could affect the timing/incorporation of Sr and Ba into the otoliths. Bath et al., (2000) found that juvenile Norfolk spot (*Leiostomus xanthrurus*, a marine fish) raised in tanks showed no statistically significant effects of precipitation rate on Sr and Ba incorporation into their otoliths, concluding that fish growth rate was similarly a weak influence.

Kalish (1989) compared the endolymph and blood elemental composition of wild and laboratory-reared fish to their otolith compositions at different temperatures. There was some evidence for an increase in otolith Sr/Ca ratios with temperature, but this might not be a direct relationship—faster growth might have affected the incorporation of trace elements into the otoliths (Kalish, 1989). Higher levels of Ca-binding proteins in the blood plasma during growth periods may lead to an increase in Sr/Ca ratios in the endolymph and hence the otoliths. This could confound studies of otolith Sr/Ca changes thought to be controlled only by changes in temperature and salinity. Ontogenetic effects have been observed in studies of fish otolith elemental compositions but have rarely been validated experimentally. A study by Walther et al., (2010), in which reef fish from three different age groups, juveniles, sub adult and adult, were raised in tanks under different temperatures and feeding regimes, found that incorporated Sr/Ca was negatively correlated with specific growth rates. These effects seem to be species specific, much like the effects of

temperature change, and so for more detailed environmental studies these need to be validated for each species involved.

Multi variate models have been used to investigate the directionality and strength of element-to-element and growth relationships, and to test hypotheses for physiological and environmental influences on otolith trace element assimilation (Grammer et al., 2017). When these models were applied to reef ocean perch (*Helicolenus percoides*), it was found that Sr/Ca and Na/Ca were mainly controlled by physiological processes, whilst Ba/Ca and Li/Ca mainly reflected environmental influences. The only elemental ratio to show a relationship with growth among individuals was Ba/Ca (Grammer et al., 2017).

Martin et al., (2013) found that otolith Ba/Ca profiles were characterised by a peak in the early life stages of the fish, followed by a progressive decrease until remaining stable in later life. This is an ontogenic signal that could not be explained by changes in the ambient water. Walther et al., (2010) found significant interactive effects between life history stage, temperature, and food quantity for Ba/Ca in the otoliths of tropical damselfish (*Acanthochromis polyacanthus*).

2.7 Application of otolith geochemistry to archaeological studies

Otoliths from archaeological sites have previously been used to deduce detailed information about past climates, fish migration patterns, ancient fishing practices, and the influence of changing environmental conditions on human populations. By targeting fish species with predictable migration patterns and basing studies on observations/records of modern fish and modern environmental conditions it is possible to build up a framework to interpret microchemical records from ancient fish otoliths. There are similar goals for understanding ancient records in other animal and human hard parts including shells (Lee and Wilson, 1969; Kennett and Voorhies, 1996; Carré et al., 2005; Colonese et al., 2017; Prendergast and Schöne, 2017; Twaddle et al., 2017), teeth and bones (Fricke et al., 1995; White et al., 2004; Fraser et al., 2008; Somerville et al., 2018; Willmes et al., 2018).

Increasingly, the chemical records preserved in fish otoliths are being used to better understand the archaeological and palaeontological record. C, Sr and O isotope ratios in otoliths were used by Carpenter et al. (2003) to interpret the migration of a selection of Cretaceous (67–65 Ma) fish. Andrus et al. (2002) used the $\delta^{18}O_{CaCO3}$

values of catfish otoliths to reconstruct past sea surface temperatures near Peru in the Mid-Holocene. They looked at variations in the $\delta^{18}O_{CaCO3}$ values of modern fish otoliths and found that El Nino events were recorded as significant negative excursions in the $\delta^{18}O_{CaCO3}$ values . The $\delta^{18}O_{CaCO3}$ values of archaeological otoliths indicated that sea surface temperatures in the Mid Holocene were ~3–4°C higher than today.

West et al. (2012) reported a study of methods for using pacific cod otoliths as palaeothermometers. They analysed otoliths from Kodiak Island, Alaska, and found that they record the Little Ice Age. Their analyses suggested that otoliths record variable mean environmental conditions over the last 500 years at the site, with mean $\delta^{18}O_{CaCO3}$ values ranging from 0.78‰ to 1.48‰. Metabolic processes did not appear to have a significant effect on the O isotope fractionation in otoliths (Thorrold et al., 1997; Campana, 1999; Høie, 2004). Mixing of freshwater (low $\delta^{18}O_{H2O}$ values) and marine water ($\delta^{18}O_{H2O} \approx 0$) affects ocean water $\delta^{18}O$ values, and this is reflected in the otoliths. West et al. (2012) assumed the $\delta^{18}O_{H2O}$ value of the prehistoric water based on contemporary conditions and compared mean annulus and mean transect values to help eliminate bias of averaged measures. Seasonal variability and ontogenetic bias may have resulted from the slower growth later in the fish's life.

Fish otolith applications to Australian archaeological sites are rarely discussed, the exception being the work by Disspain et al. (2011) who examined the Sr/Ca and Ba/Ca ratios in ancient golden perch and mulloway (*Argyrosomus japonicus*) otoliths excavated from Mid-Late Holocene archaeological shell middens in the Coorong, South Australia. They found that low Ba/Ca and high Sr/Ca were indicative of residence in marine waters, whilst the opposite indicated freshwater occupancy. By closely analysing the structure and chemical composition of the otolith edge it could be inferred that fish were caught in the warm season from freshwaters, consistent with ethnographic knowledge of aboriginal fishing strategies in the area (Disspain, 2009; Disspain et al., 2011). Studies of fish otoliths from archaeological sites have now been expanded beyond simply species identification and the determination of fish size and age, to include trace element and isotopic analyses.

2.8 Post depositional diagenetic effects

Fresh otoliths are composed of aragonite. The absence of calcite is usually a good indication that an otolith has not been affected by chemical alteration. Methods for identifying alteration/recrystallisation include scanning electron microscopy (SEM) to image differences in crystal structure, and powder X-ray diffraction (XRD) to detect the presence of calcite. Aragonite can recrystallize into calcite due to significant changes in temperature or burial, or through the influence of groundwater (Campana, 1999; Faure and Mensing, 2005).

Cook et al., (2016) found no definitive evidence for diagenetic alteration in Sr or other elements deeper than a few hundred micrometres into archaeological otoliths, making it unlikely that diagenesis will affect otolith trace elements, except in the outermost layers.

2.9 Pre-Deposition effects: cooking and waste disposal methods on otolith composition

The effects of different prehistoric cooking methods on otolith compositions has been investigated by Andrus and Crowe, (2002) and Disspain et al., (2016).

Andrus and Crowe, (2002) tested the effects of common cooking and waste disposal methods on trace elements and isotopes in Atlantic croaker (*Micropogontus undulatus*) and gafftopsail catfish (*Bagre marinus*) otoliths. Cooking methods were found to influence the trace element ratios, such as Ba/Ca and Sr/Ca, but not the $\delta^{18}O_{CaCO3}$ values, except when the otoliths were burnt (Andrus and Crowe, 2002).

Disspain et al., (2016) examined the effect of cooking treatments on the trace elemental and isotopic composition of Mulloway (*Argyrosomus japonicus*) otoliths, scales and vertebrae. The six traditional cooking practices investigated by Disspain et al., (2016) were: boiled in freshwater, boiled in saltwater, burnt completely, roasted on fire, salted or wrapped in clay. They used a LA-ICPMS system to analyse trace elements in the most recent portion of otolith growth (30 μm spot representing less than 1 month of growth) and in the juvenile portion near the nucleus.

XRD analysis of the otoliths following each treatment demonstrated that they remained aragonite, except for those that were burnt completely, which recrystallized entirely to calcite. Disspain et al., (2016) found that Sr/Ca and Mg/Ca

were relatively similar for all treatments—Ba/Ca and Mn/Ca varied between the edge and nucleus and not between treatments. The most pertinent finding of the study was that the mean $\delta^{18}O_{CaCO3}$ values differed between treatments. The $\delta^{18}O_{CaCO3}$ values of the treated otoliths was 1.09‰ to 1.47‰ lower than that of the control group. The largest difference was observed in the group burnt completely, in which the $\delta^{18}O_{CaCO3}$ value was 4.37‰ lower than the mean of the control. Aragonite is prone to alteration under increased temperature or pressure. The lower O isotope values are due to the higher temperature and longer duration of this treatment, also the change from aragonite to calcite drove the exchange of O and C in the lattice (Waite and Swart, 2015). A separate study by Guiguer et al., (2003) found no significant difference in fish otolith mean $\delta^{18}O_{CaCO3}$ and $\delta^{13}C_{CaCO3}$ when roasted at 200, 250 or 275°C for 1 h. Disspain et al., (2016) only studied edge sections of otoliths for isotopic analysis and thus provided no indication of how deeply this effect penetrates. It could be that within the inner parts of the otoliths there is no observable offset. This has implications for reconstructing lake conditions associated with the final years before the fish's death.

Disspain et al., (2016) observed changes in the O isotope values of cooked otoliths. These resulted in a predicted ambient water temperature higher by between 2.54 and 6.7˚C. When the otoliths were burnt this apparent warming could be as much as ~ 19.85°C based on warming of 1°C resulting in 0.22‰ decrease in otolith aragonite $\delta^{18}O$ values as estimated by Thorrold et al., (1997). None of the archaeological otoliths in the present project show evidence of being burnt.

If the archaeological otoliths studied for the present project were cooked in one of the ways tested by Disspain et al., (2016), other than burning, then there is the possibility that the O isotope values are slightly (1 – 2‰) lower than if the fish hadn't been cooked. Such a slight offset is only problematic in high resolution/detailed studies of temperature change where a difference of 1‰ could result in a temperature estimate 4.6°C higher or lower than the real value (Kalish, 1991).

3. Methodology: Otolith Collections, Preparation and Analysis

3.1 Introduction

Otoliths are traditionally used for age determination in modern fish growth and mortality studies (Anderson et al., 1992a; Secor et al., 1995; Campana, 2001). The preparation of otoliths for age determination requires only that the annual age increments are present and clearly visible—they do not necessarily need to be exposed. Age increments of small otoliths (< 300 μm) can be viewed without further preparation (Secor et al., 1992). For larger otoliths thin sections must be prepared to obtain high visibility of the internal structures for age determination (Secor et al., 1992; Jenke, 2002).

New analytical capabilities allow for the analysis of isotopes and trace elements within and across the age increments of fish otoliths. This expands the usefulness of otoliths beyond fish metrics to temperature reconstruction, radiocarbon dating, migration studies, stock identification and more. These new applications require the development of new otolith preparation methods to allow not only age determination and visibility of the internal structures but also close association between multiple analyses within these structures. This Chapter presents a summary of:

- Sample collection methods and sources
- the key requirements for *in situ* isotope analysis of otoliths using the SHRIMP;
- preparatory techniques used in the initial scoping study applied to ancient otoliths from hearths at Lake Mungo;
- experimental preparation methods applied to ancient golden perch otoliths recovered from the Lake Mungo lunettes and modern golden perch otoliths from fish caught downstream of the Menindee Lakes;
- the final improved otolith preparation method applied to all other golden perch otoliths in the present study;
- the SHRIMP and LA-ICPMS analyses and data processing methods.

The widths of increments are variable around the whole otolith. Growth is restricted on the ventral edge due to the physical contact between the otolith and the fish skull (Gauldie and Nelson, 1990; Francis and Campana, 2004). Whilst on the medial surface, material is continually deposited as shown in Figure 3.1 (Blacker, 1974; Boehlert, 1985; Anderson et al., 1992a).

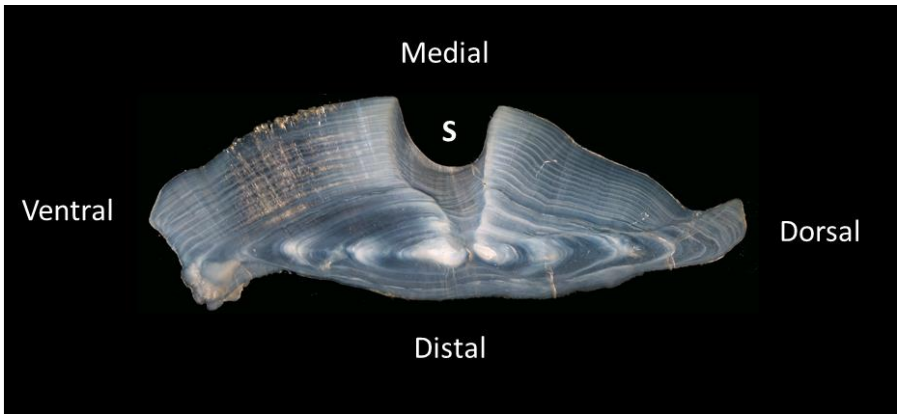

Figure 3.1: A transverse section view of a modern golden perch otolith showing restricted growth on the ventral edge and free growth on the medial edge. The sulcus (S) groove lies on the inner side of the fish.

The direction of sectioning depends on the aim of the study, for example a sagittal section (Fig. 3.2) might expose the greatest area of the otolith but may obscure increments due to changes in the growth axis over time or the establishment of secondary growth centres (Secor et al., 1992). For example, juvenile striped bass sagittae project away from the sagittal plane and therefore a sagittal section will not contain increments from the peripheral area. A transverse or frontal plan will pick up these peripheral growth increments (Secor et al., 1992). To get the best age increment readability Jenke (2002) recommend cutting perpendicularly through the age increments such that they are as narrow and well defined as possible.

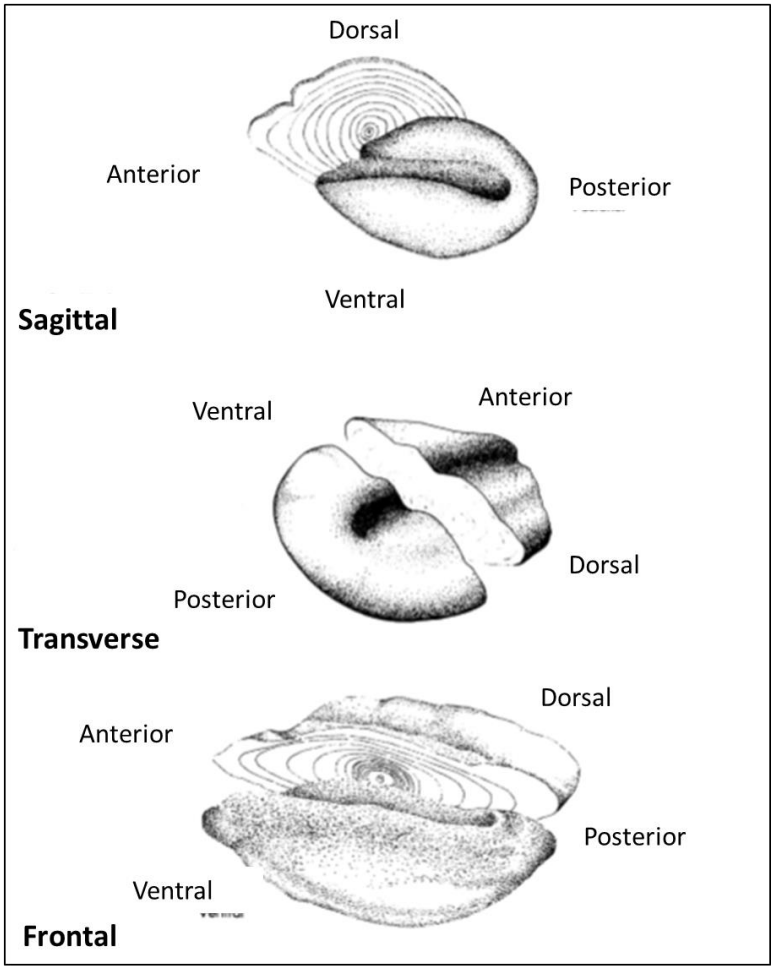

Figure 3.2: Diagrams of sagittal otoliths showing the different sectioning planes that can be used to expose the inner age increments. Adapted from Secor et al., (1992).

The initial scoping study reported by Long et al., (2014), used transverse sections of otoliths. Follow up preparation techniques experimented with different sectioning planes to improve the visibility and exposure of age increments whilst continuing to meet the preparation requirements for SHRIMP and LA-ICPMS analysis.

3.2 Sample collection

3.2.1 Modern tank otoliths

For the modern tanks study which forms Chapter 4, otoliths were obtained from the Narrandera Fisheries golden perch breeding stock. These fish were originally caught in 2007-8 from two locations in the Lachlan River; Brewster Weir and downstream of Lake Cargelligo (Fig. 3.3) and were kept in tanks for 5-6 years. A total of 26 whole otoliths were extracted from 16 modern golden perch on the 8th April 2013. Seven of the otoliths were selected for isotopic and elemental analysis (Table 3.1).

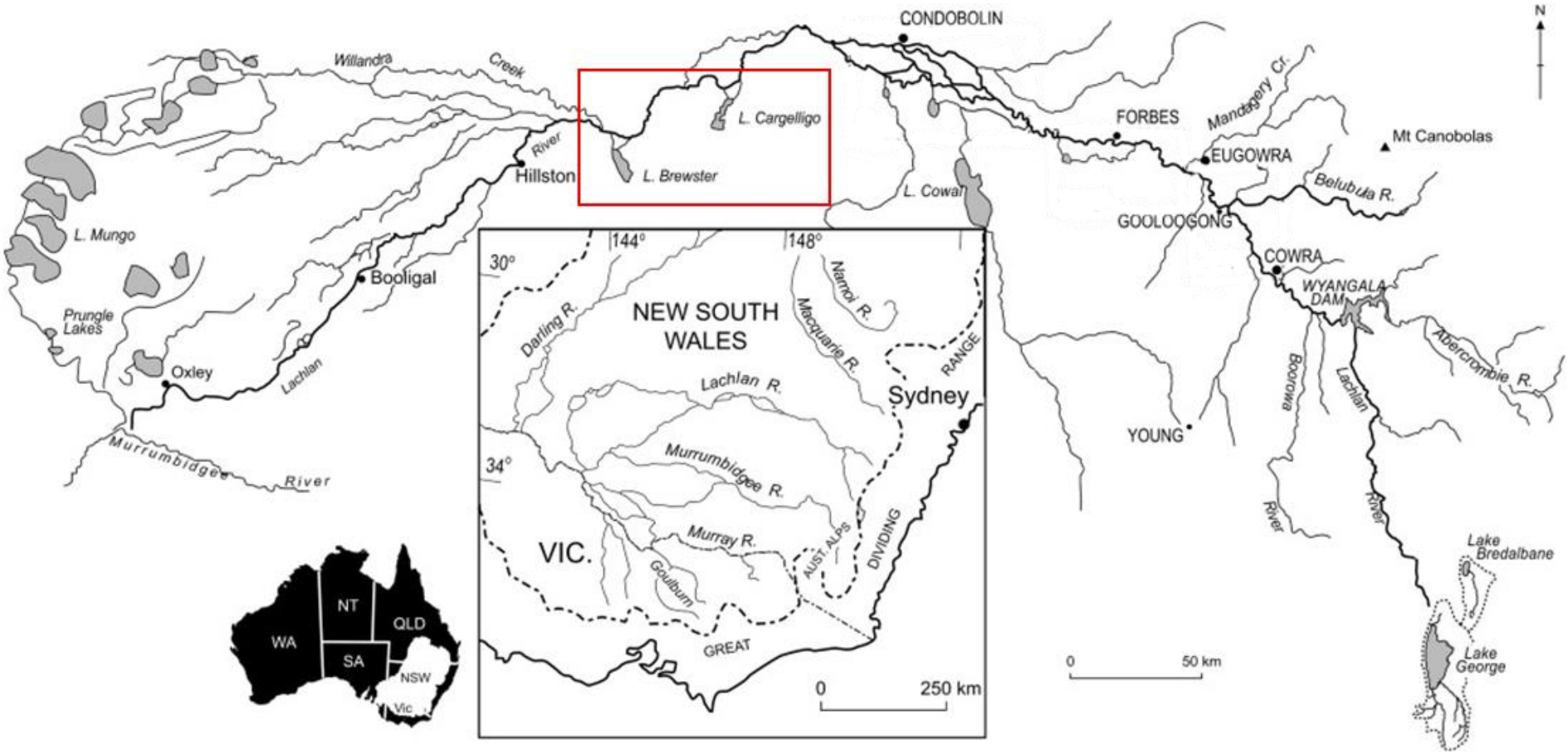

Figure 3.3: Map showing the location of Lake Cargelligo and Lake Brewster along the Lachlan River in New South Wales (Kemp and Rhodes 2010).

Table 3.1: Summary of golden perch otoliths characteristics and aging by Simon Robertson.

Sample no.	Sex	Fish Weight (g)	Fish Length (mm)	Location caught	Date caught	Otolith analysed	Age	Edge increment type	Year of spawning
3419	f	775	430	Brewster weir	May-08	Left	18	Wide Edge	1995
3422	f	710	431	Brewster weir	Jan-07	Right	14	Wide Edge	1999
3424	m	740	393	d/stream L.Cargelligo	Nov-08	Left	9	Narrow Edge	2004
3425	m	836	430	Brewster weir	Jan-07	Left	9 (10)	Narrow Edge	2004
3428	f	1055	458	Brewster weir	Jan-07	Right	12	Wide Edge	2001
3430	m	430	331	d/stream L. Cargelligo	Nov-08	Right	9	Wide Edge	2004
3433	m	820	424	Brewster weir	Jan-07	Right	12	Wide Edge	2001

When the otoliths were extracted by staff at the Narrandera Fisheries Centre tag numbers (used to link individual fish back to the location where they were originally caught) were not recorded. Nevertheless, it was possible to assign tag numbers retrospectively based on the length and weight histories of the fish. Otoliths were prepared for SHRIMP, LA-ICPMS, micromilling and DI-MS analysis as described in section 3.4 of this Chapter.

Four water samples, from the tank in which the fish lived, were collected for O isotope analysis. Throughout the life of the fish the tank water was maintained on the same filling and flushing cycle, at similar temperatures and from the same bore water source. These breeding stock tanks (Fig. 3.4) hold approximately 5000 L and have a constant low flow of incoming bore water and therefore rarely have full water exchanges. Fish from the same catchment are discrete breeding units and so are accommodated together for most of the time during the breeding program. Fish were originally collected from the wild then held in quarantine for a fortnight before being moved into the brood stock tanks for ongoing holding. Fish were removed each year for approximately 1 week between October and February for spawning in the hatchery. When the fish were brought to the hatchery for this process they were transferred to river water for 48 hours before returning to bore water for recovery and returned to their holding tanks until the next year. The salinity of the bore water used in the tanks is generally 1000 EC, which at 25°C translates to around 0.64 ppt, so slightly more brackish than freshwater (0-0.5 ppt).

Figure 3.4: Image of the 5000L tanks at the Narrandera Fisheries where golden perch breeding stock were kept. Image courtesy of the Narrandera Fisheries Centre.

3.2.2 Modern Menindee Lakes otoliths

For the Menindee Lakes study which forms Chapter 5, ten golden perch otoliths were provided by Clayton Sharpe from the Narrandera Fisheries Centre, for O isotope and trace element analysis. These fish were caught from the Darling River 1-5 km downstream from the Menindee Main Weir (Fig. 3.5) on 28 December 2005.

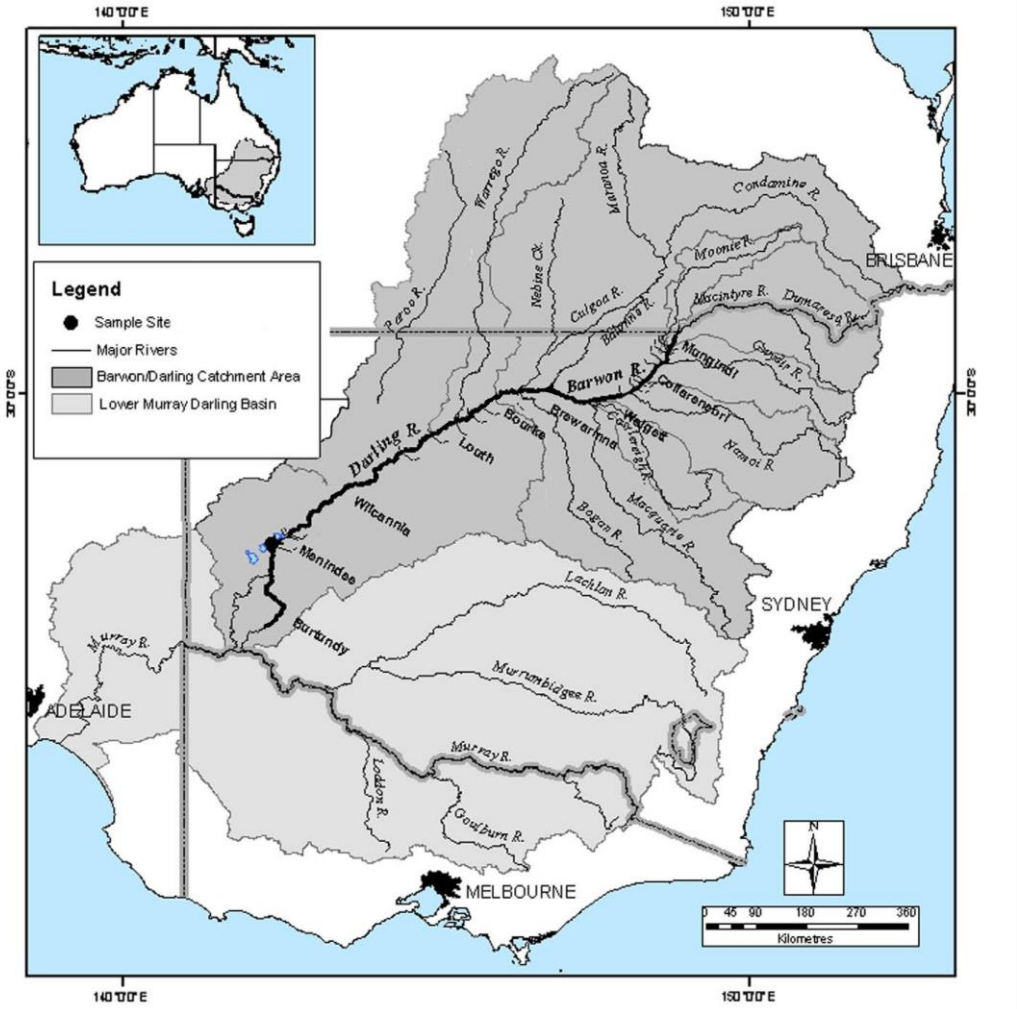

Figure 3.5: Map of the position of the Menindee Lakes sample site downstream of the Menindee Main Weir along the Barwon-Darling River system in western NSW. Image has been adapted from Meredith et al., (2009).

All fish caught were female, and the right otolith of each was provided for analysis. Eight of the otoliths were prepared for oxygen isotopic and trace elemental analysis (Table 3.2). The otolith preparation methodology is described in detail in section 3.3 below. Four of the otoliths (DSM 12-15, 12-16, 12-17 and 12-18) were prepared using the experimental thin section method described in section 3.3.4. The rest were prepared using the final improved thin section cutting and mounting method described in section 3.3.5.

Table 3.2: Summary of golden perch otoliths caught in the Darling River downstream of the Menindee Weir, provided by Dr Clayton Sharpe, Narrandera Fisheries Centre

Fish Code	Fish total length (mm)	Fish total weight (g)	Sex	Otolith weight (g)	Otolith length (mm)	Otolith width (mm)	SHRIMP & LA-ICPMS analysis
DSM 12-2	465	1432	F	0.443	16	9.4	X
DSM 12-3	419	1323	F	0.454	16	8.6	X
DSM 12-4	385	944	F	0.39	15	8.2	X
DSM 12-6	378	843	F	0.359	15	9.2	
DSM 12-12	430	1198	F	0.398	16.5	8.7	X
DSM 12-14	386	971	F	0.346	16	7.8	
DSM 12-15	415	1316	F	0.385	16	9	X
DSM 12-16	414	1256	F	0.46	16	9	X
DSM 12-17	400	1201	F	0.344	15.5	7.6	X
DSM 12-18	431	1375	F	0.515	16	9.1	X

These particular samples of golden perch otoliths were chosen for this study because information about the water composition and temperature was available for the same area and close to the same timeframe. Water samples from downstream of the Menindee Lakes were collected between 2003 and 2007 and their O isotopic composition was analysed by Karina Meredith and other hydrogeochemistry and isotope hydrology researchers from the Australian Nuclear Science and Technology Organisation (ANSTO) (Table 3.3). Temperatures were also recorded when some of the water samples were collected (Table 3.3).

Table 3.3: Summary of Menindee main Weir water measurements, provided by Katrina Meredith from ANSTO.

Sampling Date	Location	T°C	$\delta^{18}O$ (‰)	$\delta^{2}H$ (‰)
1/01/2003	Menindee Main Weir		9.91	41
11/08/2003	Menindee Main Weir		2.91	7.6
25/01/2004	Menindee Main Weir		8.06	35.1
25/01/2004	Menindee Main Weir	28	8.06	35.1
7/01/2006	Menindee Main Weir	25	3.86	14.56
16/01/2007	Menindee Main Weir	27	7.64	34.92
10/05/2007	Menindee Main Weir	18	9.31	44.9

Maximum and minimum water temperatures for the regions were estimated from air temperature records (Bureau of Meteorology BoM). Air temperature and water temperature are strongly correlated (Webb et al., 2003, Web et al., 2008), being found to follow each other closely with time lag of hours to days depending on water depth (Stefan and Preud'homme, 1993). Deviations from this relationship can occur when air temperatures are very low (< 0°C) or high (> 20°C) (Mohseni et al., 1998, Mohseni et al., 1999). Overall, water temperature is rarely higher than air temperature and, due to the high thermal inertia of water, tends to have a lower variability.

Water temperatures in rivers are a complex function of both climate and hydrological changes. Van Vliet et al., (2011) examined water temperature trends in major rivers around the world over the last 100 years and tested air-temperature-water flow models for key locations for sensitivity. The developed model was then applied to 157 river temperature discharge stations globally including the Barwon-

Darling River at Burtundy. Distinct inverse relationships between water temperature and discharge were found for most of the sites included in the study but not for the Darling river station at Burtundy. The Darling river station at Burtundy was found to have peak discharges in summer which coincided with water temperature peaks. For Burtundy, an air temperature increase of 6°C was reflected in the water temperature as an increase of 4.6°C (van Vliet et al., 2011). The optimal time lag between air temperature change and water temperature change, for Burtundy, was estimated to be 8 days (van Vliet et al., 2011).

Given that water temperatures at the upstream station of Burtundy change by 4.6°C for every 6°C of air temperature increase, it is likely that the water temperature values at Menindee are also typically lower than the air temperature values. The monthly air temperatures at Menindee, as recorded by the Bureau of Meteorology, range from a minimum of 17.3°C to a maximum of 35.6°C. To make these values a more realistic range, the predicted otolith $\delta^{18}O_{VPDB}$ values are estimated using the maximum and minimum air temperature value minus 1.6 °C as per the relationship between water temperature and air temperature change at Burtundy (van Vliet et al. 2011). Approximate water temperature range is therefore a minimum of 15.6 °C and a maximum of 34 °C.

3.3 Otolith Preparation: Experimental and improved methods

3.3.1 Requirements of SHRIMP analysis

There are a few key requirements for O isotope analysis of samples in the SHRIMP SI, one of the new generations of SHRIMP specifically designed for measurement of isotopes of low mass, or SHRIMP II, the second generation of SHRIMP after the SHRIMP I:

1. samples and standards need to be exposed on the same surface of 25mm (SHRIMP SI) or 35mm diameter round mounts (SHRIMP II)
2. for the best results samples and standards should be embedded in resin as close as possible to the centre of the mount
3. the surface of the mount needs to be clean, flat, highly polished and coated with Al

The key aims of the preparation procedures outlined here were to achieve the above requirements for SHRIMP analysis whilst also maximising the number of samples per mount, the number of spots per age increment and the visibility of age increments.

3.3.2 Initial scoping study: Mungo Hearth Otoliths

In the initial scoping study, that formed part of the work reported by Long et al. (2014) the otolith preparation process focused on preserving material and ensuring no contamination of the SHRIMP SI by conductive adhesives.

Otoliths were cut transversely through the nucleus using a diamond edged saw and again at 5mm towards the ventral axis (Fig. 3.6). The centre section was embedded in epoxy resin, with other otolith samples and the side closest to the nucleus was polished to expose age increments at the mounts surface. The two otolith end pieces (rostrum and post rostrum) were packaged separately for radiocarbon dating and amino acid racemisation (AAR) analysis (see Long et al. 2014 for hearth otolith radiocarbon dating results and Long (2012) for AAR results).

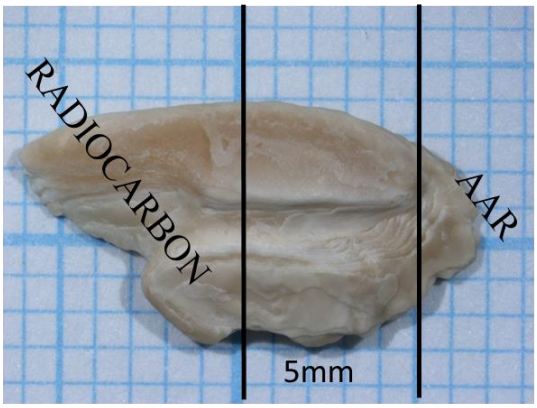

Figure 3.6: Hearth otolith 982-11. Transverse section cuts shown as black lines.

Otolith mounts were then placed within a sample holder along with standards, Davies Reef coral and NIST 612 glass, for trace element and Sr isotope analysis (Fig. 3.7).

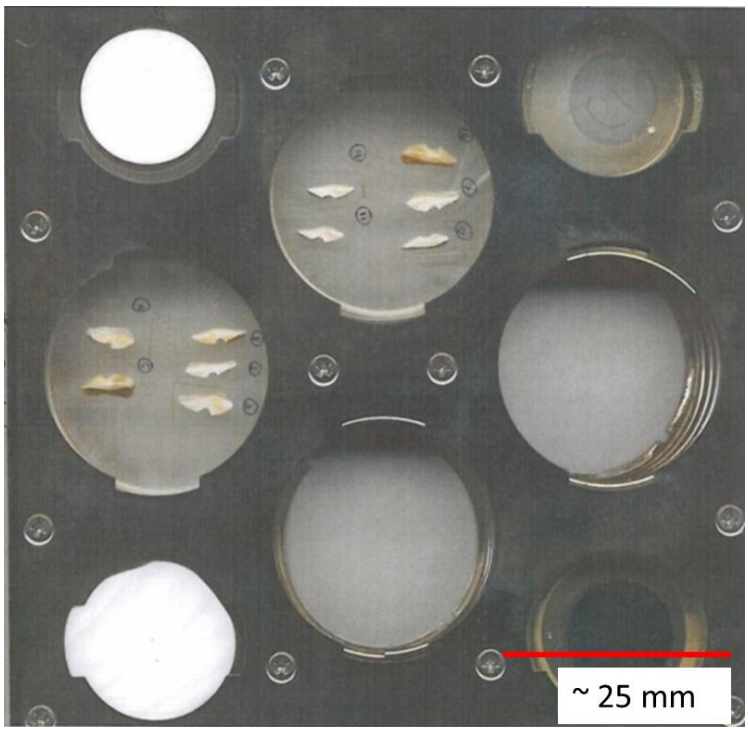

Figure 3.7: Hearth otoliths mounted in laser ablation sample holder with standards, NIST 612 glass (top right) and Davies Reef coral (bottom left).

The spot size for trace elemental measurements, using the LA-ICPMS, was 50µm and tracks were cut from the centre of each otolith out to the dorsal and ventral tips (Fig. 3.8). The spot size for Sr isotope measurements, using the laser ablation multi collector inductively coupled plasma mass spectrometer (LA-MC-ICPMS), was approximately 85µm and cut more slowly and deeply from the centre to one edge of each otolith (Fig. 3.8).

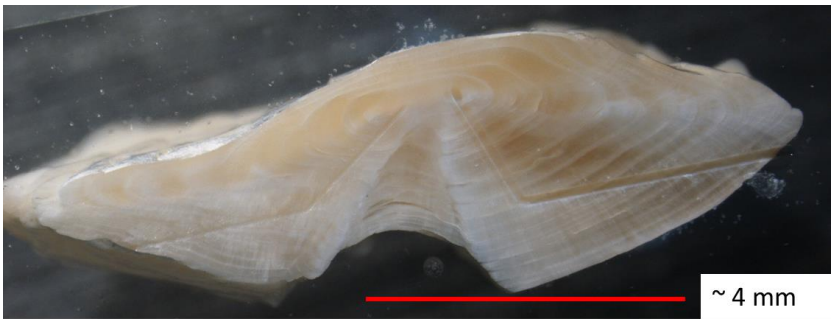

Figure 3.8: LA-ICPMS tracks (trace elements) overlain by the LA-MC-ICPMS tracks (Sr isotopes) across the age increments of a Mungo hearth otolith (982-11) from the initial scoping study.

After laser ablation the otolith mounts were wet polished to remove the analytical tracks. Each otolith was cut out from the mount, then remounted in epoxy along with standards, NBS-18 calcite and NBS-19 limestone 8544, to form smaller circular (25mm diameter) mounts typically used in the SHRIMP-SI for O isotope analysis.

The surface of each mount was cut using 1200grade SiC paper and then polished using 3 µm and 1 µm diamond paste. This polished surface was then cleaned using petroleum spirit, warm detergent solution and ultrapure water to remove contaminants, then the mount was dried for a minimum of 24 hours in a 60°C vacuum oven before being coated with a thin (~10 mm) layer of Al before being placed in the SHRIMP-SI for analysis.

High resolution photos of the embedded otolith surfaces were taken for initial age assessment. However, accurate ages could not be determined until after the analyses were complete. Following analysis, the otolith mounts were polished down from the back to create thin sections. Thin-sectioned otoliths viewed under transmitted light can be aged more accurately. The photographs taken before and after each analysis were used to match up analytical spots and tracks with age increments. In some otoliths the outer layers were lost during thin section preparation, leading to a mismatch between analyses and age increments (Long et al., 2014 Fig. 3.9).

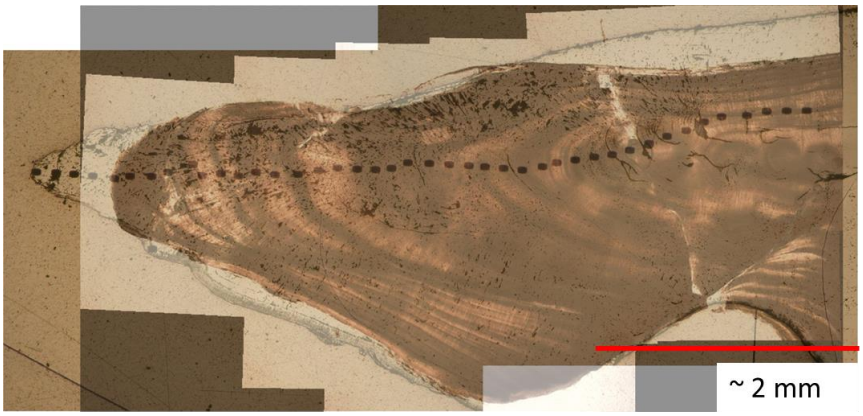

Figure 3.9: Example hearth otolith (926-3) thin section used for aging compared to the location of the SHRIMP SI spots illustrating the loss of material between sampling and aging because of polishing.

This initial scoping study demonstrated that the order of the analyses matters. If laser tracks for trace elements or Sr isotopes are cut first, then these must be polished away before the sample can be analysed in the SHRIMP. This process results in the loss of otolith material and can cause mismatches between analyses and age increments. O isotope analysis in the SHRIMP must be conducted first, preferably on thin sections of otoliths where age increments are clearly visible. LA-ICPMS analysis does not require any special preparation, apart from removing the

Al coating from the sample mounts. The SHRIMP spots can remain as guidelines for the trace element analysis.

The focus of the present study was on O isotope and trace element analyses of golden perch otoliths and how these reflect changing ambient conditions (lake levels) over the life of the fish. Therefore, the priority was to obtain O isotope and trace element measurements across the same sections of the otolith that could be closely related to each other and to age increments.

3.3.3 Experimental preparation: Lake Mungo surface otoliths

The BMLM otoliths used here were originally collected from non-cultural contexts on the surface of the northern tip of the Lake Mungo lunette by Ian Moffatt in 2007. Seven samples from this collection were radiocarbon dated to between 21,149-20,157 and 20,332–18,928 cal BP, about the time of the Last Glacial Maximum (LGM). Three were selected for isotopic analyses, the results of which were reported by Long et al., (2014). The hearth otoliths from the scoping study are of a similar antiquity, dated to between 19,490–19,330 cal BP and 19,420–19,220 cal BP. The BMLM otoliths provided an opportunity to examine the effects of different sectioning techniques on the otoliths of ancient golden perch to gain a closer approximation of how preparation methods will affect archaeologically relevant otoliths from Lake Mungo.

A common feature in teleosts (bony fish) is that the anterior portion of the sagittal otolith projects (curves) laterally within the epithelium. The sulcus and macula occur on the medial (convex) surface (Secor et al., 1992). The aim here was to test the benefits and drawbacks of exposing the age increments in the sagittal plane (Fig. 3.2). An ideal sample would be thin enough for transmitted light to pass through, with a greater area of age increments exposed on the same surface as the nucleus.

All sectioning for this experiment was completed using a precision saw equipped with a diamond wire (Fig. 3.10). Otolith BMLM 130 was embedded in resin and then sectioned transversely on the rostrum side of the nucleus (Fig. 3.10).

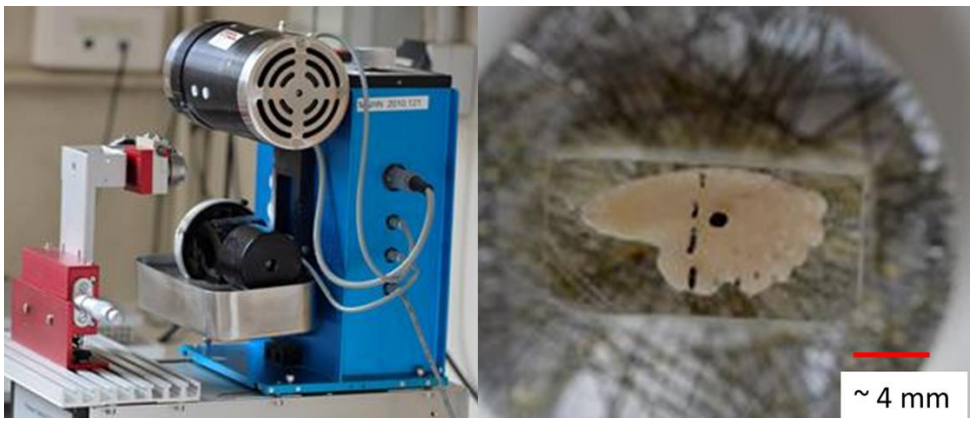

Figure 3.10: Precision saw equipped with diamond wire (left), otolith BMLM 130 attached to holders for sectioning on the precision saw (right). The nucleus and approximate sectioning line are marked in black.

Both the rostrum and post rostrum sections were polished using 500, 800 and 1200 grad SiC paper to expose the inner age increments and nucleus in the sagittal plane (Fig. 3.11).

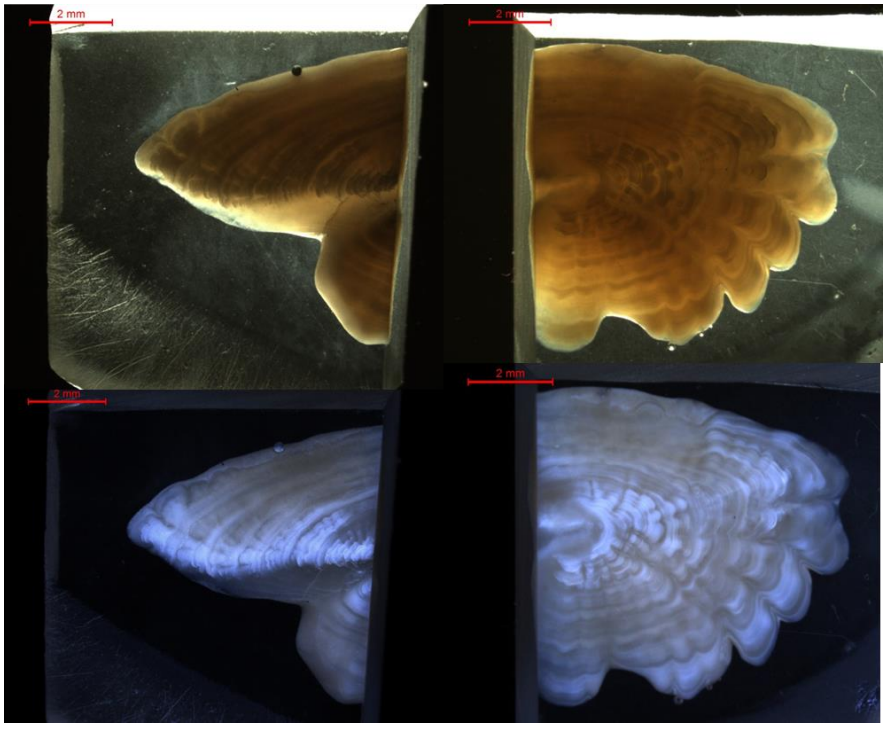

Figure 3.11: Otolith BMLM 130 after embedding in epoxy resin, sectioning and polishing to expose the nucleus. Photographs were taken using transmitted (top) and reflected light (bottom).

Otolith BMLM 167 was embedded whole in resin and ground down in the sagittal plane on the non-sulcus side until the nucleus was exposed. Only a narrow section of the otolith was exposed at the same point as the nucleus, the rest (including outer increments) remained submerged in resin (Fig. 3.12).

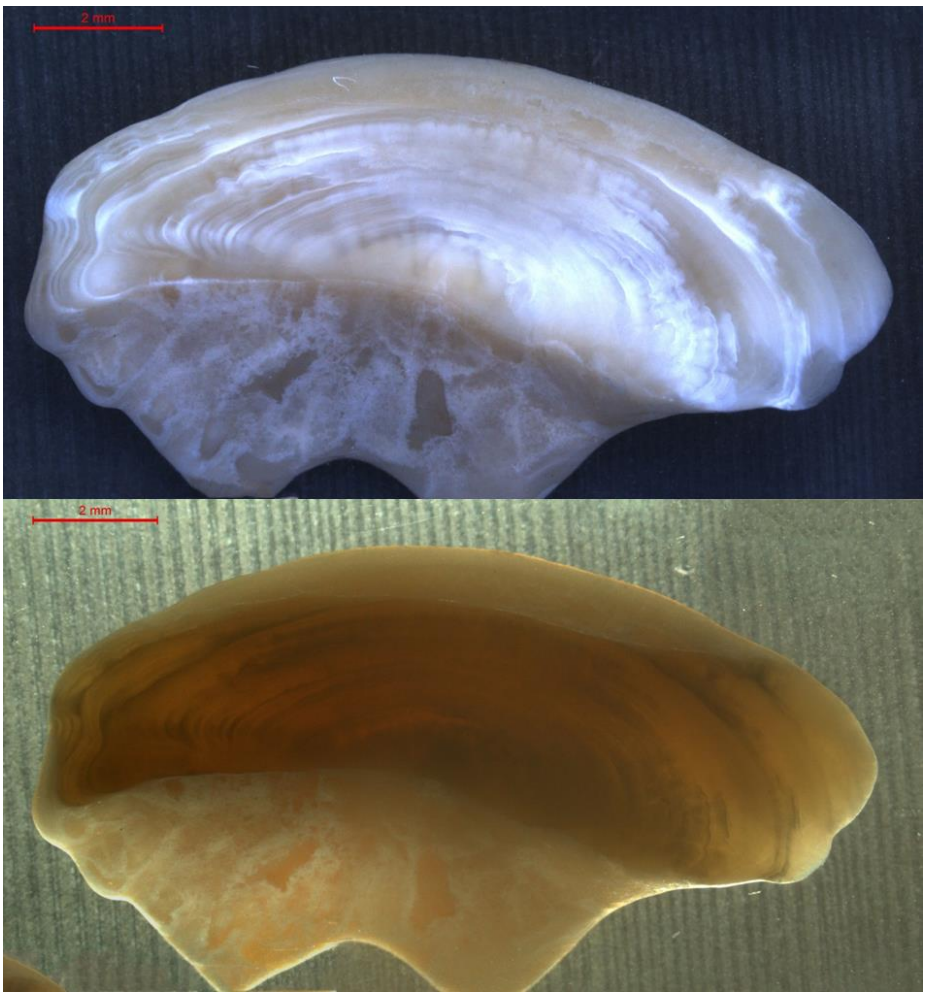

Figure 3.12: Otolith BMLM 167 after embedding in epoxy resin and polishing to expose the nucleus. Photographs were taken using transmitted (top) and reflected light (bottom).

This differential exposure is due to the curvature of the otolith. Embedding whole otoliths in resin and polishing on the sagittal plane creates a larger exposure of age increments but results in differential exposure of outer increments compared to inner as is demonstrated here with BMLM 167. This method is useful for exposing a large area of age increments in either the juvenile portion or the adult portion of the otolith but not both.

The BMLM 130 post rostrum sagittal section (Fig. 3.11) exposed a greater area of age increments but the delineation between each increment was not very clear. BMLM 167 similarly exposed a greater area of increments but left some increments covered in resin (Fig. 3.12).

A further stage of this study was to determine if the sagittal plan section (BMLM 130) was suitable for micromilling. The micromilling apparatus, shown in Figure 3.13 is the same as that used by Wurster et al., (1999). The otolith is attached

to a slide using crystal bond and then placed in the movable specimen platform positioned beneath a fixed micromilling drill bit and driven by three linear actuators.

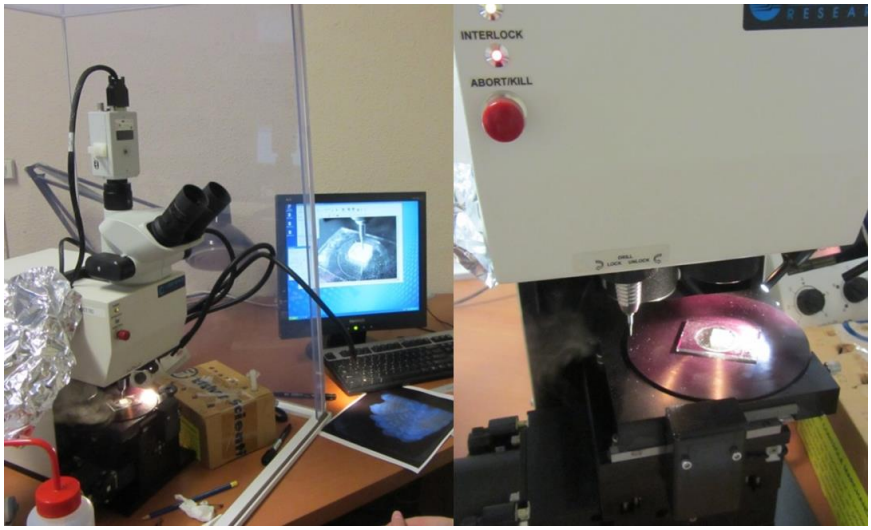

Figure 3.13: The micromilling apparatus showing the position of the otolith (BMLM 130) on the moveable stage beneath the fixed drill bit.

The main steps involved in the micromilling process are digital characterisation of the otolith surface and age increments, the calculation of intermediate sample paths and the micromilling and recovery of carbonate. These steps are outlined in greater detail in Wurster et al., (1999). Basically, a series of x-y-z coordinates were used to create a digital representation of the otolith age increments and then multiple lines are extrapolated between these. Then the stage moved the drill bit around each line to a depth of approximately 50µm into the sample (Fig. 3.14). Powdered samples were collected after each line was drilled.

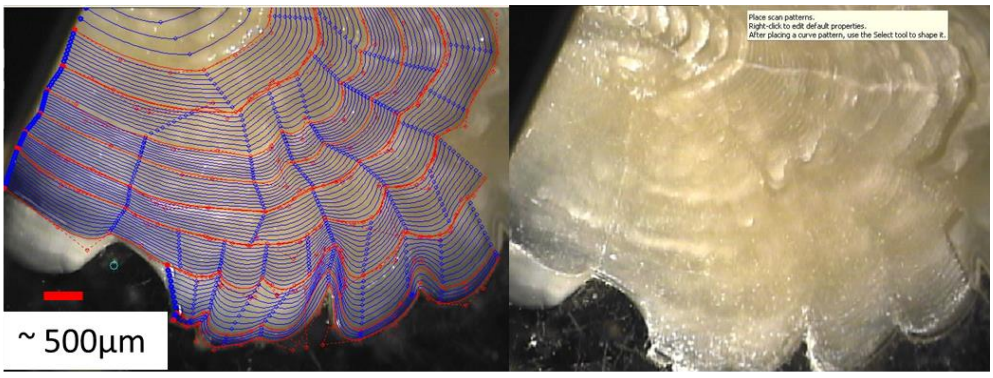

Figure 3.14: Otolith BMLM 130 surface. The main age increments are represented by the red lines, the blue lines are tracks extrapolated between these age increments (left). The image on the right is of the BMLM 130 surface after micromilling was completed.

The sagittal sectioning plane proved to be most suitable for micromilling. Within each increment, multiple powdered samples could be collected. Each was of sufficient mass for O and C isotope analyses in the Dual Inlet Mass Spectrometer (DI-MS). A total of 76 powdered samples were collected from BMLM 130.

This experimental study supported the preparation of the sagittal plane for micromilling of otoliths. However, as identified in the initial scoping study, transverse sections balance maximising the number of otoliths that can be embedded per mount, with exposing the clearest age increments and gaining the maximum number of analyses per increment. All that is needed is to create a thin enough section for age increments to be confirmed using transmitted light, whilst retaining sufficient thickness for both SHRIMP and LA-ICPMS analysis. The following section presents an experimental preparation method for creating very thin transverse otolith sections.

3.3.4 Experimental preparation methods: Downstream Menindee Lakes otoliths

The aim of this experimental preparation method was to create very thin otolith sections with age increments exposed on the same surface as the NBS-18 and NBS-19 standards. Four modern otoliths (DSM 12-15, 12-16, 12-17 and 12-18) from fish caught downstream of Menindee weir in 2015, were prepared using the following experimental technique.

The otoliths were encased in resin. A transverse centre section was cut from each otolith and ground down using 800 and then 1200 grade paper until the nucleus was almost exposed on one side. These were then embedded into a single circular resin mega mount along with the standards NBS-19 and NBS-18. The standards were embedded slightly up from the surface using double sided tape as illustrated diagrammatically in Figure 3.15.

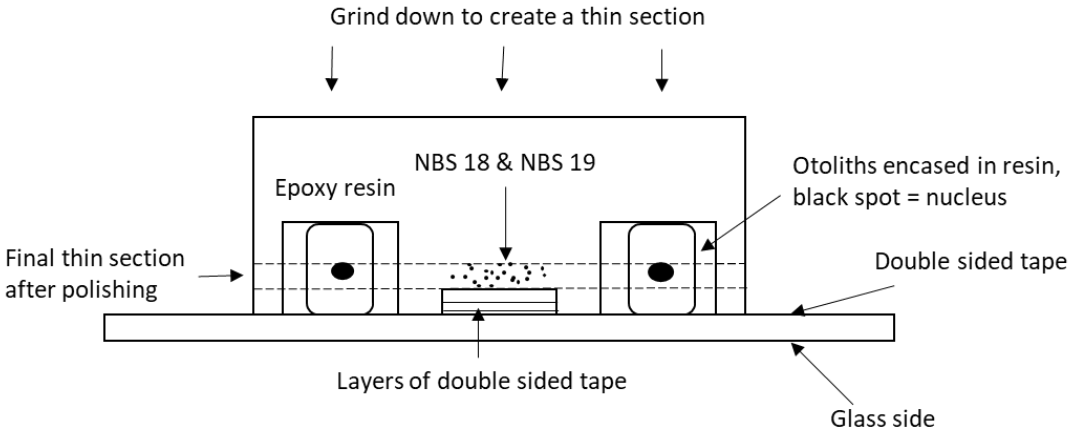

Figure 3.15: Diagrammatic representation of the preparation process for experimental thin section creation.

This mould was then handed over to one of the professional staff, John Vickers to be ground down from the back, into a 100 µm thin section with the standards and otolith age increments exposed on the surface. The thin section was then cut into a circular slide before being cleaned, dried, Al coated and mounted in the SHRIMP II.

The aim of this experimental method was to produce very thin sections with exposed age lines and standards. In this the method was successful however, the condition of the standards was poor with some falling out of the casting and others too damaged to use. None of the NBS-19 grains were fit for analysis. The NBS-18 grains survived better but were less intact than those of the initial scoping study (Fig. 3.16).

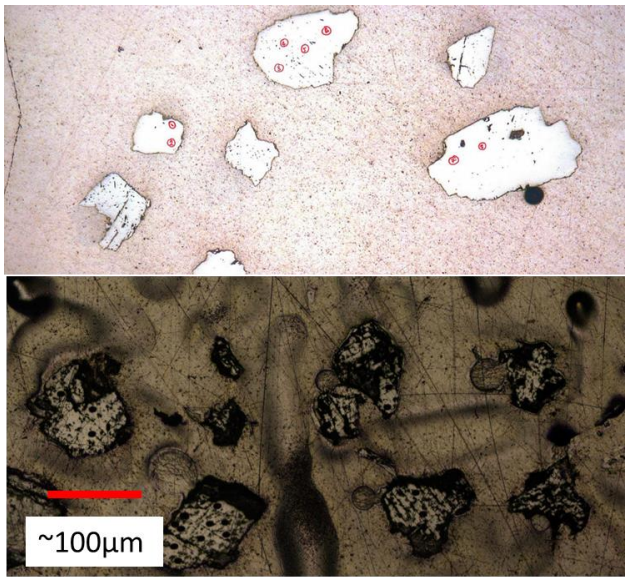

Figure 3.16: NBS 18 standard grains from the initial scoping study (top) and those of the experimental study (bottom) embedded in epoxy resin.

Age lines were faint but identifiable in all samples except DSM 12-15 (Fig. 3.17). The resulting mount was quite fragile and needed to be recast in epoxy before trace elements could be measured using the LA-ICPMS.

Figure 3.17: Reflected light image of otolith DSM-15 after thin section preparation, SHRIMP II and LA-ICPMS analysis (track visible on the right side of the otolith).

Overall, this experimental process resulted in most of the otolith being cut away and lost. Other problems included the thinness and fragility of the mount, loss of the NBS 19 standard grains and low visibility of otolith age increments.

3.3.5 Improved otolith preparation method

It was clear from these experimental preparation methods that the transverse sections used in the preliminary study are well suited for SHRIMP and LA-ICPMS analysis. The main improvement needed was thin sectioning prior to analyses. The experimental method for creating thin sections (section 3.3.4) was only moderately successful and so a second preparation technique was trialled.

Modern otoliths were embedded intact in epoxy resin. Ancient otoliths were cut transversely into three sections prior to the centre section containing the nucleus being encased in resin. The two end sections were used for radiocarbon dating. After being encased in resin multiple thin sections (500 – 700 µm thick) were cut from across the approximate location of the nucleus using a diamond edged 200 µm thick blade (Fig. 3.18). Both sides of each section were examined under a transmitted light microscope and photographed. Those sections closest to the nucleus were prepared for SHRIMP II and LA-ICPMS analysis as outlined in the analytical procedures section of this Chapter. For further details see Ickert et al. (2008) and Aubert et al. (2012).

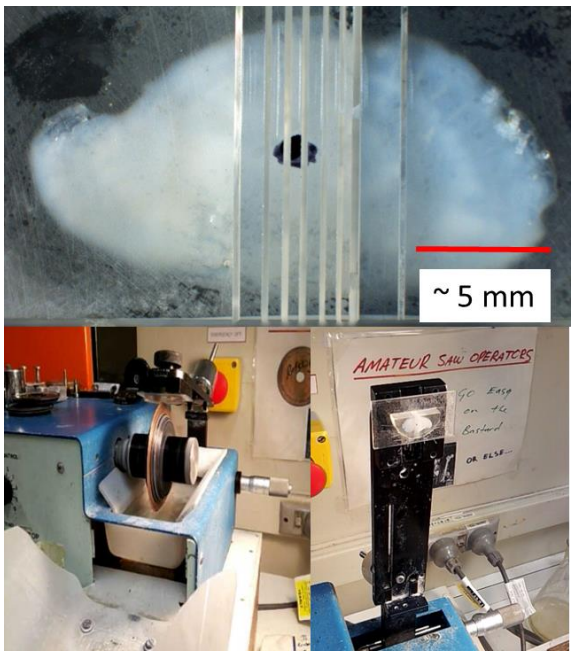

Figure 3.18: Modern golden perch otolith encased in resin (top) with multiple cuts made across the nucleus (marked in black) using a diamond edged blade (bottom). Resin encased otoliths were attached to a glass slide and then to the arm of the saw using double sided tape (bottom).

After SHRIMP II analysis the Al coating on the mounts was removed, the otoliths were photographed again and then placed in the holding unit for the LA-ICPMS along with two standards, NIST-612 and an in-house carbonate standard, a Davies Reef coral (Fig. 3.19).

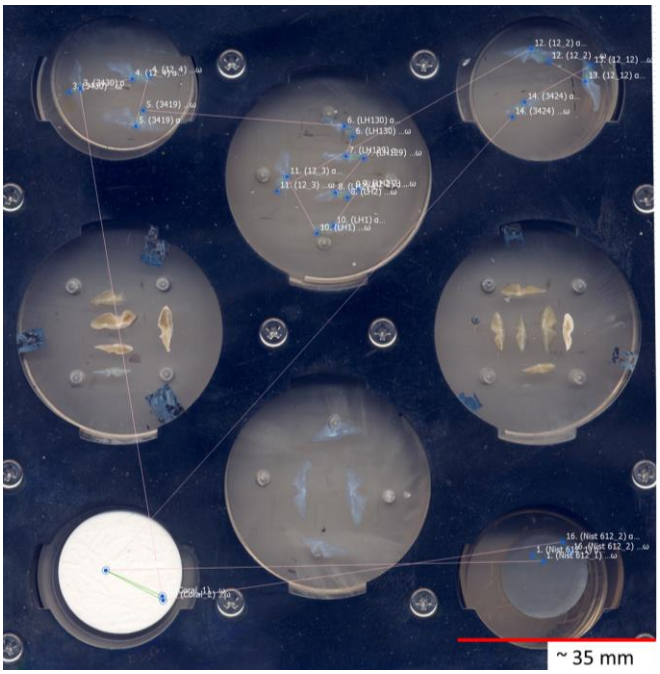

Figure 3.19: Otoliths mounted in the laser ablation sample holder with standards, NIST 612 glass (bottom right) and Davies Reef coral (bottom left). The faint pink lines show the order of laser analyses and position of the laser tracks run across each otolith.

This technique affords greater control over the thickness of otolith sections and preserves a greater proportion of the otolith for future analysis compared to the scoping study. The transverse otolith sections are smaller than sagittal sections, which means less area for analysis. However, transverse sections also exhibit clearer age increments and the small size means multiple individual otoliths can be embedded in the same mount (Fig. 3.19) and analyses in the SHRIMP can proceed more quickly.

One of the drawbacks of this method is that once the standards are embedded only a small amount of polishing can be done. This means that if the otolith sections are embedded crooked or an air bubble in the epoxy causes them to sit up from the surface (see Fig. 3.20) then they cannot be exposed on the surface of the mount by polishing without losing the standards. Another drawback is that the nucleus may accidentally be sectioned through and subsequently lost during polishing. With care and practice this can be avoided.

Figure 3.20: Ancient excavated otoliths from Lake Mungo (see Long et al., 2018) embedded in epoxy resin and photographed in reflected light. Half of one of these otoliths was lost during preparation (top) and another was lifted off the surface of the mount during the embedding by a bubble in the epoxy (second from the top).

3.4 *Analytical procedures*

3.4.1 Oxygen isotope analyses

3.4.1.1 Sensitive High Resolution Ion Microprobe (SHRIMP) II

The majority of O isotope measurements on otoliths in the present study were completed using the SHRIMP II, a high precision Secondary Ion Mass Spectrometer (SIMS) (Ireland et al., 2008). The series of SHRIMP instruments, beginning with the

SHRIMP I, were created to improve on geochemical techniques that relied on dissolving samples to determine their isotopic composition. The SHRIMP II is able to take discrete measurements of the isotopic composition across a sample, picking up small scale variations that would not be picked up by bulk analysis.

Sectioned otoliths were prepared for SHRIMP and LA-ICPMS analysis by casting in epoxy resin, with NBS-18 ($\delta^{18}O_{VPDB}$ = -23.1) and NBS-19 ($\delta^{18}O_{VPDB}$ = -2.2‰) reference calcites, to form a 35 mm diameter mount, as described in the section above. This mount was cut with 1200 grade SiC to expose the innermost growth zones, then polished with 3 and 1 µm diamond paste. After being documented by optical photomicroscopy, the samples were degreased with petroleum ether, cleaned with RBS detergent and Millipore H_2O, dried in a 60˚C vacuum oven for at least 24 hrs, coated with high purity Al and transferred to the ANU SHRIMP II for analysis using procedures based on those described in detail by Ickert et al. (2008) and Aubert et al. (2012).

In brief, a c. 15 kV beam of Cs^+ ions was focused to a c. 25 µm probe. Sputtered negative secondary ions were extracted at 10 kV and mass analysed at a resolution of c. 3000. Each analysis took c. 7 mins, consisting of 90 s preburn to stabilise the secondary ion O isotopic composition, automatic optimisation of the secondary beam trajectory, and 12 x 10 s multicollector measurements of $^{18}O/^{16}O$. Count rates of ^{16}O and internal precision for each SHRIMP session are presented in Table 3.4 and Table 3.5.

Table 3.4: Summary of SHRIMP II sessions and corrections with NBS-19 as the primary standard.

Date and otolith samples analysed	Count rates for ^{16}O (GHz)	Primary standard (NBS 19 = -2.2 ‰) standard error (‰)	Secondary standard, average (‰)	Secondary standard, standard error (‰)	Internal precision, Median (‰)	Isotopic composition for EISIE ($^{16}O/^{18}O$) was calculated separately for each session and is in the range 620-700. Baseline corrections on the low mass (LM) and high mass (HM) isotopes and gain drift corrections are outlined for each session.
N3419, 12_4, N3430	5.0	0.13	-23.3	0.14	0.15	Baseline on LM was corrected using a low order Savitzky-Golay function, baseline on the HM was corrected using a second order polynomial function. Gain drift correction: second order polynomial function
N3424, DSM 12_12, DSM 12_2	4.5	0.09	-23.36	0.16	0.15	Baseline on LM was corrected using a low order Savitzky-Golay function, the baseline on the HM was corrected using a first order polynomial function. Gain drift correction: third order polynomial function
A4/3/1, A7/8/2, B7/9/1, A7/9-10/3, A5/10/1	2.2	0.06	-23.55	0.09	0.12	Baseline on LM and HM was corrected using a second order polynomial function. Gain drift correction: second order polynomial function
B8/11/1, B8/12/4, B5/13/4, B4/14/2, B4/15/4, B4/20	2.1	0.05	-23.34	0.07	0.12	Baseline on LM was corrected using a low order Savitzky-Golay function, the baseline on the HM was corrected using a second order polynomial. Gain drift correction: second order polynomial function
12_3, LH129, LH130	2.2	0.05	-23.4	0.07	0.13	Baseline on LM was corrected using a low order Savitzky-Golay function, the HM was corrected using a second order polynomial. Gain drift correction: third order polynomial function
LH1, LH2	2.3	0.07	-23.2	0.06	0.11	Baseline on LM and HM were corrected using a low order Savitzky-Golay function. Gain drift correction: fourth order polynomial function
N3422, N3425, N3428, N3433	2.1	0.04	-23.1	0.08	0.10	Baseline on LM and HM were corrected using a low order Savitzky-Golay function. Gain drift correction: third order polynomial function

Table 3.5: Summary of SHRIMP II sessions and corrections with NBS-18 as the primary standard.

Otolith samples analysed	Count rates for ^{16}O (Ghz)	Primary standard (NBS 18 = -24.1‰), standard error (‰)	Secondary standard, average (‰)	Secondary standard, standard error (‰)	Internal precision, Median (‰)	Isotopic composition for the EISIE ($^{16}O/^{18}O$) was 590. Baseline corrections on the low mass (LM) and high mass (HM) isotopes and gain drift corrections are outlined for each session.
DSM15, DSM16, DSM17, DSM18	4.7	0.08	N/A	N/A	0.16	Baseline on LM and HM corrected using a low order Savitzky Golay function. Gain drift correction: Second order polynomial function.

Between 20 and 70 evenly spaced spots were analysed in a near linear profile across the age increments of each otolith. Profile areas were chosen based on ease of distinguishing different age increments, size of the increments and lack of cracks or other potential contaminating areas. SHRIMP II analytical spots are about 30 μm wide and 1-2 μm deep. In the early growth rings this allowed for high coverage of the age increments by multiple analytical spots but in the outer rings only one or two spots were possible (Fig. 3.21).

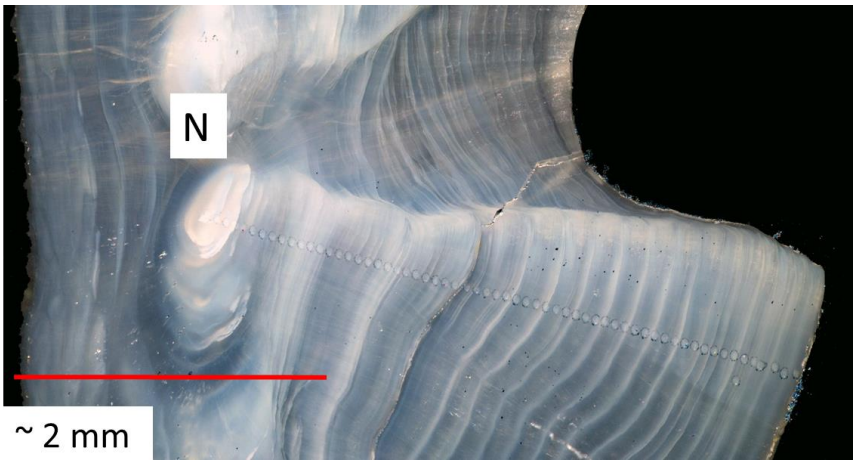

Figure 3.21: Modern golden perch otolith section after SHRIMP analysis photographed in reflected light. Each thin white line coupled with a thicker bluish translucent represents one year of growth. The tiny spots that run in a straight line from the nucleus (N) to the edge of the otoliths are the SHRIMP analytical spots.

For the Menindee otolith study that forms Chapter 6 between 49 and 53 spots were measured in a near linear profile across each otolith. For two of the Menindee otolith samples (DSM 12-18 and 12-16) a parallel profile with half the spot spacing (double density) was run over the last few age increments to improve the spatial resolution of the measurements where the increments were very thin.

Corrections for instrument drift and electron-induced secondary ion emission (EISIE: Ickert *et al.*, 2008) were made using the POXI MC program. In the POXI MC program drift in the low mass (^{16}O) and high mass (^{18}O) detector baseline count rates was corrected by fitting a function to the data. The functions used for each SHRIMP session are described in Table 3.4 and 3.5. An EISIE (Electron Induced Secondary Ion Emission) correction was applied to the data to account for the electron-induced production of low-energy ions not related to the sample. Typically, the EISIE contributes about 0.1% of the total measured ^{16}O ions. The range of EISIE corrections for the sample sessions is shown in Tables 3.4 and 3.5. A correction for

machine fractionation effects was then applied to all samples in the session. This involved fitting a simple function to the primary standard ratios. This function was then used to correct all (secondary standard and unknowns) $\delta^{18}O$ for instrumental drift (using time stamps). Sample $\delta^{18}O_{VPDB}$ values were normalized to the primary standard (NBS-19) which has a known $\delta^{18}O_{VPDB}$ values of -2.2 ‰. In the session in which Menindee otolith samples (DSM-15, 16, 17 and 18) were analysed the primary standard used was NBS-18 ($\delta^{18}O_{VPDB}$ = -23.1 ‰) due to the loss of NBS-19 grains during mount preparation (Table 3.5).

3.4.1.2 Micromilling and Dual Inlet Mass Spectrometer analysis

As a comparison to SHRIMP analysis the outer increments of three otoliths from tank raised fish were micromilled and the powder run in a Thermo MAT 253 + Kiel IV Dual Inlet Mass Spectrometer (DI-MS) under the supervision of lab manager Joe Cali.

A 200 µm drill bit running at 10,000 rpm was used to mill 50 µm into the edge of the otolith sample and along the age increments related to tank occupation. It was only possible to obtain four samples from three otoliths (N3419, N3424, N3430) because the drill bit broke after six runs.

The DI-MS produces very high precision $\delta^{18}O$ values in very small carbonate samples (preferred 40 to 180 µg). The external precision for $\delta^{18}O$ is ± 0.06‰. A minimum of 25 µg of powdered sample was required for each analysis. Most of the otolith micromilled age increment samples were too small, so some needed to be combined. The carbonate sample for N3424 represents the last year of growth, ages 8 – 9. Two samples were analysed for N3419, one combined ages 16 – 17, and the second combined ages 12 – 15. The carbonate sample for N3430 represents ages 5 – 9. The powdered samples weighed between 28 and 60 µg.

Ten standards, NBS-18, NBS-19 and ANU M2 (an in-house marble standard), weighing between 40 and 60 µg were also analysed. The raw otolith $\delta^{18}O$ values were corrected by Heather Gagan by comparing the known $\delta^{18}O$ values of the standards to mean $\delta^{18}O$ values measured during the session. The standard deviation for $\delta^{18}O$ values of the NBS19 standard was ± 0.039 ‰. A full summary of the results from the DI-MS analyses are at Appendix 9.1.

3.4.1.3 Tank water analysis

A picarro continuous flow isotope ratio mass spectrometer was used to analyse the $\delta^{18}O$ values of the four tank water samples. Analyses were run by Dr Hilary Stuart-Williams in the stable isotope laboratory at the Research School of Biology, ANU. Some evaporation may have occurred between when the water samples were collected and when they were analysed, but this unlikely to have had a major effect on the $\delta^{18}O_{H2O}$ values given that the bottles were sealed and there was no change in water height.

3.4.2 Tank Temperatures

For the tank study which forms Chapter 4, a water temperature logger recorded water temperatures in the tanks hourly from September 2009 to April 2013 with a short gap from June to August 2010. It should be noted that this temperature data logger was only in one tank and this was not the same tank from which the golden perch fish were collected. However, there should only be minimal temperature differences between tanks. Maximum and minimum temperatures were used in the fractionation equation for freshwater fish otoliths (Equation 2.10, Patterson et al., 1993) to generate a predicted range for tank occupation otolith $\delta^{18}O$. Measured otolith $\delta^{18}O_{CaCO3}$ values are expected to fluctuate within the predicted range during tank occupation.

3.4.3 Trace element analysis: Laser ablation inductively coupled plasma mass spectrometer (LA-ICPMS)

Trace elements were measured using laser ablation *in situ* microsampling coupled to a Varian 820 quadrupole ICP-MS at the Research School of Earth Science, ANU under the supervision of Les Kinsley. Otolith samples were ablated in a He atmosphere, using a 193 nm ArF excimer laser with aperture imaging optics producing an energy density at the sample surface of approximately 5 J/cm^2. This system uses a single long working distance lense to project and demagnify (by a factor of 30) the image of a laser-illuminated aperture onto a sample surface, enabling ablation of a range of sample structures with boundary dimensions of between ~5 and 400µm (Eggins et al., 1998). Samples were mounted in an ANU "Helex" 2-volume sample cell, with rapid flushing of the ablation volume, minimising smearing of fluctuations in the signal originating from compositional variations at the sampling site.

An initial spot size of ~140µm, a laser pulse rate of 10Hz with a fluence of 5 J/cm^2 was run at 200µm per second across the otolith sampling area to remove surface contaminates. Then a spot size of 50µm was run at 10µm per second from the centre to the edge of each otolith. All ablation tracks were run from the core to the edge of the otoliths and 12 elements were analysed (^{11}B, ^{24}Mg, ^{31}P, ^{43}Ca, ^{55}Mn, ^{86}Sr, ^{88}Sr, ^{89}Y, ^{137}Ba, ^{138}Ba, ^{232}Th and ^{238}U). Data reduction was conducted using an in-house MATLAB program designed by Les Kinsley. This program enabled background subtraction, calculation of element to Ca ratio and treated the data to remove anomalous intensity spikes following the protocols outlined in Longerich et al., (1996). In brief 100 seconds of gas background intensity was measured at the beginning and end of each session and 30 seconds measured before and after each ablation, these were used to calculate mean background intensity. The naturally occurring element, ^{43}Ca, was used as an internal standard. Ca concentration in the otoliths was assumed, from the stoichiometry of calcium carbonate, to be 400 000 µg g^{-1} and the concentration of other elements were estimated against the Ca concentration. The use of Ca as an internal standard is consistent with previous applications of LA-ICPMS to measure elements in otoliths (e.g. Milton and Chenery, 1998; Hamer et al., 2003; Tabouret et al., 2011).

After signal intensities were normalized to ^{43}Ca they were then drift corrected based on the standards, NIST 612 and an in house coral standard, Davies reef coral (see Alibert et al., 2003), which were measured at the beginning and end of each session. Typically, 12 to 18 otolith tracks were run per session. Elemental ratios and concentrations were calibration against the NIST-612 glass standard. All otoliths were run on the laser over two days, the analytical parameters for each session can be found at Appendix 9.2.

Laser tracks were placed as close as possible to the SHRIMP spots without obscuring them. This allowed for close comparison between the O isotope values, trace element ratios and the annual increments within which they were located. Sr/Ca and Ba/Ca ratios were plotted against distance (mm) and then against annual increments to provide the closest possible spatial link between the measurements of trace elements and $\delta^{18}O_{CaCO3}$ values.

3.5 Matching up analyses and age increments

High quality images of the otolith and analytical spots/tracks are essential for matching up analyses and age increments. All otoliths were photographed in both reflected and transmitted light using a Leica microscope at the Research School of Earth Sciences, ANU.

The thin opaque bands representing winter growth (Anderson et al., 1992) were used for otolith aging by Simon Robertson as described in section 2.4. The location of each SHRIMP spot was measured as a straight-line distance from the spot closest to the nucleus. Likewise, the location of each age increment was measured as a distance from the same nuclear SHRIMP spot. These measurements were used to graph O isotope results in comparison to their relative position within each age increment rather than just presenting results compared to distance. For LA-ICPMS measurements the total length of each track was divided by the number of individual measurements. This provided a distance per measurement which could be compared, in a similar way to those from the SHRIMP, to the distance of the age increments from the start of the laser track. This process could not be applied to the four DSM otoliths prepared using the experimental method described in section 3.3.4 because the SHRIMP spots were lost, and age increments were not visible in the final mounts. Only the double density O isotope results (DSM 12-16 and 12-18) were secure enough in relation to the age increments to be considered in Chapter 5.

4. Tank Study: The relationship between $\delta^{18}O_{CaCO3}$ values in golden perch otoliths, $\delta^{18}O_{H2O}$ values and seasonal temperature change

Chapter 2 outlined the current state of fish otolith geochemical research and highlighted the lack of validation studies for freshwater fish otoliths. This chapter, which tests the assumption that golden perch otoliths form in equilibrium with their environment, contributes to addressing this deficiency. The methods described in Chapter 3 are employed here to more closely examine seasonal patterns in oxygen isotope fluctuations and validate the use of oxygen isotopes as recorders of past environments and fish migration.

4.1 Introduction

Fish otoliths are paired calcium carbonate structures that form within the inner ears of bony fish. $\delta^{18}O_{CaCO3}$ values in otoliths from a range of modern and ancient fish species have previously been used to reconstruct changes in lake water levels (Long et al., 2014), water temperature (Wurster and Patterson, 2001; Andrus et al., 2002; Rowell et al., 2008; Wang et al., 2011) and fish migration patterns (Carpenter et al., 2003). At the world heritage site of Lake Mungo in New South Wales, Australia, golden perch otoliths from hearth sites and sediments relating to human occupation 20,000-40,000 years ago preserve a record of past water level fluctuations experienced by the fish (Long et al., 2014).

The golden perch (*Macquaria ambigua*) is an Australian freshwater fish species found mostly in lowland, slow flowing rivers. It is a long-lived species with a maximum validated age of 26 years (Stuart, 2006). Males mature at 2 years and females at 4 years. They generally spawn in floods during spring and summer when the water temperature exceeds about 23°C (Llewellyn and MacDonald, 1980; Reynolds, 1983; Koehn and O'Connor, 1990; Humphries et al., 1999). Golden perch have been observed to migrate up to 1000 km upstream, but outside the breeding season these fish occupy home ranges of about 100 m for weeks or months before relocating (O'Connor et al., 2005). The effects of ambient conditions on golden perch otolith microchemistry are not well understood. Recent studies have focused on the use of stable isotopes (^{137}Ba, ^{138}Ba, ^{87}Sr, ^{86}Sr, ^{26}Mg, ^{25}Mg, ^{24}Mg) for batch marking larval golden perch to distinguish between stocked versus non-stocked fish (Munro et al., 2008; Woodcock et al., 2011). This technique could also be used for tracking

the movements of released adult fish. Isotopic signatures in the golden perch otoliths were found to be reflective of the water composition for Sr and Ba isotopes. Otolith Mg values were only slightly different between experiments and were not reflective of the water values.

Sr/Ca ratios tend to be higher in marine waters than fresh (Campana, 1999; Secor and Rooker, 2000) whilst Ba/Ca ratios are lower (Elsdon and Gillanders, 2005a, 2005b; Tabouret et al., 2011). These differences are reflected in fish otoliths of a range of species and can be used to track fish movement between marine and freshwater residency (Elsdon and Gillanders, 2005a; McCulloch et al., 2005; Collingsworth et al., 2010). Some studies have found relationships between temperature, salinity and otolith Sr/Ca and Ba/Ca ratios (Elsdon and Gillanders, 2002; Martin et al., 2004; Miller, 2009, 2011; Collingsworth et al., 2010) but overall the largest influence is the composition of the ambient water (Chesney et al., 1998; Elsdon and Gillanders, 2003, 2005b; Wells et al., 2003; Brown and Severin, 2009; Gibson-Reinemer et al., 2009; Collingsworth et al., 2010). Ontogenic effects on otolith trace element compositions appear to be species specific. No ontogenic effects were observed by Elsdon and Gillanders (2005a) in a study of tank reared black bream, but Martin et al., (2013) observed peaks in Ba/Ca ratios in the early life stage of Atlantic salmon (*Salmo salar*) otoliths, followed by a progressive decrease and then stability in later years, an ontogenic signal that could not be explained by changes in the ambient water.

The Sr/Ca and Ba/Ca ratios of the tank waters were not measured in the present study, but as the tanks were refilled regularly from the same water source, values should have remained stable over time. Based on the strong relationship between otolith Ba/Ca and Sr/Ca and ambient water in other fish species it was expected that the golden perch otoliths would have more variable Sr/Ca and Ba/Ca ratios in the portion related to river occupation and more stable values in the portion related to tank occupation.

Golden perch age increment periodicity has been validated up to 26 years (Anderson et al., 1992b; Mallen-Cooper and Stuart, 2003; Stuart, 2006b). When golden perch otolith thin sections are viewed under transmitted light slow winter growth appears as an opaque (dark) band and faster summer growth as a translucent (light) band (Anderson et al., 1992b). Previous studies have used $\delta^{18}O$ values as a way of

confirming the relationship between the formation of opaque versus translucent bands and seasonal temperature change. Høie and Folkvord (2006) determined $\delta^{18}O_{CaCO3}$ values across the age increments of Atlantic cod raised under known temperature conditions for 4-6 years. The translucent zones in years 3 and 4 were deposited at the seasonally highest temperature in later summer and early autumn, whereas in years 5 and 6 of the older fish no significant correlation with temperature was observed. Høie and Folkvord (2006) suggested that this may have been caused by stress during gonad development or starvation during the spawning period.

Seasonal changes have also been observed in $\delta^{18}O$ values across the age increments of archaeological and modern catfish (*Ariopsis felis*) otoliths and *Mercenaria campechiensis* shells (Wang et al., 2011). The dark bands indicating growth cessation generally coincided with the most positive $\delta^{18}O$ values indicative of winter temperatures. This pattern was not observed in all otoliths for all ages, suggesting biological influences as well as temperature (Wang et al., 2011). Long et al., (2018) observed that water evaporation is recorded in golden perch otoliths as an increase in $\delta^{18}O_{CaCO3}$ values, but a direct relationship between the $\delta^{18}O_{H2O}$ values of the water, ambient temperature and golden perch otolith $\delta^{18}O_{CaCO3}$ values needs to be validated.

High resolution analyses have been successfully applied to measuring O isotopes across the age rings of Atlantic salmon (*Salmo salar*) to identify changes between freshwater and marine water occupation and to link these to macroscopic changes in otolith structure (Hanson et al., 2010). The spatial resolution and precision of two analytical techniques were compared. Secondary ion mass spectrometry (SIMS), which uses an ion microprobe to analyse discrete spots across otolith increments, obtained higher spatial and hence temporal resolution of measurements (Hanson et al., 2010) compared to a two-stage process of micromilling and O isotope analysis in a continuous flow isotope ratio mass spectrometer (CF-IRMS). However, the CF-IRMS obtained overall higher precision measurements. For the present study, a sensitive high-resolution ion microprobe (SHRIMP) was used to obtain discrete *in situ* analyses on a 25 μm scale, allowing close comparison between O isotope values and growth increments. Oxygen isotope analysis of micromilled carbonate powder

from the outer edge of some of the otoliths using a Dual Inlet Mass Spectrometer (DI-MS) was also conducted as a comparison to the SHRIMP.

The otoliths used in this study were from golden perch that were caught in the Lachlan River system and then kept in tanks for their final 5–6 years. The oxygen isotopic composition of the tank water was measured at the time of fish collection and, because it has always come from the same bore, is unlikely to have varied much over time. In this environment, the $\delta^{18}O_{CaCO3}$ values of golden perch otoliths should fluctuate with temperature, with $\delta^{18}O$ values increasing in winter and decreasing in summer. These increases and decreases should match up with the dark and light bands of the otoliths. In this study $\delta^{18}O$, Sr/Ca and Ba/Ca ratios were measured across otolith age increments relating to early life in the river system and those formed during tank occupation. Otolith tank occupation O isotope values were compared to predicated values using the Patterson et al., (1993) current aragonite temperature fractionation equation for freshwater fish (Equation 2.10).

4.2 Materials and Methods

The collection, preparation and analysis of otolith and water samples is described in detail in Chapter 3.

4.3 Results

4.3.1 SHRIMP $\delta^{18}O$ values and trace element results

The otolith $\delta^{18}O_{CaCO3}$ values start between -5 and -1‰, then increases steadily and fluctuates widely before dropping sharply as the fish enter the tanks (Fig. 4.1). The drop in $\delta^{18}O_{CaCO3}$ values is between 4.4 and 9.9‰ and occurs at 4-6 years before death. Otoliths N3424, N3425 and N3430 also display an earlier drop in $\delta^{18}O_{CaCO3}$ values. In N3424 this drop occurs at age 3, from c. 2 to -4‰. Values increase again to c. 2‰ at age 4 before the drop associated with tank entry, which occurs at age 5. The initial drop in N3430 occurs at age 3.5 years, from c. 3.4‰ to a minimum of -1.6‰, before rising steadily to 3.4‰ until the second drop at age 4. The initial drop in N3425 occurs at age 4, from c. 1.7‰ to a minimum of -4.1‰ in that year. Values increased to -1.2‰ just before the second drop occurred at age 5. Both N3424 and N3430 fish were originally sourced from Lake Cargelligo and this similar initial drop in $\delta^{18}O$ may indicate migration to waters with lower $\delta^{18}O_{H2O}$ values before returning to Lake Cargelligo.

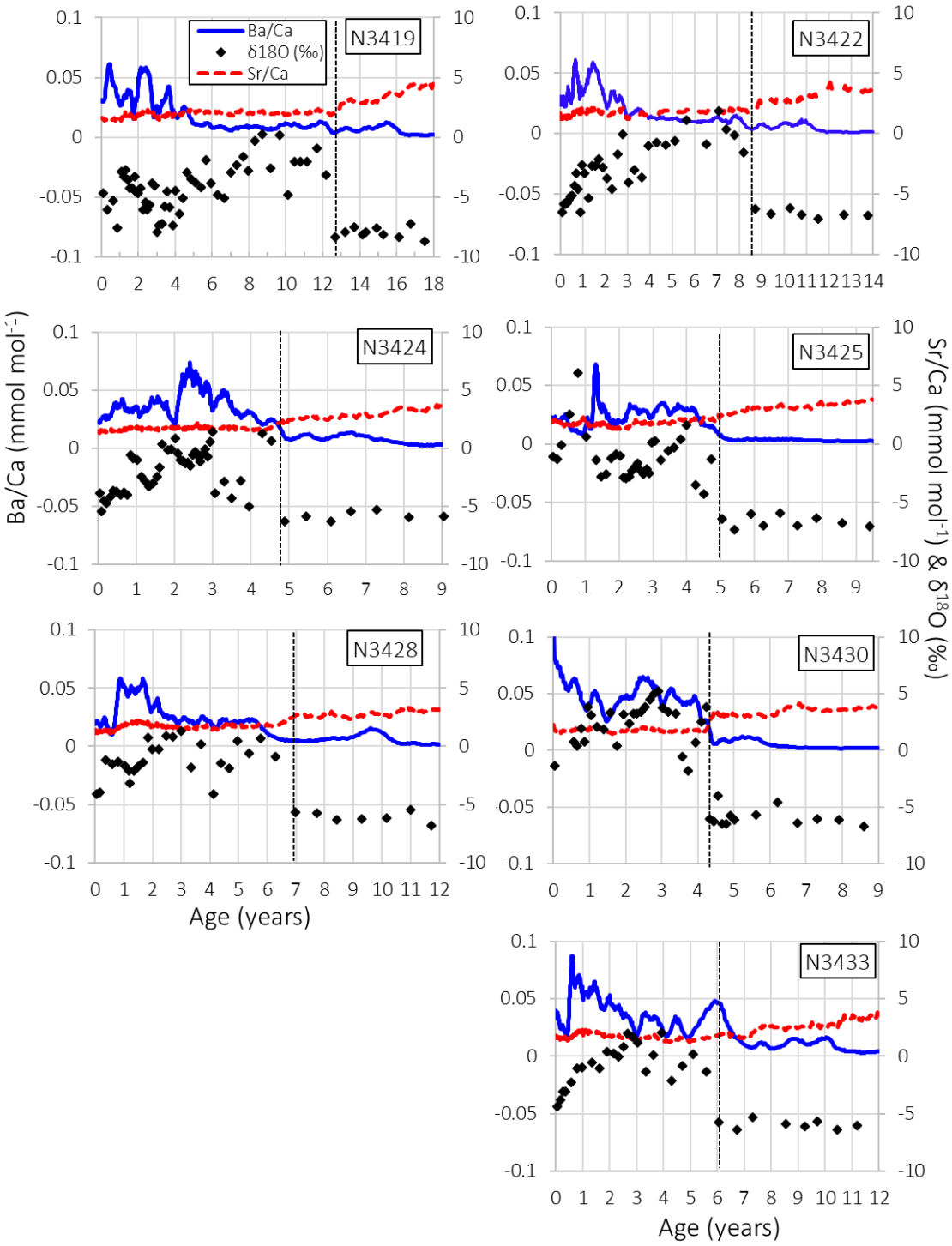

Figure 4.1: Combined $\delta^{18}O$ values, Sr/Ca and Ba/Ca ratios compared to age increments of the wild-collected tank-held golden perch otoliths. Age is from birth (left) to death (right). The black dashed vertical line indicates the approximate time of fish entry into the tanks.

The measured Ba/Ca and Sr/Ca ratios in the earliest portions of all otoliths are highly varied (Fig. 4.2). Most Ba/Ca values start at between 0.01 and 0.03 mmol.mol^{-1}, except for N3430, which starts higher, at c. 0.1 mmol.mol^{-1}. The Sr/Ca ratios start low, with minor fluctuations (1.0 – 2.5 mmol mol^{-1}). There are clear similarities between the Sr/Ca and Ba/Ca fluctuations from ages 0 to 4 in most fish. In N3433 the fluctuations in Sr/Ca and Ba/Ca ratios are almost identical up to age 6. In some otoliths a jump in Sr/Ca values by ~2 mmol mol^{-1} occurs when the fish enters the tanks (N3430, N3419) but in others there is a less sharp increasing trend (N3424, N3425). Final Sr/Ca ratios are between 3 and 4.5 mmol mol^{-1}.

Fluctuations in Sr/Ca and Ba/Ca are expected for a fish living in a natural river system where water trace element compositions vary between systems due to differences in the geological characteristics of drainage basins, weathering of different lithologies and related soils (Dalai et al., 2002; Rondeau et al., 2005) as well as changing over time due to fluctuations in biological uptake and regeneration of organic matter (Santschi, 1988) and long term climatic changes in precipitation (Shiller, 1997). In most otoliths, the Ba/Ca ratios drop between ages 4 and 5 (in N3428 this happens slightly later between ages 5 and 6). This drop in some fish coincides with tank entry (black line in Figs 4.1, 4.2), but in others it occurs regardless of the timing of tank entry. For example, in N3419 Ba/Ca ratios fluctuate from birth to age 5 and then drop and stay low until death at age 18. There is only a second slight decrease at the point at which the fish enters the tanks. The same pattern is seen in N3422, except that the original decrease occurs between ages 3 and 4 rather than at 5.

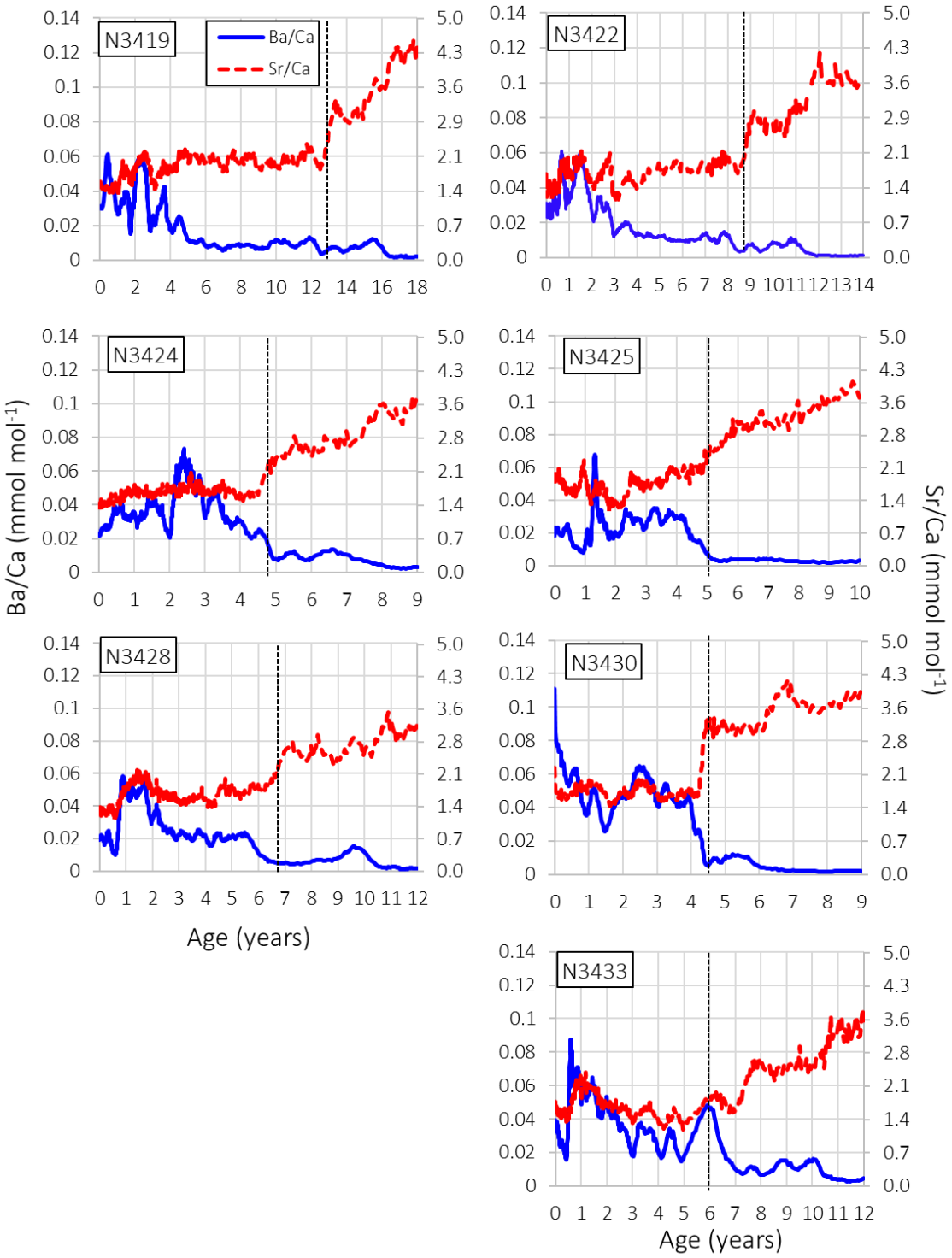

Figure 4.2: Rescaled combined Sr/Ca and Ba/Ca ratios compared to the annual age increments of the wild-collected tank-held golden perch otoliths. Age is from birth (left) to death (right). The black dashed vertical line indicates the approximate time of fish entry into the tanks.

4.3.2 Tank Temperature and water $\delta^{18}O$ values

The hourly temperature measurements have been averaged for each month. Temperatures from August 2009 to April 2013 are plotted in Figure 4.3. The

maximum temperature measured was 23.5°C and the minimum temperature was 14.8°C.

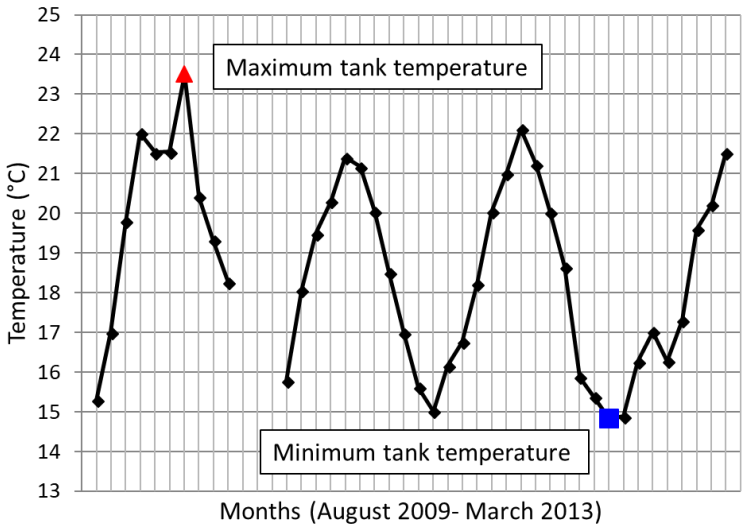

Figure 4.3: Temperature records from the Narrandera tanks. Hourly records were averaged for each month. Each increment on the x-axis represents one month from August 2009 to March 2013. The maximum and minimum tank temperatures and highlighted as a red triangle and a blue square respectively.

The tank water $\delta^{18}O$ values ranged from -5.95 to -6.45‰$_{VSMOW}$ (Table 4.1), with a standard deviation of 0.2‰ and an average water value of -6.3‰.

Table 4.1: Summary of tank water $\delta^{18}O$ values. All samples are from the same tank taken at the same time and stored in the same location.

	Tank water $\delta^{18}O_{VSMOW}$ (‰)
Sample #1	-5.95
Sample #2	-6.45
Sample #3	-6.23
Sample #4	-6.42
Average	**-6.26**

4.3.3 Predicted and measured otolith $\delta^{18}O$ values

The maximum and minimum ranges of otolith $\delta^{18}O_{CaCO3}$ values were predicted by entering the water temperature and $\delta^{18}O_{H2O}$ values into the following equation for freshwater fish otolith aragonite from Patterson et al. (1993):

$$10^3 ln\alpha_{otolith-water} = 18.56\,(10^3/T) - 33.49 \quad (4.1)$$

Where $\alpha_{\text{otolith-water}}$ is the fractionation factor between the otolith and the water

$$\alpha = \frac{\delta^{18}0_{aragonite}+1000}{\delta^{18}0_{water}+1000} \quad (4.2)$$

and T is temperature in Kelvin (K = °C + 273). To be used in this equation the value of the tank water must to be converted from VSMOW into VPDB using the following equation originally from Friedmann and O'Neil (1977) but updated based on the work of Coplen, (1996), can be used to convert $\delta^{18}O_{H2O}$ values from VSMOW to VPDB

$$\delta^{18}O_{(VPDB)} = \left(0.97001 * (\delta^{18}O_{VSMOW})\right) - 29.29 \quad (4.3)$$

The Patterson et al. (1993) equation can be re-written to include the above equations:

$$\delta^{18}O_{otolith\ (VPDB)} = \left(\frac{18560}{(T°C+273)}\right) + (0.97001 * \delta^{18}O_{water\ (VSMOW)} - 29.29) - 33.49 \quad (4.4)$$

When the tank water value (-6.3‰) and the temperature values for summer (23.5°C) and winter (14.8°C) are entered in the above equation, the expected range in otolith $\delta^{18}O_{CaCO3}$ values is -6.9 to -5.1‰. Most of the measured otolith $\delta^{18}O$ values are within this range (Fig. 4.4). A few have one or two values that fall outside this range such as N3419, N3430 and N3425. All DI-MS measurements (N3419, N3424 and N3430) fall within the expected range.

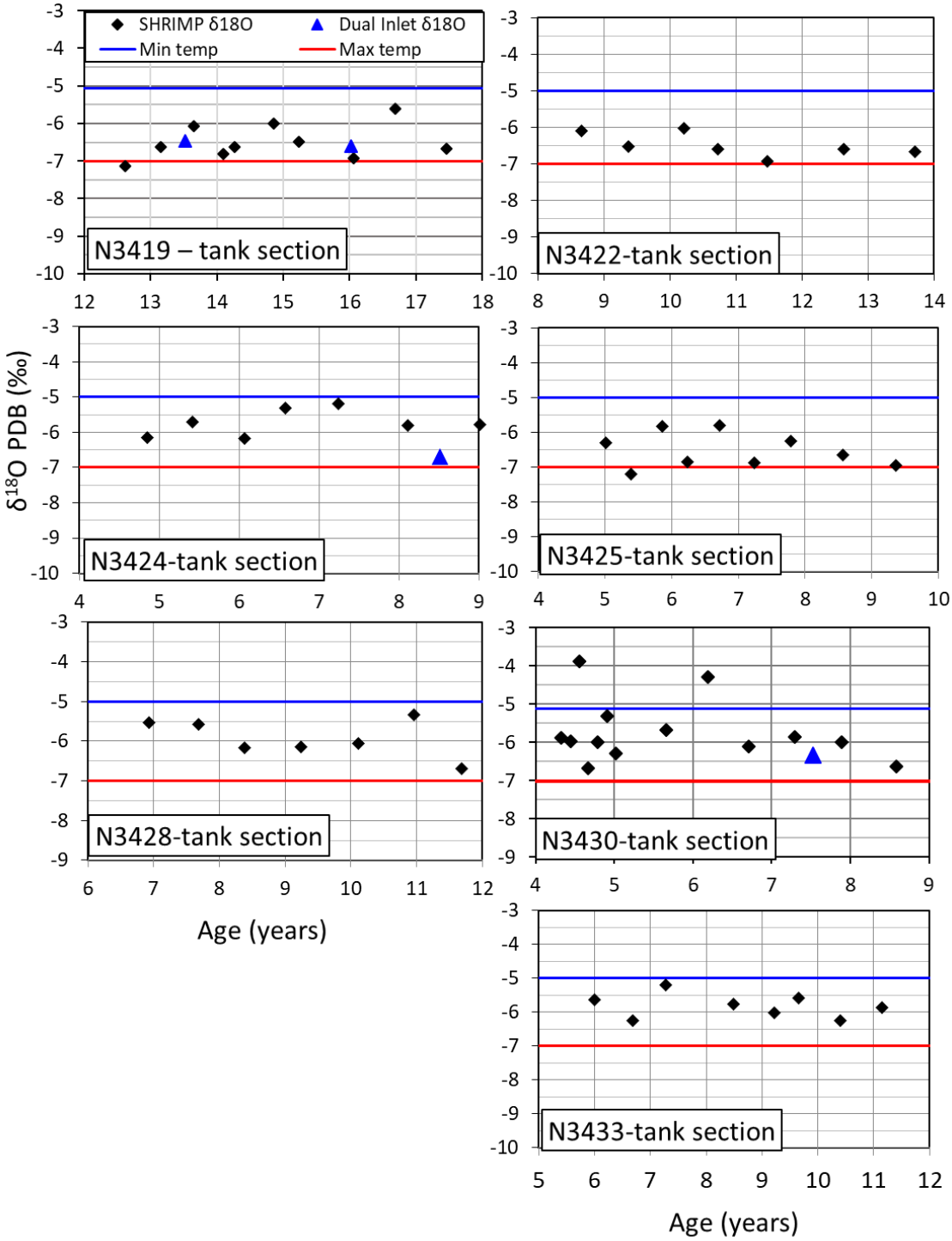

Figure 4.4: $\delta^{18}O_{CaCO3}$ values compared to the age increments formed during tank occupation of the golden perch otoliths. DI-MS $\delta^{18}O$ values are represented by blue triangles. The predicted ranges of $\delta^{18}O$ values are represented by the blue and red lines for minimum temperature and maximum temperatures respectively (maximum temperature line is always lighter, more negative than the minimum temperature line).

Seasonal fluctuations in $\delta^{18}O$ values are evident in N3425 (Fig. 4.5) with values being slightly higher in or near the thin dark increments (represented by the black vertical lines), suggesting lower temperatures, and slightly lower in the thick translucent increments (the spaces between the vertical lines), suggesting higher temperatures. This is consistent with previous observations of golden perch dark increments forming in winter (Anderson et al., 1992b). However, consistent seasonal fluctuations were not apparent in any of the other otoliths and not enough measurements within the thin dark increments have been made to conclusively link their formation to lower temperatures.

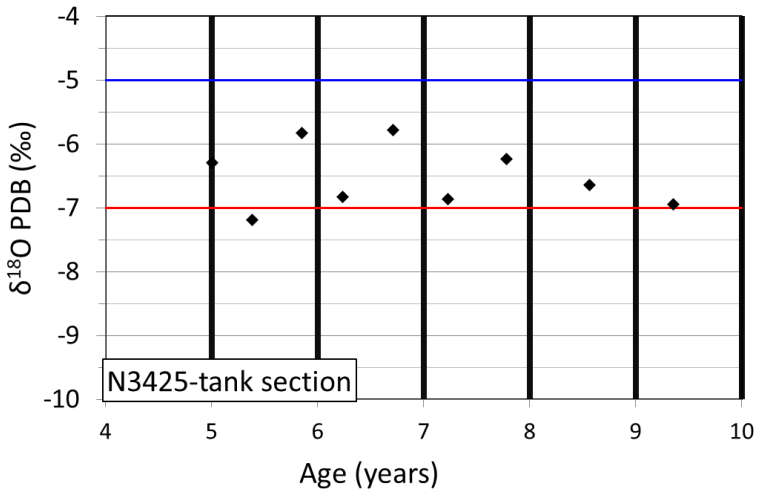

Figure 4.5: $\delta^{18}O_{CaCO3}$ values of otolith N3425 compared to age increments. The black thick vertical lines represent the opaque age increments formed during slow fish growth in winter. The predicted $\delta^{18}O$ ranges are represented by the blue and red lines for minimum temperature and maximum temperatures respectively (maximum temperature line is always lighter, more negative, than the minimum temperature line).

In Figures 4.6A – 4.6C the $\delta^{18}O_{CaCO3}$ values of the otoliths are mapped from a common time of death, allowing closer comparison of those collected from the same river. It is expected that fish caught from the same location at the same time should have similar $\delta^{18}O_{CaCO3}$ values in their otoliths. This is the case for the five fish otoliths from Brewster Weir. Even N3419, which was caught in 2008, a year later than the other Brewster Weir fish, has similar fluctuations in its $\delta^{18}O_{CaCO3}$ values (Fig. 4.6A). On the other hand, the two otoliths from Lake Cargelligo exhibit a 2 – 4‰ offset between their pre-capture $\delta^{18}O_{CaCO3}$ values (Fig. 4.6B), suggesting different life histories. The fluctuations in values are similar, but N3430 has consistently lower $\delta^{18}O_{CaCO3}$ values than N3424 during early river and/or lake occupation. As identified in the results section, N3425 also exhibits similar fluctuations to N3430 and N3424, most notably

a drop in $\delta^{18}O_{CaCO3}$ values before the drop associated with tank entry. In fact, when N3424 is compared directly to N3425 (Fig. 4.6C) their $\delta^{18}O$ values closely align (Fig. 4.6C).

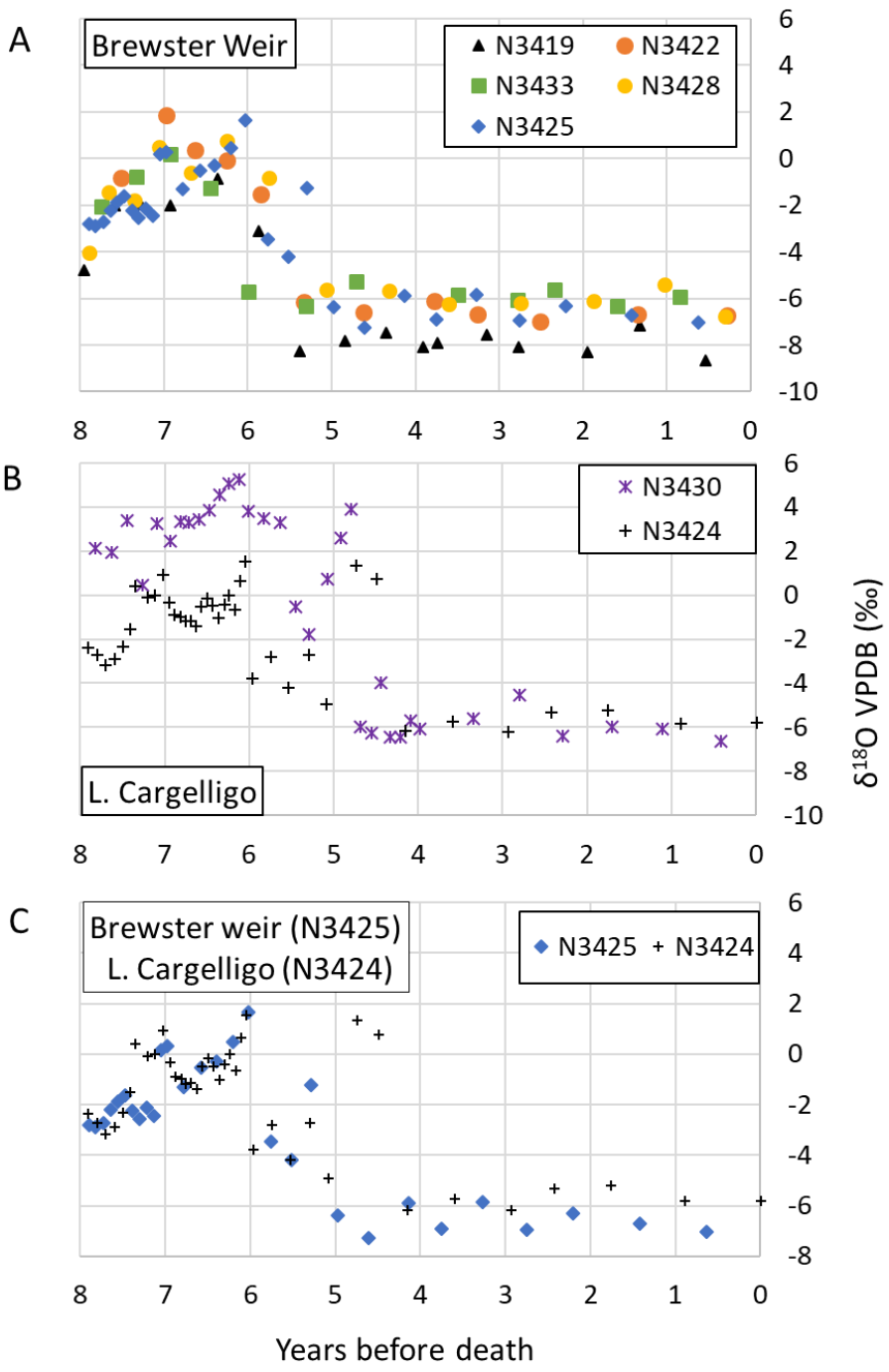

Figure 4.6: $\delta^{18}O_{CaCO3}$ values of otoliths from Brewster Weir and Lake Cargelligo compared to age increments plotted from time of death (right).

4.4 Discussion

4.4.1 Tracking fish movement using microchemistry

Previous studies have identified clear changes in the trace element and isotopic composition of otoliths with fish movement to different waters (Dufour et al., 1998; Carpenter et al., 2003; Hanson et al., 2010; Newman et al., 2011). Likewise, the present study has identified a marked change in the microchemistry of golden perch otoliths between river and tank occupation. Fish entry into the tanks is recorded as a sudden drop in the $\delta^{18}O_{CaCO3}$ values (Fig. 4.1), a slight drop in the Ba/Ca ratios and an increasing trend in the Sr/Ca ratios (Figs 4.2, 4.3). The golden perch entered the tanks at c. 4-6 years before death, recorded as a sharp change in the $\delta^{18}O_{CaCO3}$ values with tank entry, marked by a drop of between 5 and 9‰.

Tank water $\delta^{18}O_{VSMOW}$ values were relatively stable (-5.95 and -6.45‰), whilst river values are much more variable. A wide variety of environmental factors can drive temporal shifts in riverine $\delta^{18}O_{H2O}$ values, including temperature, the amount of precipitation and evaporation, contributions from groundwater and storm events (Kendall and Coplen, 2001; Andrus, 2011). Studies of the Barwon-Darling River (Meredith et al., 2009) found that water $\delta^{18}O$ values change temporally (up to 20‰ in one year) and spatially (9‰ in a 99 km stretch of river). Early fluctuations in the otolith $\delta^{18}O_{CaCO3}$ values are likely to be a result of variations in ambient water values due to flooding, evaporation and fish migration.

The differences in the oxygen isotope fluctuations between N3430 and N3424, which were both caught from Lake Cargellico (Fig. 4.6), but similarities between N3424 and N3425 suggests that N3424 was assigned to the wrong location. However, there is a major deviation between N3425 and N3424 at 5 years before death when the $\delta^{18}O_{CaCO3}$ values of N3424 increase dramatically, but N3425 drops. It is at this point that N3425 was captured from Brewster Weir and placed in the Narrandera tanks, whilst N3424 evaded capture and returned to Lake Cargelligo where it was caught almost a year later. Lake Brewster and Lake Cargelligo are within c. 50 km of each other (Fig. 3.3), so the movement of fish between the two in early life are likely. In summary, fish N3424 may have started out near Brewster weir, but ended up in Lake Cargelligo where it was captured. Fish N3430 has consistently higher $\delta^{18}O_{CaCO3}$ values in the years before entry into the tanks, suggesting it remained in Lake Cargelligo. The similarity in early fluctuations

between N3424 and N3430, but not actual $\delta^{18}O$ values, may be down to similar temperatures and flow patterns but different ambient water compositions.

There is a strong correlation between otolith Sr/Ca and Ba/Ca ratios and those of the ambient water (Bath et al., 2000; Elsdon and Gillanders, 2003; de Vries et al., 2005; Hamer et al., 2006; Walther and Thorrold, 2009; Miller, 2011; Tabouret et al., 2011; Martin et al., 2013). It was expected that the trace element values in the otoliths would fluctuate widely in the early life of the fish, reflecting movement through natural waters, which can vary greatly over time and space (Hamer et al., 2006), and that these would stabilise when the fish entered the tanks.

As expected there was variability in the early Sr/Ca and Ba/Ca ratios of the otoliths—what was not expected was the increase in Sr/Ca ratios and drop in Ba/Ca ratios (Figs 4.1, 4.2). The Sr/Ca ratios are anything but stable, instead they increase gradually, with periodic fluctuations of up to 1 mmol mol^{-1} in some otoliths (N3424, N3430, N3428; Fig. 4.2). During tank occupation Ba/Ca ratios fluctuate slightly in some otoliths (N3433, N3422; Fig. 4.2), but there is a decrease with tank entry common across all otoliths. The composition of the tank waters was not measured when the fish were obtained, but it is safe to assume that it would not change very much, given that the water filling the tanks is from the same deep source. If the observed slight fluctuations in Sr/Ca and Ba/Ca were the result of changes in the ambient water values at times when the tanks were refilled, the fluctuations should be periodic and seen in all otoliths. Similarly, if the increase in Sr/Ca ratios of the otoliths was due to evaporation, it would be expected that Sr, Ba and Ca all concentrate in the tank water, with no change in Sr/Ca or Ba/Ca ratios.

One possibility is that the stress of entering the tanks caused the fish to take up more Sr compared to Ca. Sr competes with Ca for binding sites during otolith accretion (Chowdhury and Blust, 2001, 2011). Therefore, if there was no change in the ambient Sr or Ca values then something else, perhaps physiological like stress, affected the ability of the fish to discriminate against Sr. These fish could have been stressed during tank occupation and this resulted in the increasing trend in the Sr/Ca ratios. This possibility for stress influence on Sr/Ca ratios is also considered in Long et al., (2018) for fish that died in an evaporating lake. Their otoliths all showed increasing trends in Sr/Ca ratios that could not be explained by ambient water changes. Without analysing the tank water for Sr/Ca and Ba/Ca ratios the

possibility of ambient water changes cannot be ruled out. Regardless of the reason for these changes, it is evident that they can be used to distinguish between river and tank occupation.

The changes in trace element ratios are less abrupt than $\delta^{18}O_{CaCO3}$ values, and when compared to each other without the $\delta^{18}O_{CaCO3}$ values, some otoliths show a clearer distinction between tank and river than others (Figs 4.1, 4.2). The Sr/Ca ratios in some otoliths increase sharply and distinctly at the time of tank occupation (N3430), but in others there is a steady increase rather than an abrupt change. Otolith N3425, for example, exhibits an increase in Sr/Ca from c. 2 years of age, with only a minor step on tank entry 3 years later. The same is seen in N3428, in which Sr/Ca increases steadily from the age of 4 years, and only shows a deviation after age 6, which coincides with tank entry. The Sr/Ca in otolith N3433 falls on entry to the tank, resuming its rise about a year later. This suggests that change in the ambient water composition with fish movement into the tanks is not immediately integrated into the otoliths of each fish. In some there is a sharp change, in others an incremental change, in others a delay.

The response of the Ba/Ca ratios to tank entry is varied (Figs 4.1, 4.2). In most otoliths a small drop in Ba/Ca ratio occurs at the point of tank entry (N3430, N3428) and tank occupation values are lower and more stable than in the earlier years. In some the values drop off dramatically at a point before fish entry into the tanks (around the age of maturation in N3419 and N3422) and there is only a barely observable dip when the fish entered the tanks. In N3419 there is a rise back up to pre-tank, post maturation levels before a final decrease. Ba/Ca values have been observed to reflect changes in ambient water composition (Bath et al., 2000), but the effect of biological changes, such as maturation or spawning (Martin et al., 2013), cannot be discounted. Golden perch mature at age 4 for females and age 2-3 for males (Harris and Rowland, 1996; Lintermans, 2007). In all otoliths except N3433 fluctuations in Ba/Ca decrease after the age of 4. In some, but not all, this almost coincides with tank entry.

During river occupation the Ba/Ca ratios are higher than during tank occupation, and in some cases coincide with fluctuating $\delta^{18}O$ values. In the case of N3424 (Fig. 4.1) Ba/Ca ratios peak when $\delta^{18}O$ values trough. N3430 displays the opposite effect with Ba/Ca and $\delta^{18}O$ values increasing and decreasing at similar points. Peaks in

Ba/Ca and drops in $\delta^{18}O$ values could reflect periods of incoming floodwaters, raising the Ba concentration in the water and bringing in freshwater with lower $\delta^{18}O_{H2O}$ values. In some otoliths, there are multiple drops in Ba/Ca ratios that, when viewed alone, could throw off identification of tank entry.

When Ba/Ca and Sr/Ca ratios are plotted together the change in values (drop in Ba/Ca and increase in Sr/Ca creating a kind of scissor effect) is clearer in younger fish than in older (Fig. 4.2). For example, in N3430 and N3424, the two youngest fish, the change in Sr/Ca and Ba/Ca ratios at the time of tank entry is very distinctive and could be picked up without looking at the $\delta^{18}O$ values. In the otoliths of the older fish, N3419 and N3422, there is a dramatic increase in Sr/Ca ratios with tank entry but the change in Ba/Ca is much less distinct. In both the older otoliths there is an earlier point in the fish's life when Ba/Ca ratios drop and Sr/Ca ratios increase. In the absence of $\delta^{18}O_{CaCO3}$ values this could be misinterpreted as tank entry.

There can be lags of more than 15 days between the changes in water composition and changes in the elemental composition of the otoliths (Elsdon and Gillanders, 2005b; Lowe et al., 2009; Macdonald and Crook, 2010). Miller (2011) detected changes in water composition in the otoliths of juvenile chinook salmon within 2-3 days, but it took up to 14 days for the values to stabilise.

By measuring both Sr/Ca and Ba/Ca ratios, a close approximation to the time of tank entry is possible, but only by including O isotope analyses can correct and consistent identification of the occurrence and timing of fish movement between two different water bodies be assured.

Further work is needed to determine exactly what is causing the changes in Sr/Ca and Ba/Ca ratios. It is likely to be a combination of salinity, stress and ambient water composition.

4.4.2 Sr/Ca and Ba/Ca ratios in juvenile portion of the otoliths

In almost all otoliths, the Sr/Ca and Ba/Ca ratios in the first few years of life fluctuate in harmony (Fig. 4.2). Peaks and troughs align well. The overall values and relative magnitude of the fluctuations are very different, however. Ba/Ca ratios display relatively large fluctuations between <x and 0.1 mmol mol^{-1}, where x is the detection limit, and Sr/Ca ratios fluctuate between 1.4 and 3 mmol mol^{-1}, but the timing of these fluctuations are very similar.

The co-fluctuations of Sr/Ca and Ba/Ca ratios do not always line up. There appears to be a time lag between changes in Sr/Ca and Ba/Ca. In N3425, for example, there is a clear Sr/Ca peak at age 1, but Ba/Ca doesn't peak until several months later (Fig. 4.2). This lag is in the same direction as that observed in a study by Macdonald and Crook (2010) of Ba/Ca and Sr/Ca responses to changing salinity (ambient water) in Australian bass otoliths. They found that Ba/Ca ratios responded more gradually than Sr/Ca to equivalent salinity (ambient water) changes. Not only that, they also identified a substantial time lag in elemental uptake for both Sr/Ca and Ba/Ca. Sr/Ca took ≤ 40 d and Ba/Ca ≤ 30 d for concentrations to reach equilibrium.

Previous studies have indicated that otolith Sr/Ca and Ba/Ca ratios relate closely to the ambient water composition. In general Sr/Ca ratios are higher and Ba/Ca ratios are lower in marine waters (Martin and Whitfield, 1983; Capo et al., 1998; Shaw et al., 1998; Gaillardet et al., 2003), so increases in Sr/Ca and/or decreases in Ba/Ca ratios of otoliths are used to indicate diadromous fish entry into marine waters (Milton and Chenery, 2001; Elsdon and Gillanders 2005b; McCulloch et al., 2005).

Movement between marine and fresh water is not applicable as an explanation for the changes in Ba/Ca and Sr/Ca in the otoliths of the Lachlan River golden perch, leaving three other broad possibilities:

1) The otolith Sr/Ca and Ba/Ca ratios are reflecting changes in ambient water Sr/Ca and Ba/Ca ratios, or other exogenous influences (temperature, light intensity, evaporation, flooding, food availability etc.) or,

2) The otolith Sr/Ca and Ba/Ca ratios are reflecting the condition of the fish, such as stress, age, growth rate, metabolism or other endogenous influences or,

3) Interactions between endogenous and exogenous influences are causing the Sr/Ca and Ba/Ca to fluctuate.

The fluctuations in Sr/Ca and Ba/Ca in the fish studied are closely correlated only in the subadult (or in the case of N3433 early adult) portion of the otoliths. Depending on the age of the fish, this close correlation ceases before or as the fish enter the tanks. The correlated fluctuations in N3419 cease at about the age of 4, but the fish was not captured and placed in a tank until the age of 12-13. Similarly, the co-fluctuations in N3422 seem to cease at age 4, although tank entry is at age 9 (Fig.

4.2). In both cases, however, when the co-fluctuations cease the Ba/Ca and Sr/Ca stabilise. The very similar ages at which the co-fluctuations cease (around age 4, except in N3433) indicates that they may be, at least partially, linked to the life history stage of the fish.

4.4.2.1 Stress, growth and other endogenous factors

Sturrock et al. (2015) measured the composition of seawater and the blood plasma of mature and immature plaice in a one-year experiment. They found seasonal variations in otolith elemental compositions that did not track seawater concentrations, but reflected physiological controls, most likely moderated by ambient temperature. These physiological effects were particularly evident for Sr/Ca. Otolith Sr/Ca and Ba/Ca was negatively correlated with ambient concentrations, salinity and temperature.

In a study of adult and juvenile snapper from tanks and the wild, Hamer et al. (2006) found that Ba incorporation in otoliths was positively correlated with ambient levels. It was not affected by temperature, the age of the fish or life history stage, and no seasonal cycles were evident.

More than 80% of the Sr and 95% of the Ba in otoliths originates from water sources— the remainder comes from diet (Farrell and Campana, 1996; Walther and Thorrold, 2006). A change in diet from juvenile to adulthood could contribute to the changes observed in this study but given the small percentage that diet contributes to the otoliths, it is much more likely that otolith Sr and Ba levels reflect changes in the ambient water or a factor affecting ambient water uptake.

Martin et al. (2013) observed a peak in Ba/Ca ratios in the section of Atlantic salmon (*Salmo salar*) otoliths related to early life stages, followed by a progressive decrease and then stability. This peak could not be explained by ambient water values and so was interpreted as an ontogenic signal.

Otolith elemental ratios may respond to compositional changes in the plasma and endolymph organic compounds associated with growth or stress (Walther et al., 2010). Higher somatic growth rate caused a decrease in the otolith elemental ratios and maturation state had a confounding effect. Stress promotes the production of cortisol, a glucocorticoid hormone involved in the regulation of calcium ion transport across membranes (Mommsen et al., 1999). Stress can alter the relative

proportion of proteins and carbonate laid down (Payan et al., 2004). Stress has also been cited as a possible influence on Sr/Ca ratios in salmon otoliths (Kalish, 1992), but the extent of this influence across species is still unclear.

4.4.2.2 Ambient water and other exogenous factors

Ambient temperature and salinity can affect otolith composition (e.g. Secor et al., 1995; Bath et al., 2000; Elsdon and Gillanders, 2002) and influence the effect of ambient concentrations on otolith Ba/Ca (Bath et al., 2000; Elsdon and Gillanders, 2004). Typically, the effects of temperature and salinity on otolith Ba/Ca are minimal compared to the effects of ambient Ba/Ca (Bath et al., 2000; Elsdon and Gillanders, 2003; de Vries et al., 2005; Hamer et al., 2006; Walther and Thorrold, 2009; Miller, 2011; Tabouret et al., 2011; Martin et al., 2013). In a study of wild black bream from fresh and salt water locations, Elsdon and Gillanders (2005b) identified higher Ba/Ca ratios in the otoliths from the freshwater fish. The magnitude of differences in the otolith compositions between these locations differed between winter and summer seasons. This was interpreted as reflecting higher freshwater inflow in winter than in summer. In contrast, peaks and troughs in Ba/Ca transects in Elsdon and Gillanders' (2005b) study commonly showed no relationship to annuli, suggesting no seasonal change in ambient Ba/Ca within locations over time.

Macdonald and Crook (2010) conducted a study of Ba/Ca and Sr/Ca ratios in Australian bass (*Macquaria novemaculeata*) across a salinity gradient. They found a decreasing non-linear relationship between otolith and water Ba/Ca as salinity increased. In contrast, Martin and Wuenschel (2006) found that, over a range of salinities from 5 to 45 ppt, there was no observable relationship between otolith Ba/Ca and salinity, despite a negative exponential trend in water Ba/Ca with increasing salinity. Other studies have found that Ba incorporation varies inversely with water Ba/Ca (e.g. Miller, 2011).

Transects of Ba/Ca and Sr/Ca ratios across the otoliths of three Australian Bass showed marked cycling in Ba/Ca in the outer otolith growth region, variable patterns in Sr/Ca and no consistent positive or negative relationships between the two (Macdonald and Crook, 2010). Indeed, there appeared to be an inverse relationship between Sr/Ca and Ba/Ca ratios near the otolith core, but a positive correlation in other sections. Macdonald and Crook (2010: 158) concluded that "without intimate knowledge of the salinity, temperature and ambient elemental

concentration gradients in the Albert River over the lifetime of these bass, answering questions raised by this variability is not possible." They also urged caution in extending relationships between elemental concentrations and otolith concentrations in juvenile fish to adult without first assessing any age-related effects.

To untangle these early life effects and determine the cause of the common fluctuations in Ba/Ca and Sr/Ca, it would be necessary to know more about the ambient Sr/Ca and Ba/Ca within the river system. This would make it possible to determine whether the fish was moving between locations of different Sr/Ca and Ba/Ca ratios, or there is some other ambient or internal influence causing the similar fluctuations. If the Sr/Ca and Ba/Ca ratios of the ambient water change in concert then other effects can be ruled out, if not, then something else is causing these similar patterns.

4.4.2.3 Interactive effects

Interactive effects between exogenous and endogenous factors are rarely studied exclusively or comprehensively. Walther et al. (2010) conducted experiments manipulating temperature and diet for juvenile, sub adult and adult tropical damselfish (*Acanthochomis polyacanthus*) from the south-west Pacific Ocean. They identified significant interactive effects between life history stage, temperature and quantity of food for otolith Ba/Ca ratios. For Sr/Ca ratios life history stage and food effects interacted. This shows that the controls of Sr/Ca and Ba/Ca ratios in otoliths are complex and are the result of both exogenous and endogenous factors.

Elsdon and Gillanders (2004), in a comprehensive study of black bream (*Acapanthagos butcheri*) raised in tanks under different conditions, detected interactions between temperature and ambient elemental concentration such that at low temperature there was a reduced effect of ambient elemental Sr on otolith composition compared to higher temperatures. The same effects of concentration and temperature on Ba/Ca were also observed.

4.4.3 Seasonal Fluctuations: Actual vs predicted otolith isotopic values

Otolith $\delta^{18}O_{CaCO3}$ values during tank occupation was found to fluctuate within a 2‰ range, consistent with the seasonal change in tank water temperature. All $\delta^{18}O$ values fall within or near the predicted ranges. There was an 8.7°C difference

between tank water maximum (23.5°C) and minimum (14.8°C) temperatures during fish occupation (Fig. 4.3). The average tank water $\delta^{18}O_{VSMOW}$ was -6.26‰. When these values are entered into the temperature fractionation equation for freshwater fish (Patterson et al., 1993), the predicted $\delta^{18}O_{VPDB}$ values of the otoliths ranges from -6.9 and -5.1‰ (Fig. 4.4)

All DI-MS and most of the SHRIMP otolith $\delta^{18}O_{VPDB}$ values fall within the predicted range. This indicates that golden perch otoliths form with minimal vital effects at or near isotopic equilibrium with the surrounding water, as has been found in previous studies of different fish species (Patterson et al., 1993; Weidman and Millner, 2000; Høie, 2004; Sako et al., 2007; Matta et al., 2013). A small number of the SHRIMP $\delta^{18}O_{VPDB}$ values fall outside the predicted range. Slight deviations in the SHRIMP $\delta^{18}O_{VPDB}$ values could be picking up the time each fish spent in the spawning ponds fed by fresher river water, which would have had lower $\delta^{18}O_{VSMOW}$ values. However, Otolith N3430 has two SHRIMP measurements one within age 4 and one in 6 that are 1.3‰ and 0.6‰ higher than predicted (c. -3.8 and-4.5‰ respectively). This indicates slightly lower temperatures or heavier tank water $\delta^{18}O_{SMOW}$. Given the increased density of otolith age increments in these later years, the effects of a particularly cold winter might be recorded in this otolith but not others.

4.4.4 Seasonal fluctuations: relationship between $\delta^{18}O$ values and age increments

4.4.4.1 Oxygen isotopes

Otolith $\delta^{18}O_{VPDB}$ values fluctuated by 1–2‰ during the time that the fish were in the tanks. In otoliths N3424 and N3425 higher $\delta^{18}O_{VPDB}$ values are associated with the thinner dark growth increments, indicating lower temperatures (Figs 4.4, 4.5). This is consistent with previous interpretations that dark increments in otoliths relate to slower growth during winter (Anderson et al., 1992b; Mallen-Cooper and Stuart, 2003; Stuart, 2006). Otolith N3425 shows a regular 1.5‰ change in $\delta^{18}O_{VPDB}$ values within each age increment (Fig. 4.5). These fluctuations are closer to the warmest predicted value, suggesting higher temperatures in both winter and summer than recorded, or lower water values than those used in the prediction equation. It is possible that the dark rings are the result of a lack of growth over winter, as is the case with freshwater drum (*Aplodinotus grunniens*), whose otoliths stop growing at 10°C (C. Wurster and Patterson, 2001) and then start growing again in spring. This

would also partially explain why the micromilled $\delta^{18}O_{VPDB}$ values are consistently lower. Micromilling averages the growth year and since the translucent bands relating to summer growth are thicker they make up a higher proportion of the samples leading to an overall lower $\delta^{18}O_{VPDB}$ values. No other otoliths show regular changes in the $\delta^{18}O_{VPDB}$ values during tank occupation that could be related to seasonal increment formation. Further high-resolution work is needed to confirm the link between $\delta^{18}O_{VPDB}$ values and seasonal increment formation in golden perch otoliths.

4.4.4.2 Trace elements

The relationship between Sr/Ca and Ba/Ca ratios and temperature is unclear. As covered in Chapter 2, most studies focus on Sr/Ca ratios and in those that identify a temperature effect the direction of this differs—some found a negative relationship (Radtke, 1989; Townsend et al., 1992; Secor et al., 1995; Sturrock et al., 2015), some find a positive or insignificant relationship (Kalish, 1989; Fowler et al., 1995; Tzeng, 1996; Chesney et al., 1998; Dorval et al., 2007) and still others suggest interactive effects between salinity, temperature, ambient composition and fish biological state (Elsdon and Gillanders, 2004, 2005a, 2005b). The fluctuations reported in the present study are similarly indistinct. There are regular fluctuations observed in Sr/Ca and Ba/Ca ratios in the early life of most fish (Fig. 4.1, 4.2), related to river occupation and lower values/troughs tend to match up with the thin dark increments related to winter growth (N3433, N3419, N3424, N3422). There are exceptions, however, where increases in trace elemental ratios also occur in some winter growth periods (N3419 at age 2, N3433 at age 6). The degree of change in the ratios within a year is also quite variable. Possible reasons for these yearly fluctuations could be periodic movement of fish to Ba and Sr rich waters, seasonal temperature change, and/or increased food consumption in summer leading to higher ratios. These are all discussed above in section 4.4.3. In the tank portion of the otoliths, when the fish were living in bore water, the Ba/Ca ratios are quite low and stable. N3433 does show some mound like fluctuations but the relationship between these and temperature/age increments is unclear. Peaks and troughs are less pronounced suggesting this is unlikely to be just a temperature effect, a combination of periodic behaviour and circumstances experienced by the fish.

Possible seasonal fluctuations between Ba/Ca, Sr/Ca and O isotopes warrants further investigation.

4.5 Conclusions

This study supports the use of O isotopes, Sr/Ca and Ba/Ca rations for identifying broad changes in fish lives such as migration from one water body to another. The $\delta^{18}O_{CaCO3}$ values of golden perch are closely related to changes in the ambient environment, picking up fish movement into tanks as a sharp drop in $\delta^{18}O$ values. Similarly, Sr/Ca and Ba/Ca ratios also track fish movement but do not display as clearly marked a change in all cases as the $\delta^{18}O_{CaCO3}$ values . Once the fish are living in the tanks the fluctuations in their $\delta^{18}O_{CaCO3}$ values are solely due to temperature change. Sr/Ca and Ba/Ca ratios show some fluctuations during tank occupation, but these do not seem to be seasonal. First and foremost, Sr/Ca and Ba/Ca ratios reflect the ambient water composition (Fowler et al., 1995; Milton and Chenery, 2001; Collingsworth et al., 2010; Elsdon and Gillanders 2004; 2005a; 2005b) and the lack of substantial change in Ba/Ca ratios suggests that the ambient values are stable. The continual increase in Sr/Ca ratios could be related to stress of fish living in the tanks as has been observed in fish living in an evaporating lake (Long et al., 2018).

Most $\delta^{18}O_{CaCO3}$ values for the otolith increments formed during tank occupation fall within the predicted range. This suggests that golden perch otoliths form in O isotopic equilibrium with the surrounding water consistent with previous studies of other fish species (Patterson et al., 1993; Høie, 2004; Sako et al., 2007; Matta et al., 2013).

There were few otoliths that showed consistent seasonal fluctuations in the $\delta^{18}O_{CaCO3}$ values or trace element ratios that could be matched to dark or light band formation. There were some regular fluctuations in the $\delta^{18}O_{CaCO3}$ values of N3425 during tank occupation which were consistent with expectations; slightly higher $\delta^{18}O_{CaCO3}$ values in or close to the opaque dark thin bands, suggesting lower temperatures, and slightly lower $\delta^{18}O_{CaCO3}$ values during the translucent summer portion. Further work is needed to confirm the use of $\delta^{18}O_{CaCO3}$ values for identifying seasonal temperature fluctuations and their influence on annual increment formation.

The co-fluctuations in Sr/Ca and Ba/Ca ratios in the early years of fish life warrant further investigations. These values could be reflecting changes in the ambient water values but given that co-fluctuations only occur in the early life of the fish (before age 4-6) they must at least partially be related to fish ontogeny. Whether this is a result of an internal biological change irrespective of external conditions or one that is due to ambient environment change affecting the uptake or deposition of trace elements remains unclear.

5. Menindee otoliths: oxygen isotope and trace element records across the otoliths of wild caught golden perch

The studies of modern otoliths described in Chapter 4 and part of Long et al., (2018) examined the relationships between O isotope compositions of otoliths and known ambient conditions. In Chapter 4 it was demonstrated that golden perch otoliths form in isotopic equilibrium with the ambient water and that the expected range of golden perch otolith $\delta^{18}O_{CaCO3}$ values can be predicted using the Patterson et al., (1993) O isotope fractionation equation, when the temperature and $\delta^{18}O_{H2O}$ values of the ambient water are known. The Long et al., (2018) study demonstrated that known evaporative trends and flood events in a lake system were recorded in the $\delta^{18}O_{CaCO3}$ values of golden perch otoliths. This Chapter further investigates the relationship between otolith $\delta^{18}O_{CaCO3}$ values and ambient environmental conditions. Here the $\delta^{18}O_{CaCO3}$ values of golden perch otoliths fished from the Barwon-Darling River system are compared to commensurate records of water $\delta^{18}O$ values, temperature and known flooding and drying events.

5.1 Introduction

Golden perch otoliths have been shown to form in or near to O isotopic equilibrium with the surrounding water (Chapter 4) and can therefore be used as recorders of broad changes in ambient water $\delta^{18}O$ values resulting from fish migration or local evaporation, rainfall or flooding events. This study examines the extent to which otolith $\delta^{18}O_{CaCO3}$ values can be used to compare and understand the life histories of individual fish caught at the same place at the same time.

This study also investigates the relationship between the $\delta^{18}O_{CaCO3}$ values of the final layer of otolith growth and the ambient conditions (temperature and $\delta^{18}O_{H2O}$ values) of the river water where the fish were caught. As in Chapter 4, the Patterson et al., (1993) palaeotemperature fractionation equation for freshwater fish is used here to predict the $\delta^{18}O_{CaCO3}$ values of the outer otolith age increments based on the known water $\delta^{18}O$ values and expected maximum and minimum temperatures.

As part of the study Sr/Ca and Ba/Ca ratios were also measured across the otoliths of wild caught golden perch otoliths to determine if these record similar fluctuations to the $\delta^{18}O_{CaCO3}$ with flooding and evaporation events, and whether similar fluctuations to those identified in Chapter 4 and Long et al., (2018) were present.

Trace element ratios in otoliths, (Sr/Ca and Ba/Ca), have also been shown to be closely related to ambient Sr/Ca and Ba/Ca ratios in fresh, marine and brackish waters (Fowler et al., 1995; Milton and Chenery, 2001; McCulloch et al., 2005; Hamer et al., 2006; Collingsworth et al., 2010). Some studies have found relationships between otolith trace elements and temperature (Radtke, 1989; Townsend et al., 1992; Secor et al., 1995; Elsdon and Gillanders, 2003) and/or salinity (Zimmerman, 2005; Diouf et al., 2006; Sturrock et al., 2015). As explained in Chapter 2, the relationship with salinity seems mainly to be a result of the ambient water Sr/Ca and Ba/Ca ratios also changing with salinity. Relationships with temperature are inconsistent with some studies showing positive relationships (Kalish, 1989; Bath et al., 2000; Elsdon and Gillanders, 2002; Collingsworth et al., 2010) others showing negative relationships (Radtke, 1989; Townsend et al., 1992) or no relationship (Kalish, 1991; Chesney et al., 1998; Arai, 2010).

Ba/Ca ratios in golden perch otoliths have been shown to be relatively high in the subadult portion of the otolith and lower in the adult portions, suggesting an ontogenetic relationship (Chapter 4). Co-fluctuations in Ba/Ca and Sr/Ca ratios have been found in the portion of otoliths related to occupation of rivers and lakes in subadult life, but not in the portion of the otolith related to adult-hood and occupation of tanks with controlled, stable water compositions (Chapter 4).

5.2 Study Location

The Menindee lakes are a chain of shallow ephemeral freshwater lakes connected to the Barwon-Darling River system in western NSW (Fig. 3.5). The Barwon-Darling River system experiences high flow periods following rainfall at the headwaters. One discharge event occurred at Bourke in 2001 (Murray Darling Basin Authority, 2018) and five flow events occurred during the drought dominated period 2002-2005. Hughes et al., (2012) report the timing and approximate volume of these flow events at Bourke to be as follows: Mar-Apr 2003 (~ 1.3 x 10^8 m^3); Jan-Feb 2004 (~ 3.85 x 10^8 m^3); Mar-Apr 2004 (~ 2 x 10^8 m^3); Dec 2004-Jan 2005 (~ 4.8 x 10^8 m^3); Jul-Aug 2005 (~ 2.2 x 10^8 m^3). During this period flows at Wilcannia measured only 16 % of the average flow and only 25% of the flow at Wilcannia made it to beyond the Menindee lakes to eventually discharge into the Murray river (Hughes et al., 2012). High water $\delta^{18}O_{VSMOW}$ values were recorded throughout the system. Two of the most enriched locations were Lake Copi Hollow (+16.19 ‰), a small lake

situated between Lake Pamamaroo and Lake Menindee, during the 2003-2004 drought and Burtundy in February 2004 (+16.22 ‰) (Hughes et al., 2012). The reasons for the elevated $\delta^{18}O_{VSMOW}$ values at Burtundy was that the first flood event in Mar-Apr 2003 did not reach beyond the Menindee Lakes, only the flood event of Jan-Feb 2004 managed to pass through the lakes system and reach the Murray River. Meredith et al., (2009) took monthly measurements of the water composition (trace elements and $\delta^{18}O$ values) of the Barwon-Darling river between Bourke and Wilcannia from 2002 – 2007. During low flow systematic increases were observed in water Cl^- Na^+, Mg^{2+}, SO_4^{2-} and $\delta^{18}O_{VSMOW}$ values. Discharge events introduced water with lower $\delta^{18}O$ values to the system.

The golden perch whose otoliths were analysed as part of the present study would have been living in the Barwon-Darling river system during the same period that the above water $\delta^{18}O_{VSMOW}$ values were recorded. It is expected that the $\delta^{18}O_{CaCO3}$ values of their otoliths should reflect the drought and discharge conditions reported in the aforementioned studies, with increasing trends evident of drying waters and sudden drops evidence of flood events.

5.3 Materials and Methods

The collection, preparation and analysis of otoliths is described in detail in Chapter 3. The SHRIMP II was used for high resolution in situ measurement of $\delta^{18}O$ across the age increments of the otoliths. Trace elements were measured using laser ablation in situ microsampling and a Varian quadrupole ICPMS. These methods are described in detail in Chapter 3.

5.4 Results and Discussion

5.4.1 Predicting final otolith $\delta^{18}O$ value range

The relationship between the $\delta^{18}O$ values of ambient water and that of precipitated aragonite is a function of temperature (Kim et al., 2007). In most species of fish this relationship between temperature, water and the O isotopic composition of aragonitic otoliths is similar to that of inorganic aragonite (Patterson et al., 1993; Thorrold et al., 1997; Kim et al., 2007). Here, the $\delta^{18}O_{VPDB}$ values at the edge of each otolith is expected to be similar between individuals, as they were occupying the same water body at the time of collection. Firstly, the recorded water $\delta^{18}O$ values for the Menindee Main Weir in January 2006 (3.86 ‰; Table 3.3) and estimated water

temperature based on the measured values for January 2004 (28 °C; Table 3.3) were entered into the Patterson et al., (1993) fractionation equation to predict the expected $\delta^{18}O$ of the DSM otoliths. Maximum and minimum water temperatures estimated from air temperature records were also entered in to the equation to predict the seasonal range of otolith $\delta^{18}O$ values expected if the water $\delta^{18}O$ value is temporally stable. The resulting predicted otolith $\delta^{18}O$ values are summarised in Table 5.1.

Table 5.1: Summary of the otolith $\delta^{18}O_{VPDB}$ values predicted by entering measured and estimated water temperature and known water $\delta^{18}O_{VSMOW}$ values into the Patterson et al. (1993) temperature fractionation equation.

Water sample collection date	**Water $\delta^{18}O_{VSMOW}$ values**	**Predicted otolith $\delta^{18}O_{VPDB}$ values**		
		Jan 2004 water temp. (28°C)	**Min water temp. (15.7°C)**	**Max water temp. (34°C)**
1/01/2003	9.91	7.79	10.42	6.59
11/08/2003	2.91	1.00	3.63	-0.20
25/01/2004	8.06	6.00	8.62	4.79
7/01/2006	3.86	1.92	4.55	0.72
16/01/2007	7.64	5.59	8.22	4.38
10/05/2007	9.31	7.21	9.84	6.00

The result of this calculation compared to actual measurements of each otolith's edge $\delta^{18}O$ values is shown in Figure 5.1 as a dashed line. If the water $\delta^{18}O$ value was temporally stable this is the otolith $\delta^{18}O$ values that would result, given a water temperature of ~ 28 °C. The otolith $\delta^{18}O$ value range predicted for maximum (34 °C) and minimum (15.7 °C) water temperatures are shown respectively as solid blue and red horizontal lines (Fig. 5.1). This range also assumes that the water $\delta^{18}O$ value is temporally stable and only temperature change is affecting the otolith $\delta^{18}O$ values.

As can be seen in Figure 5.1, none of the otolith edge $\delta^{18}O$ values are equal to the predicted otolith $\delta^{18}O$ values when a water temperature of 28°C and $\delta^{18}O$ value of 3.86‰ are used. Some otoliths (e.g. DSM 12-12) have edge $\delta^{18}O$ values within 1 or 2‰ of those predicted. This could reflect different temperatures at the time of

collection. Most of the edge otolith $\delta^{18}O$ values fall within the seasonal predicted otolith $\delta^{18}O$ range, maximum and minimum estimated water temperature represented by the red and blue horizontal lines in Figure 5.1. Otolith DSM 12-3 however has a final $\delta^{18}O$ value that is unexpectedly low (-0.7 ‰) and suggests that either the temperature of the water is much higher, >41 °C, which seems unlikely, or the water $\delta^{18}O$ value is lower than that recorded. This anomalous $\delta^{18}O_{VPDB}$ value could be a short term drop in water $\delta^{18}O_{VSMOW}$ values only picked up in this fish because of a faster growth rate.

It is also possible that the water $\delta^{18}O_{H2O}$ value downstream of Lake Menindee is not temporally stable even for the 1-month period between fish collection (Dec 2005) and water collection (Jan 2006). This is also suggested by the significant variation in water $\delta^{18}O$ values sampled between the years 2003 and 2007, which range from a maximum of 9.91‰ in January 2003 and a minimum of 2.91 ‰ in August of the same year (Table 3.3). Having said this, many of the otolith $\delta^{18}O$ values in the final 1-2 years fall within the predicted temperature range for the measured water $\delta^{18}O_{VSMOW}$ value of 3.86‰ supporting the notion that it is representative of the water the fish were living in over this period.

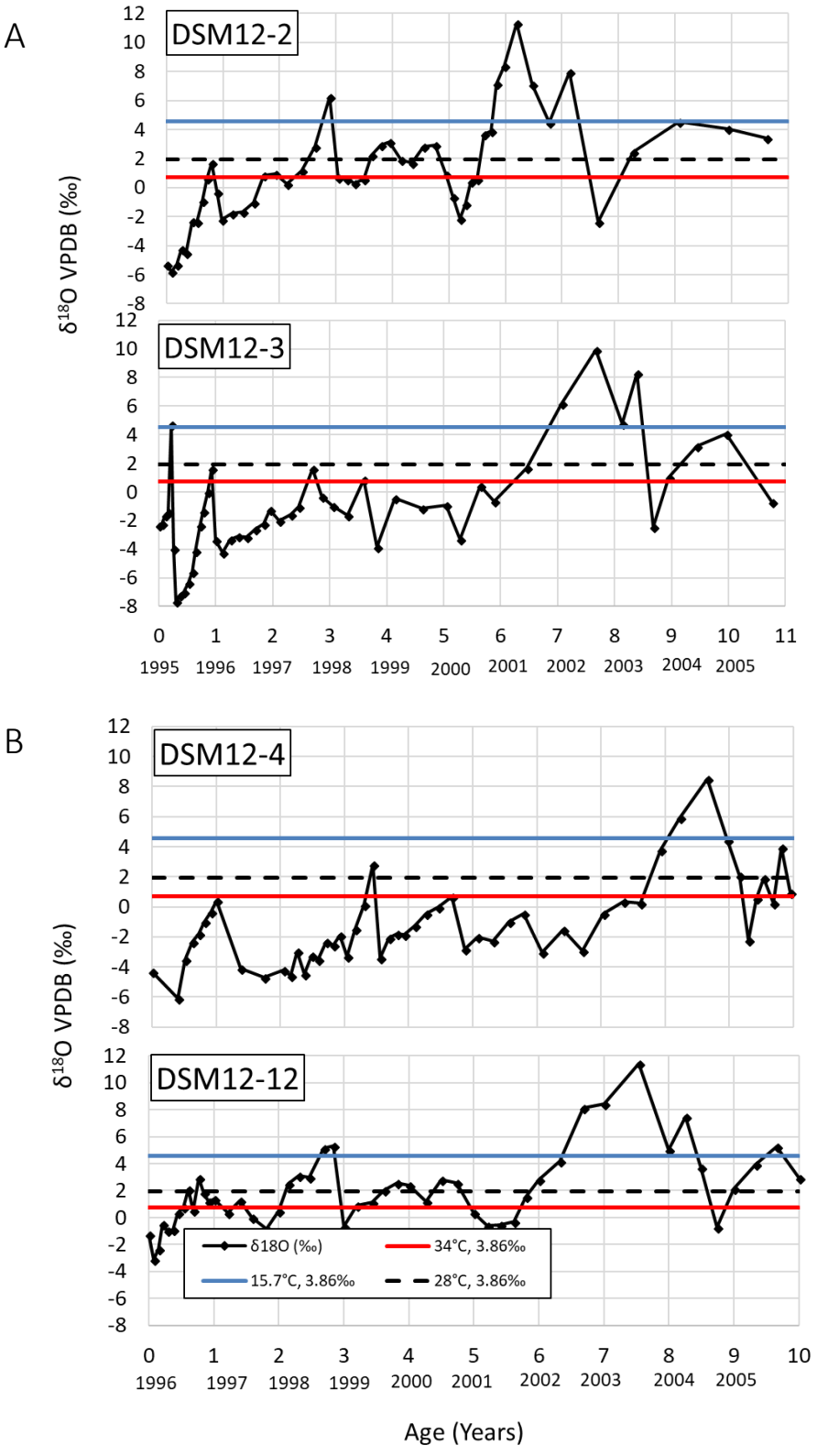

Figure 5.1: $\delta^{18}O_{CaCO3}$ values measured across the age increments (birth on the left, death/edge on the right) of DSM 12-2, DSM 12-3, DSM 12-4 and DSM 12-12 otoliths. The black dashed horizontal line is the $\delta^{18}O$ value in $‰_{VPDB}$ calculated using measured water temperature for January 2004 and the measured water $\delta^{18}O$ value in $‰_{VSMOW}$ for January 2006 (Tables 3.3, 5.1). The blue and red horizontal lines indicate expected range of $\delta^{18}O_{CaCO3}$ values predicted using the same water $\delta^{18}O$ value in $‰_{VSMOW}$ and estimated mean water minimum and maximum temperature for the Menindee region respectively.

5.4.2 Comparison between otolith $\delta^{18}O$ values and flood events

The $\delta^{18}O‰_{VPDB}$ results are plotted from birth to death for the two 11-year-old fish DSM12-2 and DSM12-3 in Figure 5.1A and for the two 10-year-old fish, DSM12-4 and DSM 12-12 in Figure 5.1B. Recorded under the x-axis are the approximate calendar years which the otolith age increments relate to. Each vertical grey line on the graphs is roughly equivalent to the location of an opaque increment on the otoliths which formed during slow winter growth. There are very similar trends in the $\delta^{18}O_{CaCO3}$ values of all otoliths suggesting fish occupation of the same water bodies but the timing of major fluctuations in the otolith $\delta^{18}O$ values do not match up, differing even between fish of the same age.

All otolith $\delta^{18}O$ values start low (-6 to -1 ‰), then there is an overall increasing trend, with some major fluctuations, of ~ 6 ‰ or more. The increasing trend goes up to a peak which differs slightly in magnitude and timing. In the two 11-year-old fish a peak of 11.5 $‰_{VPDB}$ occurs at age 6 for DSM 12-2 and a peak of 10 $‰_{VPDB}$ occurs at between age 7 and 8 for DSM 12-3. In the two 10-year-old fish the peak is 8 $‰_{VPDB}$ at between ages 8 and 9 for DSM 12-4 and the peak is 11.4 $‰_{VPDB}$ between ages 7 and 8 for DSM 12-12. This peak is followed by a drop to ~ 4 $‰_{VPDB}$ in all otoliths. In otolith DSM12-4 this decreasing trend continues to ~ -3 $‰_{VPDB}$, whilst in all other otoliths there is an increase up to 8$‰_{VPDB}$ before a sharp, drop to below 0 $‰_{VPDB}$. Following this the $\delta^{18}O$ values in all otoliths rises over 1-2 years to near or at 4 $‰_{VPDB}$. Then there is a drop of 2 – 4 $‰_{VPDB}$ in all otoliths except DSM 12-2 which experiences only a small drop to 3.4 $‰_{VPDB}$. The major 8 – 12 $‰_{VPDB}$ peak in the otoliths happens at different times in the lives of each of the fish.

In otolith DSM 12-2 the increase in $\delta^{18}O$ values occurs at between ages 5 – 6 (years 2000 to 2001) and the following series of drops occurs between ages 6 – 7 (years 2001 to 2002) and ages 7 – 8 (years 2002 to 2003). The drop in otolith $\delta^{18}O$ values could be the result of the discharge event that occurred at Bourke in 2001 (Murray Darling Basin Authority, 2018) and 2003 (Hughes et al., 2012). Considering these events did not reach beyond the Menindee Lakes we could interpret that the fish was occupying waters above the location where it was eventually caught (downstream of Menindee Main Weir). The other discharge events do not seem to have been recorded. This suggests that the fish was further downstream and so the discharge events did not reach it. This seems unlikely, given that the 2004 flow event

was recorded to have reached the Murray river (Hughes et al., 2012). It could be that the resolution of SHRIMP analyses in the later, thinner age increments is not high enough to pick up the other flood events.

In otolith DSM 12-3 the increase in $\delta^{18}O$ values occurs at between ages 6 – 7.5 (years 2001 to early 2003) and the two drops at age 8 (2003) and between age 8 and 9 (2003 to 2004). These could be the flood events recorded at Bourke in 2003 and 2004 (Hughes et al., 2012). The earlier and later flood events do not appear in the otolith $\delta^{18}O$ record. Again, this could be because the fish was not close enough to them or because the resolution of the SHRIMP analyses is not high enough to pick these short-term flood events at least in the outer rings.

In otolith DSM 12-4 and DSM 12-12 the increases and decreases in the $\delta^{18}O$ values occur slightly later that in the first two otoliths. In DSM12-4 there is only one major drop at age 9 (early 2005) which could be recording the 2005 flood event at Bourke. In DSM12-12 there is a drop between ages 7 and 8 (2003-2004), which could be one of the 2004 flood events. A second drop occurs between ages 8 and 9 (2004 to 2005) which could be one of the 2004 flood events or the 2005 flood event. Again, in these otoliths not all of the known flood events are recorded.

In summary the differences in timing between the increases and decreases in otolith $\delta^{18}O$ values could be due to each fish occupying a different part of the river system when flooding and drying events occurred. The discharge events at Bourke were not of the same magnitude and most did not reach all the way downstream. It is possible that if one fish was downstream from Bourke when a small discharge event occurred then it might not record the decrease in the water $\delta^{18}O$ values in its otoliths, whereas a fish closer to Bourke would. The other option is that the fish otoliths are recording the same flooding and drying events and the offset between the peaks is a result of different otolith growth rates. Some fish otoliths could have been growing faster and forming an opaque band earlier than the others.

The increasing trend in the otolith $\delta^{18}O$ records up to the first high peak at between ages 6 to 10 indicates that either, the fish is moving to waters with higher $\delta^{18}O$ values or the fish is not moving and the $\delta^{18}O$ value of the water it is occupying is increasing. Water $\delta^{18}O$ values increase during evaporation, when the lighter isotope, (^{16}O) enters vapour more readily than the heavier isotope, (^{18}O) leaving behind a body of water enriched in the heavier isotope thereby increasing $\delta^{18}O$ values. Examination

of water $\delta^{18}O$ values along the Barwon-Darling River system with distance upstream from the Murray River shows that the water $\delta^{18}O$ is heavier near the confluence with Murray and lighter near the headwaters (Hughes et al., 2012). The trend in the otolith $\delta^{18}O$ of starting lighter and getting consistently heavier over time suggests that the fish spawned upstream and moved downstream, eventually ending up downstream of the Menindee lakes.

5.4.3 Comparison between otolith trace element (Sr/Ca, Ba/Ca), and $\delta^{18}O$ records

The $\delta^{18}O$ results are compared to the Sr/Ca ratios in Figure 5.2 and to the Ba/Ca ratios in Figure 5.3. Sr/Ca and Ba/Ca ratios are plotted together in Figure 5.4.

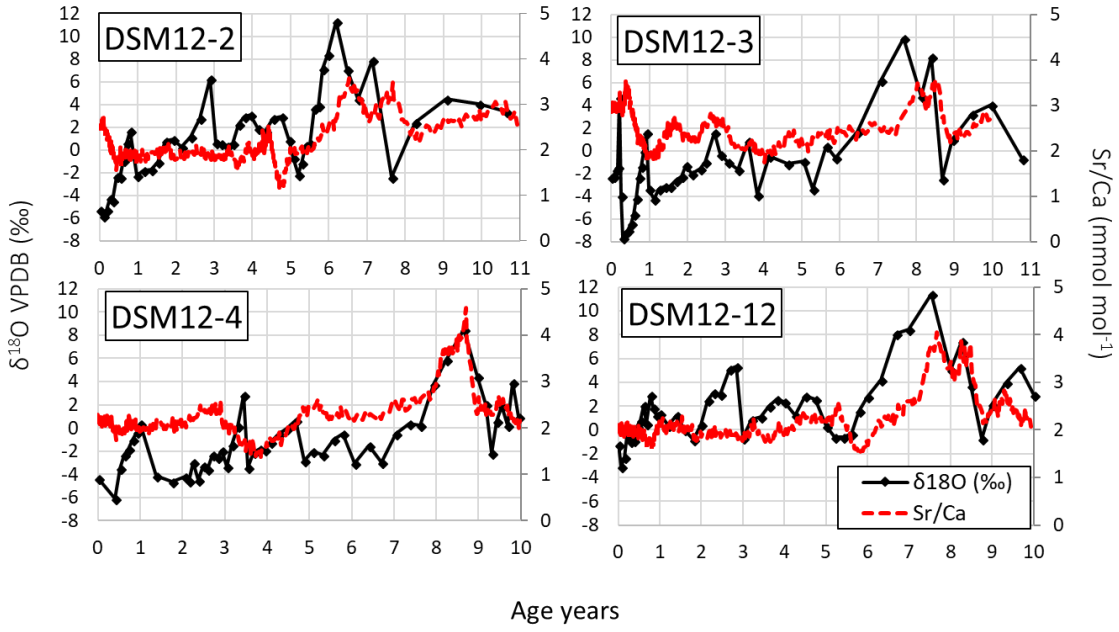

Figure 5.2: Downstream Menindee otolith $\delta^{18}O_{CaCO3}$ values and Sr/Ca ratios plotted from birth (left) to death (right)

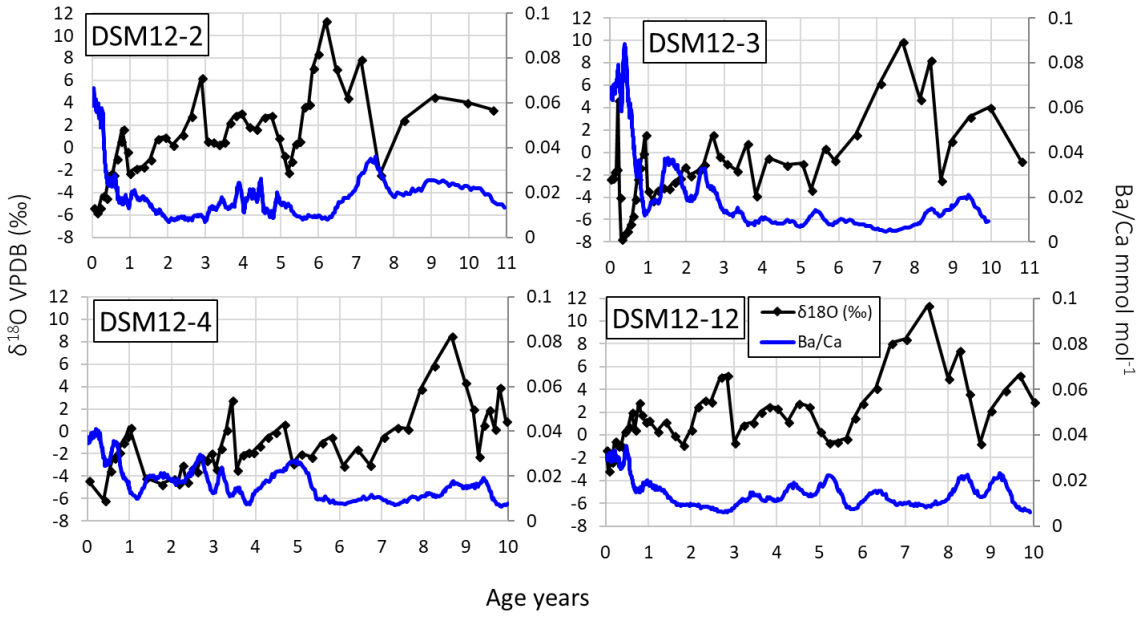

Figure 5.3: Downstream Menindee otolith $\delta^{18}O_{CaCO3}$ values and Ba/Ca ratios plotted from birth (left) to death (right)

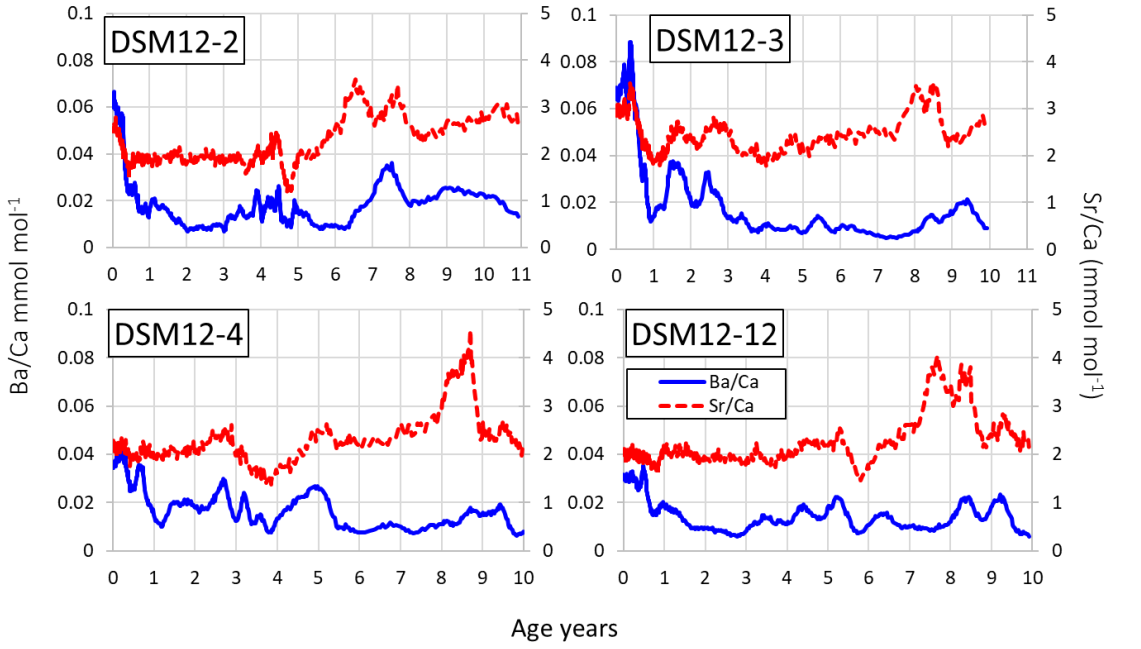

Figure 5.4: Downstream Menindee otolith Ba/Ca and Sr/Ca ratios plotted from birth (left) to death (right)

Fluctuations in the Sr/Ca ratios align closely with those in the $\delta^{18}O$ values. All Sr/Ca ratios fluctuate between 1 and 5 mmol.mol^{-1}. The peaks and troughs in the Sr/Ca ratios seem to match those in the $\delta^{18}O$ values. In DSM 12-4 there is a peak in the Sr/Ca ratios up to 4 mmol.mol^{-1} at the same point as the peak in $\delta^{18}O$ values at 8‰$_{VPDB}$ (Fig. 5.2). In the other otoliths there appears to be a temporal offset between peaks in the Sr/Ca ratios and in the $\delta^{18}O$ values. In otolith DSM 12-12 the

Sr/Ca ratios match closely with the second O isotope peak at between 8 and 9 years of age but there is a slight temporal offset (perhaps representing only a few months) between the initial $\delta^{18}O$ values and Sr/Ca peak at between 9 and 10 years of age. This is also the case for DSM 12-2 and 12-3.

There is a slight offset of less than 1 year between peaks and troughs in the two records, most likely due to different accumulation rates of O isotopes compared to Sr into the otolith or as the result of the different analytical methods and matching up of these records to age increments.

The similarity in trend between Sr/Ca ratios and $\delta^{18}O$ values is closest in DSM 12-12 and DSM12-4, particularly in the later years (Fig. 5.2). Sr/Ca ratios and $\delta^{18}O$ values are both purported to increase positively with salinity however this is usually in relation to mixing of marine waters (which tends to have higher $\delta^{18}O$ values and Sr/Ca ratios) with fresh water (which tends to have lower $\delta^{18}O$ values and Sr/Ca ratios). In the Barwon-Darling River system this is unlikely to occur.

Co-fluctuations in Sr/Ca and Ba/Ca ratios within the subadult portion of golden perch otoliths were identified in Chapter 4. A similar relationship is observed between the sub adult Sr/Ca and Ba/Ca ratios of the Menindee golden perch otoliths (Fig. 5.4). For DSM 12-3 both the Sr/Ca and Ba/Ca ratios increase to a peak and drop at the same time within the first year. The extent of the decrease is greater in the Ba/Ca ratios than in the Sr/Ca ratios, relative to overall amount of change in each record. Both trace element records then exhibit two peaks, one in DSM 12-3's second year and one in its third followed by a decreasing trend in both elemental ratios. The later peak in the Sr/Ca ratios between ages 6 and 10, which coincides with the peak in $\delta^{18}O$ values, is not evident in the Ba/Ca ratios (Fig. 5.3). As noted in Chapter 4, the co-fluctuations between Sr/Ca and Ba/Ca ratios appears to be a subadult feature.

Sr/Ca and Ba/Ca ratios in otoliths are closely associated with ambient water Sr/Ca and Ba/Ca ratios respectively. The same is true for the $\delta^{18}O$ values of otoliths. In Long et al., (2018) increases in otolith Sr/Ca ratios were recorded coincident with lake evaporation and an increase in otolith $\delta^{18}O_{CaCO3}$ values. The Sr/Ca ratio increase was interpreted as being linked to fish stress rather than changes in the ambient Sr/Ca composition of the water. Here the Sr/Ca ratios follow the peaks and troughs in the $\delta^{18}O_{CaCO3}$ values throughout the record, not just in periods when the $\delta^{18}O_{CaCO3}$ values are increasing. This suggests fish occupation of different environments or

water bodies with changing $\delta^{18}O_{H2O}$ values, rather than solely the impact of increasing stress levels/biological effects of living in an evaporating lake. A future area of study area would be to examine changes in trace element records in Australian rivers and lakes to determine how closely these mirror changes in water $\delta^{18}O$ values, then compare these to the microchemical records in fish otoliths from those regions. This could shed more light on the links between golden perch otolith trace element records with changes in ambient chemistry as opposed to biological condition.

5.4.4 Higher resolution sampling in outer increments

Given the poor visibility of age increments in otoliths DSM 12-15, 16, 17 and 18, due to the experimental preparation procedure (see Chapter 3, section 3.3.4), the $\delta^{18}O_{CaCO3}$ values measurements are not considered as part of the main life history study. Two of these otoliths were sampled at a higher resolution than the others and the results of this are shown here. This higher resolution sampling involved measuring double the amount of spots in the outer increments right next to the original wider spaced spots. This sampling of DSM 12-16 and 12-18 allowed us to pick up finer detail in the pronounced $\delta^{18}O$ value peak in the final years (Fig. 5.5). This is most obvious in 12-16 where step-wise changes in $\delta^{18}O$ values were observed in the double density sampling but not in the original profile. Without this extra detail a straight decline in $\delta^{18}O$ values would be assumed.

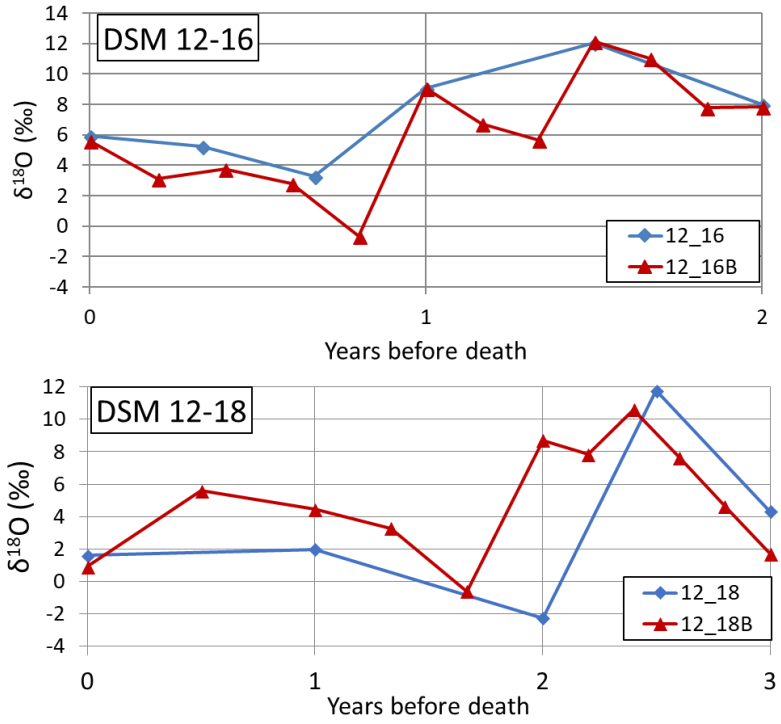

Figure 5.5: $\delta^{18}O_{CaCO3}$ values resulting from higher resolution sampling in outer increments of DSM 12-16 and DSM 12-18. Analyses are plotted as years before death; otolith edge is on the left. The original SHRIMP spot sampling is in blue and the higher resolution sampling is in red.

In DSM12-18, the $\delta^{18}O_{CaCO3}$ values from 12-18B tracks alongside in a steady increase from 3 years before death to 2.5 years before death. A slight drop and rise are seen in 12-18B but not in the original track and further differences are evident between 2 and 0. The 12-18B ratios increase to around 6‰$_{VPDB}$ whilst the original track only increases a far as 2‰$_{VPDB}$. Nevertheless, there is a close association between the timing and type of changes in the ratios of each original track with the higher resolution sampling results. This is a useful method for elucidating fine structure in data, and similar methods have previously been employed to create sub seasonal records of $\delta^{18}O_{CaCO3}$ values across otolith age increments (Matta et al., 2013).

5.5 Conclusions

The Menindee otoliths analysed here show similar peaks and troughs in their $\delta^{18}O$ records however the timing of these peaks and troughs differ between individuals. All otoliths pick up evaporation and discharge events. The discharge events can be matched approximately to the timing of known discharge events in the system. From this study the movement of fish through the system could not be separated from changes in ambient water $\delta^{18}O$ values at a single location caused by discharge and drying events. A closer examination of the otolith records in comparison to more

detailed temperature and water $\delta^{18}O$ records could help to elucidate this but there will likely always be some obscurity in the results.

The overall increasing trend observed in otolith $\delta^{18}O$ values likely relates to fish moving from the upstream river waters with relatively low $\delta^{18}O$ values to the waters downstream with relatively high $\delta^{18}O$ values.

Otolith $\delta^{18}O$ values should reflect the $\delta^{18}O$ value of the water in which the fish is living with a temperature dependent overprint. Here it was found that the range of outer edge $\delta^{18}O$ values of most otoliths could be predicted using the Patterson et al. (1993) fractionation equation, seasonal water temperature range and known water $\delta^{18}O$ value. One otolith had an outer edge $\delta^{18}O_{CaCO3}$ value that was much lower than predicted. It is unlikely that this anomalous otolith $\delta^{18}O$ value is due to a period of increased temperature but could be a short term drop in water $\delta^{18}O$ value only picked up in this fish because of a faster growth rate.

Overall, the Menindee otoliths recorded a signature of flooding and drying cycles, which we know, dominate the water $\delta^{18}O$ records of the Barwon-Darling system (Meredith et al., 2009, Meredith et al., 2013, Meredith et al., 2015; Hughes et al., 2012). Further information about the fish movement or more detailed water $\delta^{18}O$ surveys and temperature records are required for a more comprehensive interpretation.

This study identified co-fluctuations in $\delta^{18}O$ values and Sr/Ca ratios within the otoliths. This could be reflecting ambient water compositional changes, increases and decreases in both Sr/Ca and $\delta^{18}O$ values or periodic flooding that brought in both water with a lower $\delta^{18}O$ value and Sr/Ca ratio to dilute the higher Sr/Ca ratio of the water the fish was living in. A detailed record of water $\delta^{18}O$ values and trace element values for the Barwon-Darling river region as well as direct water temperature measurements taken at the same time as fish collection would greatly assist in untangling the influence of ambient water composition vs biological effects on the otolith Sr/Ca and Ba/Ca ratios.

6. Using simple mass balance equations to gain a more quantitative understanding of past lake level and water O isotope change in the Willandra Lakes

The previous chapters have focused on validating the effects of ambient conditions (temperature, evaporation, flooding) on the oxygen isotope and trace element compositions of golden perch otoliths in modern settings. This chapter focuses on how mass balance models and ancient otolith oxygen isotopes records can be used to test scenarios of lake level change at Lake Mungo. This involves examining the broader lake system and Lake Mungo's position within it to determine how flooding and drying scenarios would have affected the oxygen isotopic composition of the water. The modelled variability in $\delta^{18}O_{H2O}$ values is compared to the $\delta^{18}O_{CaCO3}$ values preserved in ancient hearth otoliths to assess theories for lake level changes and human occupation during the Last Glacial Maximum. The MATLAB code, developed for this study by David Heslop, can be found at the back of this thesis.

6.1 Introduction

The Willandra lakes are a series of dry inter-connected basins in south western NSW that were once filled by the Lachlan River via the Willandra Creek (Bowler et al., 2012; Fitzsimmons et al., 2014). The Lachlan river shifted its course resulting in the drying of the Willandra lakes, and for the last ~ 15,000 years has flowed directly into the Murrumbidgee. Today the Lachlan River rises in the Australian highlands and flows east terminating, except when in flood, in ephemeral wetlands and lakes (Kemp, 2004; Kemp and Rhodes, 2010). At various times in the past during periods of increased and more effective precipitation, the Willandra Lakes formed a cascading sequence that overflowed at its lower end into the Murray River (Bowler et al., 2012; Kemp et al., 2017). Large pulses of water, flowed from the Lachlan River into the Willandra creek filling the uppermost lake, (Mulurulu), before moving down the system sequentially filling lakes Garnpung and Leaghur (Fig. 6.1). Lake Leaghur overflows into Lake Mungo which was the only terminal Lake in the system. The creek continued past Leaghur to Outer Arumpo/Chibnalwood feeding lakes further to the south (Bowler and Price, 1998; Cohen et al., 2012).

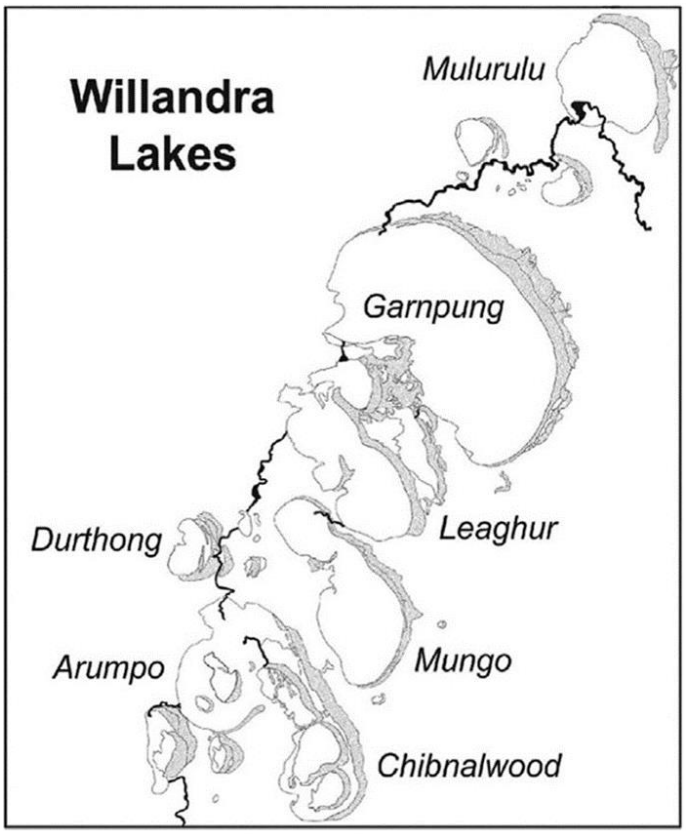

Figure 6.1: Map of the Willandra Lakes system adapted from Bowler (1998).

The lakeshore dunes of Lake Mungo contain a record of lake level changes stretching back throughout the Quaternary. A significant amount of archaeological material has been uncovered within these dunes (Bowler et al., 1970; Bowler, 1998; Fitzsimmons et al., 2014; Stern, 2015). A key focus of research in the area has been on linking environmental conditions with lake level changes with periods of human occupation. Initial studies of the dunes and their stratigraphy focused on the southern tip of the Mungo lunettes (Bowler et al., 1970; Bowler, 1998), whilst more recent work focuses on the central lunettes where erosion has uncovered an array of archaeological and stratigraphic features (Fitzsimmons et al., 2014; Stern, 2015). A key difficulty identified for matching up lake levels and archaeological traces at Lake Mungo is that human occupation events occur over much shorter time periods than the formation of the sedimentary lake records and it can be difficult to reconcile the two (Holdaway et al., 2010). However, as has been described in Chapter 2, the Mungo Archaeology Project, led by Nicola Stern have developed an appropriate methodology for generating paleoenvironmental and behavioural information at the same scale. The sediment in which archaeological traces lie provide information

about past hydrologic conditions and palaeoenvironmental recorders such as otoliths, can provide additional detail to these records.

Otoliths grow within the inner ears of bony fish by the incremental deposition of calcium carbonate (aragonite) forming annual rings (Campana, 1999). As otoliths grow they preserve a record of the ambient $\delta^{18}O_{H2O}$ values, with a slight temperature overprint (Campana, 1999). Changes in water $\delta^{18}O$ values are forced by evaporation and flooding events which, in turn, are recorded in the otoliths.

At Lake Mungo a series of fish-bone hearth sites found in the central lunettes, offered an opportunity to relate microchemical records of otoliths directly to human occupation and to assess their usefulness for building up chronological records of ancient lake conditions. The hearth sites were uncovered within Unit E (Arumpo/Zanci) which straddles the Last Glacial Maximum (LGM), the period when global ice sheets were at their greatest extent. Eighteen OSL dates from Unit E show that these alternating sands and clays accumulated between about 25 and 14 ka (Fitzsimmons et al., 2014). Radiocarbon dates of the hearth site otoliths place them between an upper limit of 19,490 – 19,330 and lower limit of 19,420 – 19,220 cal BP at 95.4% probability (Long et al., 2014). At this probability all hearths were made within a time span of between zero and 240 years, with the shorter duration more likely (Long et al., 2014). A small number of OSL dates from the central Mungo lunette indicate that final drying of the lake did not occur until 14.5-14ka (Fitzsimmons et al 2014). Unit E not only contains multiple hearth sites but also large amounts of stone tools and other archaeological materials (Stern et al., 2015).

Trace elements and $\delta^{18}O_{CaCO3}$ values were measured across the age increments of the hearth otoliths. Increases in the Sr/Ca ratios were interpreted as relating to fish entry into an increasingly saline Lake Mungo (Long et al., 2014). The $\delta^{18}O$ values exhibited an increasing trend of between 4 and 6‰$_{VPDB}$ from the point at which Sr/Ca ratios increased to fish death (Fig. 6.2, Long et al., 2014). This was interpreted as evidence for evaporation and a decrease in lake level (Long et al., 2014) and seemed to support the Easy Prey Hypothesis that suggests large quantities of fish migrated into Lake Mungo after a flood pulse, were trapped by evaporative conditions and targeted by human occupants who took advantage of the supine state of the fish to "scoop [them] up in shallow waters" (Bowler 1998: 146). However as noted in Chapter 2 such low quantities of fish (~ 2 to 26) are much more likely to be

the result of spearing or netting. This Chapter adds further evidence to contest the hypothesis that these fish died when trapped in an evaporating lake cut off from the river system.

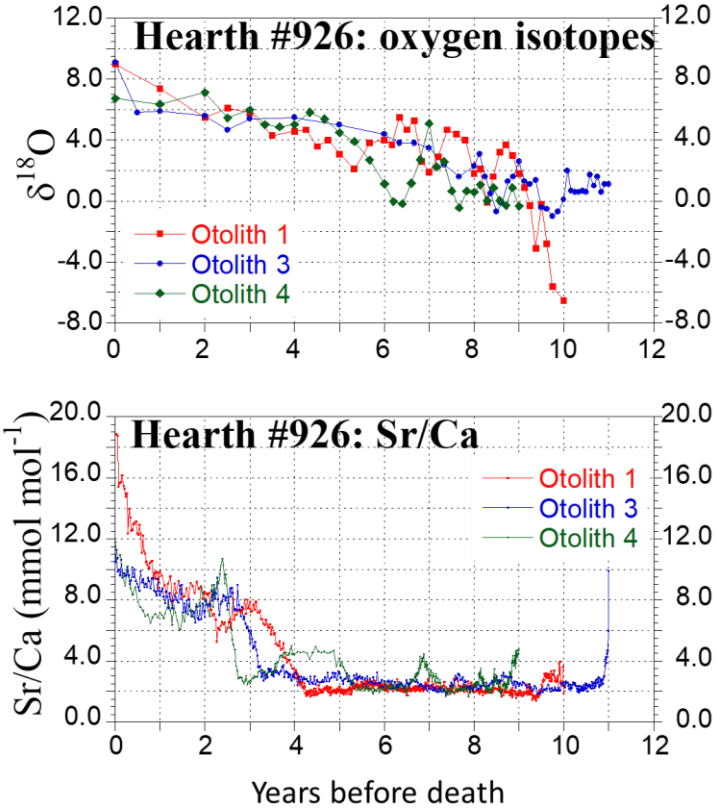

Figure 6.2: The $\delta^{18}O$ values and Sr/Ca ratios plotted against otolith age lines as years before death for each of the otoliths collected from hearth #926 (Long et al. 2014).

Here a simple model is constructed to test the lake desiccation scenario suggested by the otolith records, and to more broadly understand how changes in lake level would have been reflected in $\delta^{18}O_{H2O}$ values. In brief, a model is developed in which the Willandra Lakes are maintained in mass balance and allowed to approach isotopic equilibrium between incoming and outgoing $\delta^{18}O_{H2O}$ values over 20 years. After 20 years, inflow to Lake Mungo is cut off and evaporation proceeds unimpeded. The effect on the $\delta^{18}O$ values of the lake waters is recorded over time. The model can also be used to show what happens to the $\delta^{18}O$ value of Lake Mungo water when the lake is filled and maintained at different depths for different periods of time.

Understanding the hydrological context of the lake system and how this affects the water $\delta^{18}O$ values is imperative for understanding the $\delta^{18}O_{CaCO3}$ records preserved

in the otoliths of fish that once lived within these lakes. These records are also useful for understanding past human activity but the isotope record, on its own, cannot solve the problem of how fish were caught; that requires zooarchaeological information as well as ecological information. The latter will be critical for developing an integrated understanding of what was fished, when and how.

Changes in lake levels over time reflect the integration of mean net precipitation over the catchment area and evaporation from the lakes surface area (Rohling, 2013). The surface area of lakes varies with lake level, at Lake Mungo increases in lake level results in increased surface area. The $\delta^{2}H_{H2O}$ and $\delta^{18}O_{H2O}$ values of evaporating water bodies are controlled by several variables including the initial isotope value of the water, temperature, relative humidity, ambient vapor isotopic composition, diffusion and/or mixing at the water-air interface, wind stress and the thermodynamic activity (salinity) of the water (Gonfiantini, 1986; Edwards, 2004; Jones et al., 2005; Rohling, 2013; Steinman and Abbott, 2013; Gibson et al., 2016).

The $\delta^{18}O_{CaCO3}$ values of fish otoliths is a product of the temperature and $\delta^{18}O_{H2O}$ values of the water in which the fish has lived. If the ambient water $\delta^{18}O$ value remains constant, a change of 1‰ in otolith $\delta^{18}O$ values would reflect a ~ 4°C change in temperature (Kalish 1991). As well as the water balance and climatic conditions described above, the size, shape and depth profile of the lakes also plays a role in influencing the water $\delta^{18}O$ value reached over time.

In the Willandra Lakes system, any change in climate which affects the hydrologic balance of the system will be felt and expressed differently in each of the Lakes. Responses to changes in climate will depend on the shape, size and position of the lakes within the Willandra chain (Bowler et al., 2012). For example, Mulurulu, which is positioned closer to the source channel, will retain water for longer periods than those lakes further down the chain (such as Lake Mungo).

The shoreline dunes of the Willandra Lakes preserve a sedimentary record of fluctuating lake conditions stretching from beyond the last interglacial (Marine Isotope substage (MIS) 5e) to the present (Bowler and Price, 1998; Fitzsimmons et al., 2014). When humans first settled the area at ~45 ka Lake Mungo was full. From ~ 40 ka onwards the lakes start to oscillate, recorded as alternating layers of quartz sand, representing periods of high lake levels, and pelletal clays which formed as lake levels dropped exposing the clayey lake floor (Bowler 1998, Bowler et al 2012,

Fitzsimmons et al., 2014). The hydrology of the Willandra Lakes system most closely reflects runoff from the south-eastern highlands rather than local climatic conditions.

Unlike most other modelling sites (Jones et al., 2001; Rohling, 2013, 2016), Lake Mungo contains no modern water to measure or hydrological patterns to observe. The initial water $\delta^{18}O$ value for the model can be approximated based on nearby river systems but humidity over the lake surface and the $\delta^{18}O$ value of the evaporated vapour is unknown.

Isotopic mass balance models provide a theoretical framework to simulate and quantitatively interpret isotopic variability in lakes (Gibson et al., 2016). Under constant forcing a closed lake will eventually reach a steady state if the amounts of evaporation and incoming water are balanced. There have been many studies that have investigated water and isotopic mass balance approaches in both modern (Dinçer, 1968; Gonfiantini, 1986; Gat, 1995) and ancient (Jones et al., 2005; Steinman and Abbott, 2013; Rohling, 2016) systems. The degree of quantification for Lake Mungo is limited, due to a lack of records of past climate (humidity, temperature, wind stress etc), but simple models can be very effective at ruling out certain hydrological scenarios (see Rohling, 2016).

Steinman and Abbott, (2013) used coupled lake-catchment isotope mass balance models, forced with temperature, relative humidity and precipitation data and compared these to reconstructed surface elevations and sediment core oxygen isotope values. The strongest control on lake isotopic and hydrologic dynamics suggested by the simulation was precipitation. Secondary to this was temperature and relative humidity. Jones et al. (2005) compared an 80-year varve oxygen isotope record from Turkey with instrumental records. Significant relationships between the isotope record, summer temperature and evaporation were identified suggesting these as the dominant controls on isotope hydrology.

The relationships between these influences were able to be tested independently through modelling of the stable isotope hydrology of the lake system. Findings from the independent modelling suggested that the isotope records for the lakes were less sensitive to evaporation and temperature than suggested by the initial climate calibration. Rohling et al., (2016) used a simple framework of equations to investigate the causal link between lake level changes and agricultural productivity.

The study demonstrated that in some cases crop growing potential could be improving at the same time as lake levels are dropping.

6.2 Constructing and running a Steady State Model (Methods and Results)

To study the movement of Lake Mungo $\delta^{18}O_{H2O}$ values towards equilibrium it is first necessary to determine the volume and surface area of each lake in the Willandra Lakes system. Maximum water levels are controlled by the height of the overflow outlet connecting each basin to the next in the chain (Bowler et al., 2012). These heights were defined using a digital elevation model (DEM) from the scanning radar topography mission (SRTM), provided by Geoscience Australia. Topographic lake contours were examined at 1 m intervals and the maximum fill height for each lake was set as the highest closed contour line, which resulted in separate basins. To establish the surface areas and volumes of the lakes, all contours that fell outside of the maximum contour line boundary that defined each lake were excluded. Surface area was calculated as the number of pixels within the lake contour, where each pixel represents a known area. Using MATLAB, the surface area at 10 cm height intervals from the base of the lake to the top was calculated and then integrated to get the lake volume at each height. The surface area and volume for Lake Mungo at a given water level is shown in Figure 6.3.

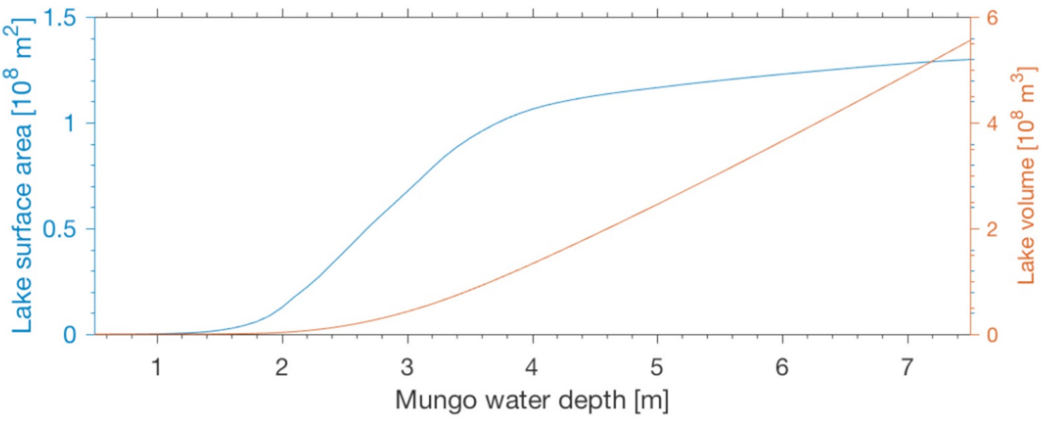

Figure 6.3: Modelled change in Lake Mungo water levels and volume with depth.

The volume of the lakes gives the amount of water needed to fill the lakes but to maintain those levels it is necessary to consider water fluxes; specifically, evaporation from each lake surface and the additional water that is needed to push water from one lake to the next. The modern average annual pan evaporation rate for the Willandra Lakes region, ~ 2000 mm (BoM) was used as a starting point for

calculating the amount of water needed to fill all the upper lakes and maintain Lake Mungo at a given height. The relationship between water fluxes representing the inflow, evaporation and outflow required to maintain lakes in mass balance is given by:

$$F_w = F_E + F_{out} \quad (6.1)$$

Where F_w is the water flux entering the lakes, F_E is the flux of water lost to evaporation and F_{out} is the water flux that flows out to the next lake. When $F_w = F_E + F_{out}$ then the lake level is stable, when $F_w < F_E + F_{out}$ the water level falls, when $F_w > F_E + F_{out}$ the water level rises.

For the purposes of this study the Willandra Lakes can be treated as a system that ends with the fluxes exiting Lake Mungo. Outer Arumpo, and lakes further down the sequence can be disregarded as they are not directly connected to Lake Mungo (Fig. 6.1). In the future this model could be extended to other lakes in the system. The amount of water lost to evaporation from the first lake in the system is its surface area (SA) multiplied by the evaporation rate. The amount of outflow required is SA multiplied by the evaporation rate for each lake further down the system (see Fig. 6.4).

This water flux entering the Willandra Lakes system can be expressed as:

$$F_w = SA_1E + SA_2E + SA_3E + SA_4E \quad (6.2)$$

Where F_w is water flux entering the system, SA_1, SA_2… is the surface area of each lake from top to the bottom of the sequence and E is the evaporation rate for the region. If no water flows out of Lake Mungo, then to maintain stable lake levels throughout the model system the outflow for the top lake in the sequence must be equal the sum of the surface area multiplied by the evaporation rate for each lake further down in the sequence or:

$$F_{out} = SA_2E + SA_3E + SA_4E \quad (6.3)$$

This gives us the amount of water needed to maintain all the lakes at mass balance.

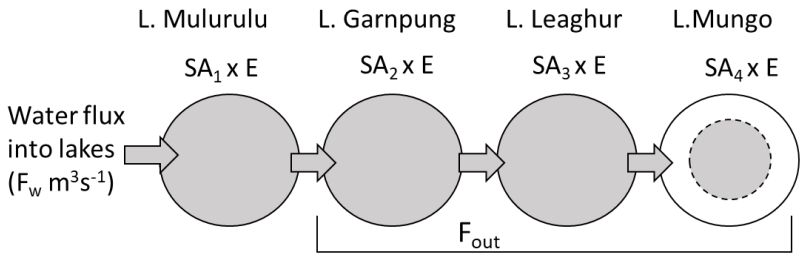

$$F_{\mathrm{w}} = SA_1\mathrm{E} + SA_2\mathrm{E} + SA_3\mathrm{E} + SA_4\mathrm{E}$$

$$F_{\mathrm{w}} = F_E + F_{out}$$

F_w is the water flux entering the lakes
F_E is the flux of water lost to evaporation
F_{out} is the water flux that flows out to the next lake

$F_w = F_E + F_{out}$ (Water level maintained)
$F_w < F_E$ (Water level lowers)
$F_w > F_E$ (Water level rises)

Figure 6.4: Diagrammatic representation of the water flux entering the Willandra Lakes as expressed by the Equations 6.1, 6.2 and 6.3.

The equation for isotopic steady state is given by:

$$F_{in}\,\Delta t\delta_P = F_E\Delta t(\delta_L - 10) + F_{out}\Delta t\delta_L \qquad (6.4)$$

Where δ_p is the isotope value of precipitation or water entering the lakes, δ_L is the isotope value of the lake water, "$\delta_L - 10$" is the depletion in the heavy oxygen isotope (^{18}O) in the vapour phase with respect to the liquid phase at a typical ambient temperature of 15-20°C (Gonfiantini, 1986; Froehlich et al., 2005; Rohling, 2016) and Δt is the time step.

The water $\delta^{18}O$ value used as a starting point for the model influences the final equilibrium $\delta^{18}O$ value but does not influence the rate or degree of change. An initial $\delta^{18}O_{H2O}$ value starting point of -8‰$_{VSMOW}$ was chosen based on studies of the $\delta^{18}O$ values of the nearby Barwon-Darling River. During high flow events, like those that once filled the Willandra Lakes, tributary rivers of the Barwon-Darling river that normally do not carry water can contribute water with significantly lower $\delta^{18}O$ values to the system. During the January 2004 flow event at Bourke, for example the $\delta^{18}O_{H2O}$ value was -8.32‰$_{VSMOW}$, compared to that upstream at Brewarrina, which was -3.23‰$_{VSMOW}$ (Hughes et al., 2012). Input of water with lower $\delta^{18}O$ values from the normally dry tributary Culgoa River forced the lower water $\delta^{18}O$ values (Hughes

et al., 2012). In the Willandra Lakes model, a large-scale flood event was assumed to fill all the lakes over a period of days. The $\delta^{18}O$ value of the source water in such a scenario is likely to be lower than the value of rainfall for the local and/or source region.

In summary the modelling process was to set up a schematic of the lake system and, fill all the lakes instantly (simulating a massive flood event) with water of $\delta^{18}O_{VSMOW}$ = -8‰. The lake water was then maintained at mass balance and the $\delta^{18}O$ value was allowed to change with evaporation and inflow according to the above equation. Once the lakes had filled they started to evaporate. The model worked by tracking the $\delta^{18}O$ value of the water remaining as water was lost incrementally, 10 cm at a time. During evaporation the $\delta^{18}O$ value of the surface layer of the water increased. This higher value surface water was then mixed through the rest of the water column, resulting in slightly higher water $\delta^{18}O$ value overall. This value was then passed on to the next lake in the sequence. The first lake was then replenished with $\delta^{18}O$ = -8‰$_{VSMOW}$ water and the cycle repeated.

As a consequence of this process, each lake down sequence was replenished by water that with slightly higher $\delta^{18}O$ value than the water that filled the previous lake. This means that lakes further from the primary water source reached higher $\delta^{18}O$ value than lakes closer to the source (Fig. 6.5). In the desiccation scenario tested here the lakes were maintained in mass balance for 20 years, after which Lake Mungo was cut off from the system and allowed to evaporate until only 10cm of water remained. The effect of this scenario on the $\delta^{18}O$ values of the Lake Mungo water is shown after the dotted line in Figure 6.5.

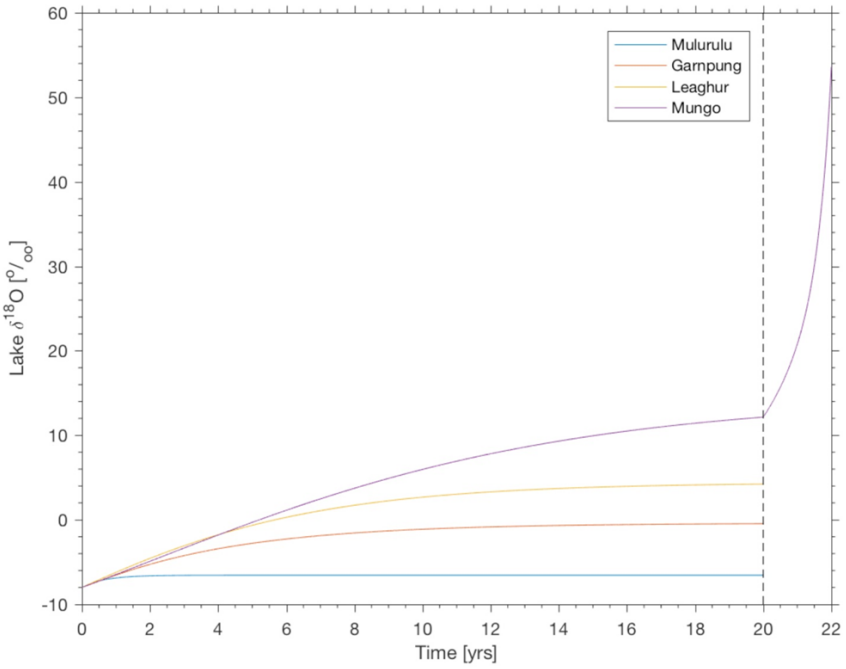

Figure 6.5: Modelled output for change in the $\delta^{18}O_{H2O}$ value of the Willandra when the lake levels are maintained in mass balance for 20 years. This graph also shows the change in water $\delta^{18}O_{H2O}$ value of Lake Mungo after 20 years, when it is cut off from the rest of lakes and left to evaporate to dryness (10 cm depth).

The progressive increase in the $\delta^{18}O_{H2O}$ value of an evaporating lake is limited by physical conditions and the rate and extent of this limitation depends on the local meteorological conditions (Gat and Levy, 1978; Gat and Gonfiantini, 1981). This limit is commonly expressed as δ^{*}:

$$\delta^{*} = \frac{(h\delta_A+\varepsilon)}{(h-\varepsilon/1000)} \quad (6.5)$$

where h is the ambient humidity normalised to the saturation vapor pressure at the temperature of the air-water interface, δ_A is the isotopic composition of ambient moisture, and $\varepsilon = \varepsilon^{*}+\varepsilon_K$ the total isotopic fractionation comprised of both equilibrium ε^{*} and kinetic ε_K components. Note that ε^{*} is a function of temperature (T), whereas ε_K is controlled by the turbulent/diffusion mass transfer mechanisms and humidity (as explained in Gibson, 2002). These variables are unknown for Lake Mungo and so it is not possible to set a limit on the evaporative trend shown in Figure 6.5. There are few records of changes in the $\delta^{18}O_{H2O}$ value of lakes evaporating to near dryness. The water $\delta^{18}O_{H2O}$ of an ephemeral lake in the Sahara reached a maximum $\delta^{18}O_{VSMOW}$ of 31.3 $‰_{VSMOW}$ as a result of evaporation at low relative humidity (Fontes and

Gonfiantini (1967), as reported in Gonfiantini (1986)). This could be used as an approximate limit for the Lake Mungo $\delta^{18}O$ values.

Once inflow to Lake Mungo is cut off $\delta^{18}O$ values increases dramatically. Evaporation causes the $\delta^{18}O$ value of the lake to jump up >20‰ within two years (Fig. 6.5). This amount of change can be compared to that observed in the hearth otolith $\delta^{18}O$ records (Long et al., 2014). The modelled increase is higher and more rapid than the $\delta^{18}O$ increase observed in the hearth otoliths, from the point at which Sr/Ca ratios increased (4 – 6‰ over the final 5 years).

Further consideration of the influencing factors on otolith Sr/Ca ratios (see Chapter 2; Chapter 4; Long et al., 2018) suggests that the increase in Sr/Ca ratios might be related more to the stress levels of the fish or change in the ambient water Sr/Ca than to increasing salinity (Chapter 5; Long et al., 2018). The increase in Sr/Ca ratios might still relate to lake entry, but the link with salinity is not supported. If the Sr/Ca ratios are ignored and the change in otolith $\delta^{18}O_{CaCO3}$ values from fish birth to death is considered instead, there is an increase in $\delta^{18}O_{CaCO3}$ values to a maximum of 16 $‰_{VPDB}$ over 10 years (Otolith 926-1; Fig. 6.2), which is still not large enough to suggest occupation of a desiccating lake.

This same steady state scenario was run without cutting the lake off from the system, to examine the influence of different lake heights on the $\delta^{18}O$ value of the water. F_w was set to result in fixed water heights/levels in Lake Mungo (1, 3, 5 and 7m) with the same annual evaporation rate (2000mm/yr) to see how the $\delta^{18}O$ value of the lake water would have changed over time. The results are illustrated in Figure 6.6.

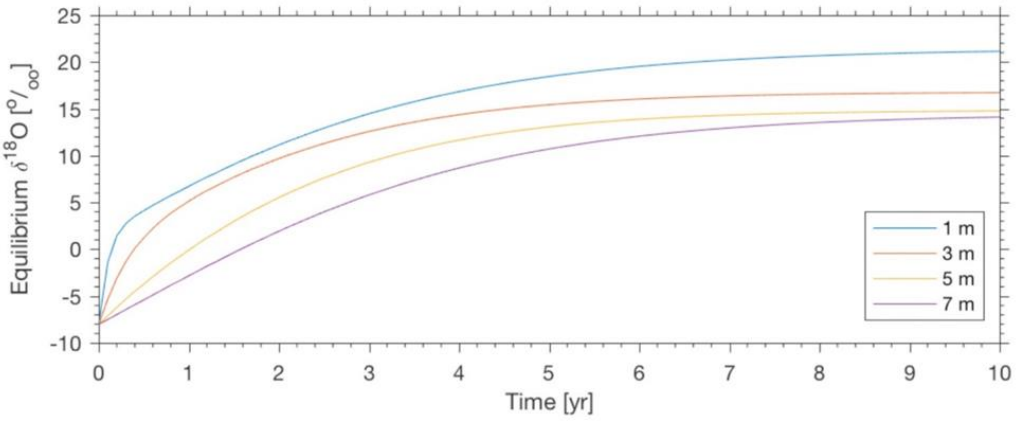

Figure 6.6: Model output results showing changes in the $\delta^{18}O$ value of the Mungo lake water reached over time (x-axis) when the lake is maintained in mass balance at fixed water heights (1, 3, 5 and 7m).

At a water depth of 1 m the $\delta^{18}O_{H2O}$ value changes more quickly and reaches a higher value after 10 years than for deeper water. The change in the lake $\delta^{18}O$ value over this time is still quite large, however, regardless of the lake level maintained. This demonstrates that, based on $\delta^{18}O_{H2O}$ values alone, a lake in steady state could be misinterpreted as evaporating towards dryness, even though no change in water level is actually taking place. This emphasizes the importance of integrating the otolith $\delta^{18}O$ records with broader information about lake hydrology generated from the sedimentary record.

Finally, the same steady state scenario used in Scenario 2 was modelled but instead of examining the change in $\delta^{18}O$ values of the water over time, water $\delta^{18}O$ values were examined as a function of water depth (0 – 7.5 m) in 10 cm increments, for four different time periods (2, 5, 10 and 200 years). Essentially, the $\delta^{18}O$ value of the water was calculated after the lake had been maintained at each depth in mass balance for each period of time. The results are illustrated in Figure 6.7 and compared to the expected change in the lake surface area and volume for each depth.

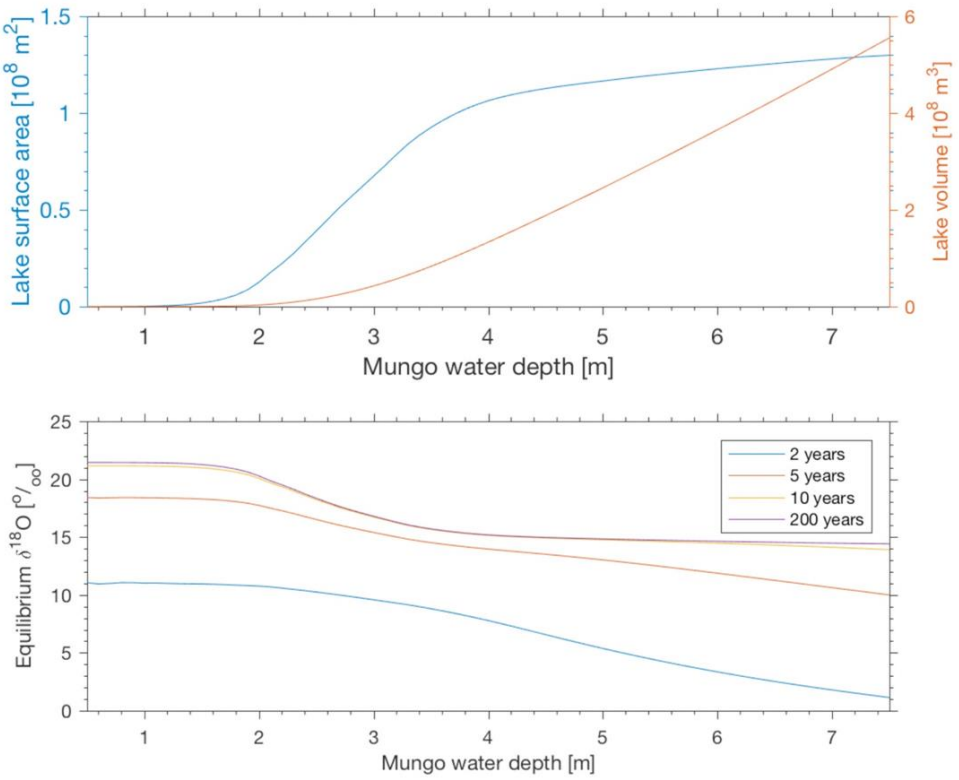

Figure 6.7: Model output results showing changes in the $\delta^{18}O$ values of the Mungo lake water reached when lake levels are maintained at certain depth (x-axis) over fixed time periods (2, 5, 10 and 200 years).

The change in the $\delta^{18}O$ value of the water reached for the time periods changes in relation to the surface area at each depth. The differences between the curves for lake $\delta^{18}O$ value at different depths (Fig. 6.7) is a result of the different surface area of water exposed at each of those levels. When the lake is maintained at 5 m the resulting curve is very similar to that for lake max/full at 7 m but is slightly steeper early on (~ 4‰ difference in $\delta^{18}O$ value reached over 3 years, with 5 m higher)

6.3 Discussion

6.3.1 Lake Mungo: cut off from the system and drying out?

In the scenario modelled here Lake Mungo continues to evaporate and $\delta^{18}O$ values continue to rise until the lake is only 10 cm deep. For fish populations living in the lake there will be a tipping point as the lake shrinks where overcrowding occurs, or water conditions deteriorate to a point at which fish start to die out and thus cease recording ambient conditions in their otoliths. When fish otoliths are found within a hearth site this suggests that the fish were caught and eaten by humans prior to their maximum life expectancy. Recent studies of modern golden perch from a

known desiccation episode at Lake Hope, South Australia (Chapter 5; Long et al., 2018), also show an increasing trend in their otolith $\delta^{18}O$ values. This would at first seem to support the interpretation of the Mungo Hearth otolith $\delta^{18}O$ record as being related to lake desiccation, but the $\delta^{18}O$ values of Lake Hope otoliths increases by 10-15‰ over 3-4 years (Long et al., 2018), whereas the $\delta^{18}O$ values of the Mungo hearth otoliths only increase by ~ 4‰ over 7-10 years (Fig. 6.2). By modelling the effect of flooding and evaporation on water $\delta^{18}O$ values and levels in the Willandra Lakes system, an alternate interpretation of the Mungo hearth otolith O isotopes records can be made. Golden perch are a hardy fish that can survive in extremes of salinity and temperature (Harris and Rowland, 1996) and recover quickly from acute stress as well as acclimatising quickly to conditions of chronic stress (Carragher and Rees, 1994). This suggests that golden perch could survive for a long time in an evaporating lake, and hence preserve a long evaporative trend record in their otolith $\delta^{18}O$ values.

The original interpretation of the 4‰ increase in otolith $\delta^{18}O$ values was that they represented a drying trend prior to fish being caught and eaten (Long et al., 2014). The lake was thought to have been cut off from the river system, evaporation caused lake levels to drop and increased salinity caused the fish to become sluggish and easy prey for past human occupants (Bowler 1998; Long et al., 2014). The modelled results for the change in Lake Mungo $\delta^{18}O_{H2O}$ values when inflow is cut off and evaporation allowed to proceed unimpeded tell a different story. During the period represented by the fish bone hearths, Lake Mungo was unlikely to have been cut off from the lake system and evaporating to dryness. Indeed, the pelletal clays found in this layer would only have formed if at least some water was present in the lake basin, if the lake is completely dry, clay deposition on the lunette would cease (Bowler, 1973). As shown in Figure 6.5, if Lake Mungo is cut off from the system after a period of relative stability the $\delta^{18}O$ value of the water increases dramatically. This increase is faster and more extreme than that recorded in the hearth otoliths, even considering that the fish died prior to the lake evaporating to dryness (captured by humans) and taking into account the offset in $\delta^{18}O$ values between otoliths and water due to temperature (~1‰ for every 4°C change in temperature; Kalish, 1991). A change of the magnitude suggested by the modelled desiccation scenario would be recorded in the otoliths of any fish living in the water at the time. The alternating pelletal clays and quartz sand of Unit E (Arumpo/Zanci) indicate

periodic flooding and drying, where water is unlikely to be lost from the lake basin entirely. This suggests that the lake was not evaporating to dryness but experiencing periodic fluctuations as the presence of water is necessary in the formation of the clay portion of the sediments in which the otoliths were found.

6.3.2 Lake Mungo: no lake level change

Some have described the Willandra Lakes during the Last Glacial Maximum as lacking in surface water and so windy and dusty that people abandoned the region (e.g. Allen and Holdaway, 2009). However, the sand and clays of the Lake Mungo lunette that formed during the LGM suggest that the lake levels varied between higher stable water levels and periods of drying which exposed the lake floor (Fitzsimmons et al., 2014; Stern et al., 2015). At least periodically water was plentiful during the LGM. Records of high lake levels during the LGM are not unique to Lake Mungo. Other lakes including Lake Urana (Page et al., 1994), Lake Kanyapella on the Murray river (Bowler, 1967, 1978) and Lake Nekeeya near the Grampians (Bowler, 1999) all remained full during the LGM due to the efficient nature of their catchments (Bowler et al., 2012).

The 4‰ change in the $\delta^{18}O$ values of the hearth otoliths could be the result of a full lake in mass balance where the $\delta^{18}O$ value of the water was increasing towards isotopic equilibrium with respect to the $\delta^{18}O$ values of incoming and outgoing water. As shown in Figure 6.5, when the lakes in the system are filled rapidly, by floodwaters for example, then maintained that level in mass balance between incoming and outgoing water, the isotope values of the water increase towards equilibrium with respect to the $\delta^{18}O$ values of the incoming and outgoing water. The degree and rate of change in the modelled lake water $\delta^{18}O$ value is very similar to the degree and rate of change in the $\delta^{18}O_{CaCO3}$ values of the Lake Mungo hearth otoliths (Fig. 6.2). Over 20 years of these mass balance conditions, the $\delta^{18}O$ of Lake Mungo water in the model increased by ~ 16‰ (Fig. 6.5). From 0 years to 7 – 10 years there was a 10 – 14 ‰ increase in $\delta^{18}O$ values. The total change in $\delta^{18}O_{CaCO3}$ values across the hearth otoliths is between 5 and 16‰ over 8 – 13 years. Otolith 926-1 records a change of 16‰ over 10 years. The level of the lake does not need to decrease for an increasing trend to be recorded in water $\delta^{18}O$ values (Fig. 6.5). This trend would have been recorded in the otoliths of fish living in the lake at the time and, given the similarities between the increase in the modelled water $\delta^{18}O$

values and in the otoliths may well be what was happening at Lake Mungo 20,000 years ago.

6.3.3 Seasonal lake level changes

The Last Glacial Maximum at Lake Mungo was a period of indeterminate hydrological conditions. The stratigraphic unit which straddles the LGM (Unit E, Arumpo/Zanci) contains alternating layers of quartz sand, indicating lake full conditions, and pelletal clay, indicating periods of drying and exposure of the lake floor. Together this alternating sediment formation suggests intermittent periods of stabilisation of lake levels followed by short term drying. However, as noted above the pelletal clays still indicate the presence of at least some water in the lake. Defining the periodicity of these clay and quartz dune increments or finding a proxy for the lake level conditions is essential for understanding how past hydrological conditions affected human habitants within their lifetimes.

The increasing trend in otolith $\delta^{18}O_{CaCO3}$ values could be recording a short term or periodic drop in lake level or as described above could be recording water $\delta^{18}O$ values approaching isotopic equilibrium, with respect to the $\delta^{18}O$ values of incoming and outgoing water, without concomitant change in lake level. Due to the narrowness of the otolith outer increments we can't pick up seasonal fluctuations in these outer otolith layers, but that doesn't mean that seasonal fluctuations weren't present.

In the earlier, subadult portion of the otoliths, there are some fluctuations that suggest seasonal cycles of changing water $\delta^{18}O$ values and/or temperatures. The lowest and highest hearth otolith $\delta^{18}O$ results for every ~6 months of otolith growth are illustrated in Figure 6.8 to better show these seasonal or near seasonal fluctuations.

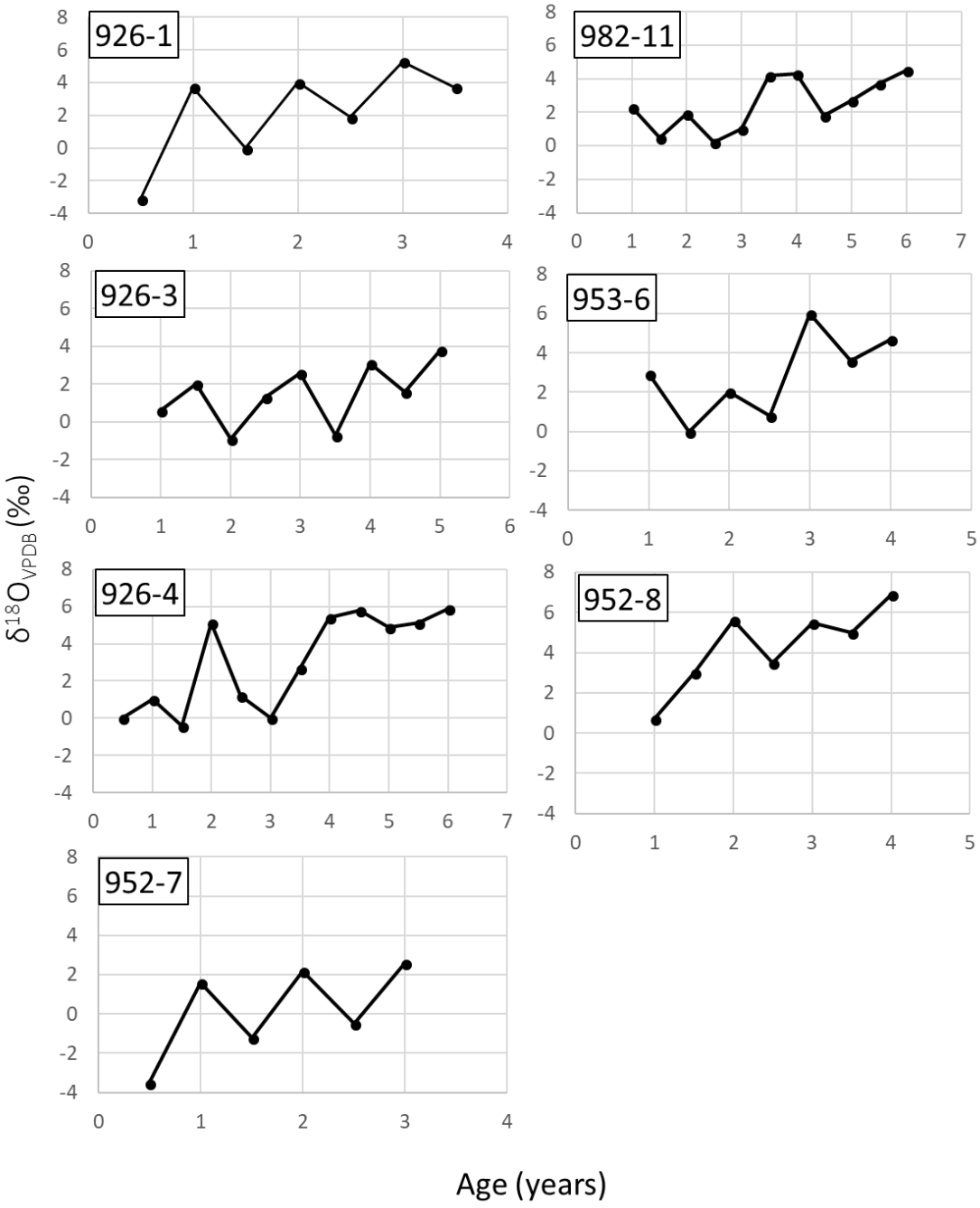

Figure 6.8: Hearth otolith $\delta^{18}O$ values related to the subadult portion of growth. Only the $\delta^{18}O$ values recorded every 6 months are included to examine sub-annual increases and decreases and pick out possible seasonal trends.

If the fluctuations in $\delta^{18}O_{CaCO3}$ values were due solely to temperature change, the range would be 1-2‰ (Chapter 4; Kalish 1991; Patterson et al., 1993) which is observed in some otoliths (e.g. 926-3). In most, however, the change within a year of growth is much larger, 3-5‰. This suggests that there is a seasonal change in ambient water composition that has a greater effect on the otolith $\delta^{18}O_{CaCO3}$ values overriding the expected temperature signal. It could be that during the LGM the lake system received seasonal snow melt from the South Eastern Highlands via the

Lachlan River. This would have resulted in waters with lower $\delta^{18}O$ values, diluting the lake waters and causing a short-term decrease in $\delta^{18}O$ values followed by progressive enrichment as evaporation resumed. These freshwater pulses may not have been seasonal prior to the LGM but further information is needed for clarification. The results from this modelling study do not rule out the possibility that Lake Mungo was experiencing short term seasonal drying or flooding, it merely rules out that the lake was cut off from the river system and evaporating to dryness.

6.3.4 Lake Mungo human occupation and fishing

The results of this simple modelling study may have some interesting implications for interpretations of human occupation, fishing practices and lake level change during the LGM. The hypothesis that people were taking advantage of sluggish oxygen starved, golden perch following a period of marked evaporation after Lake Mungo was cut off from the other lakes in the system is not supported by the $\delta^{18}O$ record preserved in the hearth otoliths. Other theories for fish collection and human lifestyles must be considered.

In modern systems, golden perch do not naturally congregate near the shoreline of lakes. They inhabit deep pools with woody debris, undercut banks or rocky ledges (Cadwallader, 1979; Battaglene and Prokop, 1987) and are usually fished using rods from small boats. This means that unless the entire lake was shallow enough for wading; spearfishing from the shoreline is unlikely. The results of the mass balance model presented here (Fig. 6.6) indicate that if the lake was maintained at the lower levels, 1m (shallow enough for wading in the outer edges of the lake) then the increase in $\delta^{18}O$ values of the water is still too rapid and too high (>10‰ in 1 year) for what has been recorded in the otoliths. From this it could be inferred that the lake was not shallow enough for wading when these fish were caught. A recent paper by Fitzsimmons et al., (2015) suggests that just prior to the LGM Lake Mungo experienced a Mega Lake Event (up to 5 m deeper than preceding or subsequent lake full events) and evidence for human presence on a small island near the Lake Leaghur water inlet implies the use of water craft. Neither the present modelling study nor the research on the Mega Lake Event can definitively support or provide evidence for the use of water craft at Lake Mungo but it is a theory that warrants further consideration.

6.4 Conclusions

Following this reappraisal of the $\delta^{18}O$ records preserved in the otoliths of golden perch it is possible to conclude with some confidence that these fish did not die in a lake that was cut off from the river system and evaporating to dryness. This was not the final lake desiccation trend. There is the possibility that lake levels remained stable whilst the fish were living there and that the increase in the $\delta^{18}O_{CaCO3}$ values was a result of the ambient water approaching isotopic balance, with respect to the $\delta^{18}O$ values of the incoming and outgoing water. There is also the possibility that this was a short-term evaporation event, as opposed to a final desiccation trend, where the lake was cut off and evaporating to dryness.

Fluctuations in the $\delta^{18}O_{CaCO3}$ values of the otoliths when the fish were young appear to be seasonal and related to changes in ambient water composition rather than temperature. Improved analytical and otolith preparation methods are required to confirm the seasonality of such fluctuations in future studies.

This study demonstrates the value of a quantitative approach using a relatively simple model to provide new insight and update interpretations of lake level records from archaeological sites.

7. Summary of Key Findings, Conclusions and Future Directions

The two main aims of the present study were to validate the use of O isotopes and trace elements (Ba and Sr) in modern golden perch otoliths for reconstructing a record of evaporation and flooding events and to apply these techniques to the archaeological and environmental history of Lake Mungo. This study also tested different methods for otolith preparation and settled on an improved methodology (Chapter 3) for creating SHRIMP-suitable mounts of multiple thin sections of otoliths with age increments clearly visible and exposed with relevant standards on the surface. The improved preparation methods meant that multiple analyses could be taken across the same area of the otoliths, with no polishing in between, allowing close association between age increments, $\delta^{18}O$ values (both SHRIMP and DI-MS) and trace element (LA-ICPMS) measurements.

The work described here has demonstrated that golden perch, as with other fish species, have otoliths that form in near O isotope equilibrium with the surrounding water, a slight offset between water and otolith $\delta^{18}O$ values resulting from the temperature dependent isotopic fractionation (Chapter 4). In Chapter 4, the relationship between water $\delta^{18}O$ values, temperature and golden perch otolith $\delta^{18}O$ values was validated based on records from fish living in tanks under known conditions. Changes in Sr/Ca and Ba/Ca ratios across the otoliths from these fish could be used to distinguish between early life in the river and later life in the tank, but the clearest change was in otolith $\delta^{18}O_{CaCO3}$ values, which dropped sharply with tank entry. A few otoliths displayed possible seasonal fluctuations in $\delta^{18}O_{CaCO3}$ values that seemed to match up with dark and light otolith banding formation, but these were not consistently found in all otoliths.

It was found that oxygen isotopes in otoliths can provide a detailed record of evaporation and flooding events, (Long et al., 2018). Otoliths from fish that died in the desiccating Lake Hope had $\delta^{18}O$ profiles reflecting earlier floods, and the progressive evaporation of the lake. The otolith Sr/Ca ratios started to follow the $\delta^{18}O$ trend only after evaporation is well advanced, probably after the fish became stressed. The examination of $\delta^{18}O$ values across the otoliths of wild golden perch fish otoliths caught from a single location, downstream of Lake Menindee, at the same time, December 2005 (Chapter 5), supports the finding of Chapter 4 concerning the relationship between golden perch $\delta^{18}O_{CaCO3}$ values, ambient water

$\delta^{18}O_{H2O}$ values and temperature. Noting that the temperature and water composition was not as well constrained as in the Narrandera tanks study. The Menindee otoliths display very similar trends in their $\delta^{18}O_{CaCO3}$ values, picking up the strong flooding and evaporation regime present in the Barwon-Darling River system of the time period. However, there were offsets between the timing of these flooding and evaporation events that warrant further investigations with better constrained, more detailed environmental and fish migration information. Similar to Long et al., (2018) Sr/Ca ratios in the Menindee otoliths (Chapter 5) tended to track closely with the $\delta^{18}O_{CaCO3}$ values during evaporation events but also seemed to track with the $\delta^{18}O_{CaCO3}$ values throughout the otolith record.

Both the tank study in Chapter 4 and the Menindee lakes study in Chapter 5 identified co-fluctuations between Sr/Ca and Ba/Ca ratios in the subadult portion of the otoliths. This and the high Ba/Ca ratios in the subadult portions of all otoliths, ancient and modern alike, seem to be ontogenetically related.

Oxygen isotope and trace element analyses were applied to otoliths related to the earliest period of human occupation of Lake Mungo (Long et al., 2018). Otoliths excavated from the shorelines of Lake Mungo in the 1970s were dated to between 37 – 42 cal kBP which supported previous OSL dating for the same section. Most of the $\delta^{18}O_{CaCO3}$ profiles across these ancient otoliths were relatively stable, with no evidence of significant lake flooding or drying. Sr/Ca ratios were similarly stable, indicating that over a period of 5 ka evaporation and inflow remained in relative balance. Peaks in Ba/Ca ratios in the subadult portion of the otolith suggest a biological relationship, but this warrants further study/investigation in a wider range of samples. An evaporation trend and increasing Sr/Ca ratios were identified in one ancient Mungo otolith, dated to 19.3 cal kBP, which was consistent with other evidence for Lake Mungo being subject to periods of drying at this time.

A simple mass balance model was successfully constructed and used to test scenarios of lake level change and evaporation for their influence on ambient water $\delta^{18}O$ (Chapter 6). Re-examination of the hearth otolith $\delta^{18}O$ records (from Long et al., 2014), considering the mass balance modelling results, suggests that these fish did not die in a lake that was cut off from the other lakes in the system and evaporating to dryness. It does, however, support the possibility that the lake was undergoing a short-term possibly seasonal evaporation trend or that the lake levels

were stable and the increase in the otolith $\delta^{18}O_{CaCO3}$ values was reflecting water $\delta^{18}O$ values increasing in an approach to isotopic equilibrium, with respect to the $\delta^{18}O$ of incoming and outgoing water.

Otoliths from freshwater fish may not provide palaeotemperatures but arguably the record of evaporation and flooding that is preserved in golden perch otoliths is of greater importance. At the site of Lake Mungo flooding and drying cycles helped to rejuvenate the system leading to an abundance of flora and fauna and are likely to be directly related to the timing and length of human occupation in the region.

Overall the results of the work described here demonstrate that the chemical and $\delta^{18}O_{CaCO3}$ values of otoliths from inland archaeological sites is a valuable tool for reconstructing past evaporation and flooding events, but temperature information remains elusive. Ongoing work in the area of clumped isotope analysis (e.g. Ghosh et al., 2007) offers a way of untangling past temperature from otolith oxygen isotope records, which as shown here for inland freshwater sites, are strongly affected by changes in the ambient water composition (either with fish migration and/or evaporation and flooding events).

Areas for future work:

- A closer study of the relationship between trace elements in otoliths and in the water is required. We developed a broad understanding of how the Sr/Ca and Ba/Ca ratios in golden perch otoliths fluctuate with evaporation, flooding and temperature but examining these in further detail might permit the generation of migration maps for the ambient water chemistry and distinguish between changes in otolith Ba/Ca and Sr/Ca arising from changes in ambient water chemistry vs possible biological effects.
- At Lake Mungo:
    - comparison between microchemical measurements across otoliths of different species from the same hearth/sedimentary layer, this would be especially valuable if one species occupies a different river/lake zone from the other or has narrower tolerances regarding salinity and temperature.
    - comparison between the $\delta^{18}O$ values in shells (mussels or snail shells) and those of otoliths within the same sedimentary unit/hearth site or that can be closely related in space and time. Shells can be limited to

one area i.e. a lake and provide a way of controlling more variables. Unfortunately, they don't occur through the whole lake system and age lines are not always as clear as those in the golden perch otoliths.

- Further lake level modelling work – can the simple mass balance model presented here be improved to test other scenarios for lake level and changing water $\delta^{18}O$ values? Can seasonal influence be taken into account?

8. References

Alibert, C., Kinsley, L., Fallon, S.J., McCulloch, M.T., Berkelmans, R., McAllister, F., 2003. Source of trace element variability in Great Barrier Reef corals affected by the Burdekin flood plumes. Geochimica et cosmochimica acta. 67(2), 231–246.

Allemand, D., Mayer-Gostan, N., De Pontual, H., Boeuf, G., Payan, P., 2007. Fish otolith calcification in relation to endolymph chemistry. In: Bauerlein, E., (Ed.) Handbook of Biomineralization. Weinheim, Germany, 291–308.

Allen, H. and Holdaway, S. 2009. The archaeology of Mungo and the Willandra Lakes: looking back, looking forward. Archaeology in Oceania. 44(2), 96–106.

Anderson, J.R., Morison, A.K., Ray, D.J.,1992a. Age and growth of Murray Cod, *Maccullochella peelii* (Perciformes: Percichthyidae), in the lower Murray-Darling Basin, Australia, from thin-sectioned otoliths. Australian Journal of Marine and Freshwater Research. 43(5), 983–1013.

Anderson, J.R., Morison, A.K., Ray, D.J.,1992b. Validation of the Use of Thin-sectioned Otoliths for Determining the Age and Growth of Golden Perch, *Macquaria ambigua* (Perciformes: Percichthyidae), in the Lower Murray-Darling Basin, Australia. Australian Journal of Marine and Freshwater Resources. 43(5), 1103–1128.

Andrus, C.F.T., Crowe, D.E., Sandweiss, D.H., Reitz, E.J., Romanek, C.S., 2002. Otolith $\delta^{18}O$ record of mid-Holocene sea surface temperatures in Peru. Science, 295(5559), 1508–1511.

Andrus, C. F. T. and Crowe, D. E. 2002. Alteration of otolith aragonite: effects of prehistoric cooking methods on otolith chemistry. Journal of Archaeological science. 29(3), 291–299.

Andrus, C.F.T. 2011. Shell midden sclerochronology. Quaternary Science Reviews. 30(21–22), 2892–2905.

Arai, T. 2010. Effect of salinity on strontium: calcium ratios in the otoliths of Sakhalin taimen, *Hucho perryi*. Fisheries Science. 76(3), 451–455.

Aubert, M., Williams, I.S., Boljkovac, K., Moffat, I., Moncel, M.H., Dufour, E., Grün, R., 2012. In situ oxygen isotope micro-analysis of faunal material and human teeth using a SHRIMP II: a new tool for palaeo-ecology and archaeology. Journal of Archaeological Science. 39(10), 3184–3194.

Bastow, T.P., Jackson, G., Edmonds, J.S., 2002, Elevated salinity and isotopic composition of fish otolith carbonated stock delineation of pink snapper, *Pagrus aurutus*, in Shark Bay, Western Australia. Marine Biology. 141(5), 801–806

Bath, G.E., Thorrold, S.R., Jones, C.M., Campana, S.E., McLaren, J.W., Lam, J.W., 2000. Strontium and barium uptake in aragonitic otoliths of marine fish. Geochimica et cosmochimica acta. 64(10), 1705–1714.

Battaglene, S. and Prokop, F. 1987. Golden Perch, Agfacts F3.2.2, Grafton, Australia: Department of Agriculture New South Wales.

Beckman, D. W. and Wilson, C. A. 1995. Seasonal timing of opaque zone formation in fish otoliths. In: Secor, D. H., Dean, J. M., and Campana, S. E. (Eds.) Recent developments in fish otolith research. Columbia: University of South Carolina Press. 27–44.

Bell, W. T. 1991. Thermoluminescence dates for the Lake Mungo aboriginal fireplaces and the implications for radiocarbon dating. Archaeometry. 33(1), 43–50.

Blacker, R. W. 1974. Recent advances in otolith studies. Sea fisheries research. 67–90.

Boehlert, G. W. 1985. Using objective criteria and multiple regression models for age determination in fishes. Fishery Bulletin. 83(2), 103–117.

Boljkovac, K. 2009. In situ SHRIMP $\delta^{18}O$ and laser ablation ICP-MS Sr/Ca and $^{87}Sr/^{86}Sr$

measurements in fossil otoliths for palaeoclimate reconstructions at the Willandra Lakes World Heritage Area. Unpublished honours thesis, Australian National University, Canberra.

Bowler, J. M. 1967. Quaternary chronology of Goulburn Valley sediments and their correlation in Southeastern Australia. Journal of the Geological Society of Australia. 14(2), 287–292.

Bowler, J.M., Jones, R., Allen, H., Thorne, A.G., 1970. Pleistocene human remains from Australia: a living site and human cremation from Lake Mungo, western New South Wales. World Archaeology. 2(1), 39–60.

Bowler, J. M. 1971. Pleistocene Salinities and Climate Change: Evidence from Lakes and Lunettes in Southeastern Australia. In: Mulvaney, D. J., Golson, J. (Eds.) Aboriginal Man and Environment in Australia, Canberra: Australian National University Press. 46-65

Bowler, J. M. 1973. Clay Dunes: their occurrence, formation and environmental significance. Earth-Science Reviews. 9(4), 315–338.

Bowler, J. M. 1976. Aridity in Australia: Age, origins and expression in aeolian landforms and sediments. Earth-Science Reviews. 12(2–3), 279–310.

Bowler, J. M. 1978. Quaternary climate and tectonics in the evolution of the Riverine Plain, southeastern Australia. In: Davies, J. L., Williams, M. A. J. (Eds.) Landform evolution in Australasia. Canberra: Australian National University Press. 70–112.

Bowler, J. M. 1998. Willandra Lakes revisited: environmental framework for human occupation. Archaeology in Oceania. 33(3), 120–155.

Bowler, J. M. and Price, D. M. 1998. Luminescence dates and stratigraphic analyses at Lake Mungo: review and new perspectives. Archaeology of Oceania. 33(3), 156–168.

Bowler, J. M. 1999. Nekeeya Lunette Assessment Study: Geomorphology, origins and evolution of the Nekeeya sand lunette. Report to Aboriginal Affairs Victoria.

Bowler, J.M., Johnston, H., Olley, J.M., Prescott, J.R., Roberts, R.G., Shawcross, W., Spooner, N.A., 2003. New Ages for human occupation and climatic change at Lake Mungo, Australia. Nature. 421(6925), 837–840.

Bowler, J.M., Gillespie, R., Johnston, H., Boljkovac, K., 2012. Wind v Water: glacial maximum records from the Willandra Lakes. In: Haberle, S. G., David, B. (Eds.) Peopled landscapes: archaeological and biogeographic approaches to landscapes. terra australis. 34, Canberra: Australian National University Press. 271–296.

Brothers, E.B., Williams, D.M. and Sale, P.F., 1983. Length of larval life in twelve families of fishes at "One Tree Lagoon", Great Barrier Reef, Australia. Marine Biology. 76(3), 319–324.

Brown, P. and Wooden, I. 2007. Age at first increment formation and validation of daily growth increments in golden perch (*Macquaria ambigua*: Percichthyidae) otoliths. New Zealand Journal of Marine and Freshwater Research. 41(2), 157–161.

Brown, R. J. and Severin, K. P. 2009. Otolith chemistry analyses indicate that water Sr:Ca is the primary factor influencing otolith Sr:Ca for freshwater and diadromous fish but not for marine fish. Canadian Journal of Fisheries and Aquatic Sciences. 66(10), 1790–1808.

Cadwallader, P. L. 1979. Distribution of native and introduced fish in the Seven Creeks River System, Victoria. Australian Journal of Ecology. 4(4), 361–385.

Campana, S. E. 1984. Interactive effects of age and environmental modifiers on the production of daily growth increments in otoliths of plainfin midshipman, *Porichthys notatus*. Fishery Bulletin. 82(1), 165–177.

Campana, S. E. 1999. Chemistry and composition of fish otoliths: pathways, mechanisms and applications. Marine Ecology Progress Series. 188, 263–297.

Campana, S. E. 2001. Accuracy, precision and quality control in age determination, including a

review of the use and abuse of age validation methods. Journal of Fish Biology. 59(2), 197–242.

Capo, R.C., Stewart, B.W., Chadwick, O.A. 1998. Strontium isotopes as tracers of ecosystem processes: theory and methods. Geoderma. 82(1–3), 197–225.

Carpenter, S.J., Erickson, J.M., Holland Jr, F.D. 2003. Migration of a Late Cretaceous fish. 423, 70–74.

Carragher, J. F. and Rees, C. M., 1994. Primary and secondary stress responses in golden perch, *Macquaria ambigua*. Comparative Biochemistry and Physiology Part A: Physiology. 107(1), 49–56.

Carré, M., Bentaleb, I., Blamart, D., Ogle, N., Cardenas, F., Zevallos, S., Kalin, R.M., Ortlieb, L. and Fontugne, M. 2005. Stable isotopes and sclerochronology of the bivalve *Mesodesma donacium*: Potential application to Peruvian paleoceanographic reconstructions. Palaeogeography, Palaeoclimatology, Palaeoecology. 228(1–2), 4–25.

Chang, C. W., Lin, S., Iizuka, Y., Tzeng, W. 2004. Relationship between Sr:Ca ratios in otoliths of grey mullet *Mugil cephalus* and ambient salinity: validation, mechanisms, and applications. Zoological Studies. 43(1), 74–85.

Chesney, E.J., McKee, B.M., Blanchard, T., Chan, L.H., 1998. Chemistry of otoliths from juvenile menhaden *Brevoortia patronus:* evaluating strontium, strontium:calcium and strontium isotope ratios as environmental indicators. Marine Ecology Progress Series. 171, 261–273

Choat, J. H. and Axe, L. M. 1996. Growth and longevity in acanthurid fishes; an analysis of otolith increments. Marine Ecology Progress Series. Inter-Research Science Center. 15–26.

Chowdhury, M. J. and Blust, R., 2001. A mechanistic model for the uptake of waterborne strontium in the common carp (*Cyprinus carpio* L.). Environmental science & technology. 35(4), 669–675.

Chowdhury, M. J. and Blust, R. 2011. Strontium. In: Wood, C. M., Farrell, A. P., Brauner, C. J., (Eds.) Fish Physiology, 31 Part B, 351–390.

Clarke, A.D., Telmer, K.H., Shrimpton, J.M., 2015. Movement patterns of fish revealed by otolith microchemistry: a comparison of putative migratory and resident species. Environmental Biology of Fishes. 98(6), 1583–1597.

Cohen, T.J., Nanson, G.C., Jansen, J.D., Jones, B.G., Jacobs, Z., Larsen, J.R., May, J.H., Treble, P., Price, D.M., Smith, A.M., 2012. Late Quaternary mega-lakes fed by the northern and southern river systems of central Australia: Varying moisture sources and increased continental aridity. Palaeogeography, Palaeoclimatology, Palaeoecology. 356–357, 89–108.

Collingsworth, P.D., Van Tassell, J.J., Olesik, J.W., Marschall, E.A., 2010. Effects of temperature and elemental concentration on the chemical composition of juvenile yellow perch (*Perca flavescens*) otoliths. Canadian Journal of Fisheries and Aquatic Sciences 67(7), 1187–1196.

Colonese, A.C., Netto, S.A., Francisco, A.S., DeBlasis, P., Villagran, X.S., Ponzoni, R.D.A.R., Hancock, Y., Hausmann, N., de Farias, D.S.E., Prendergast, A., Schöne, B.R., 2017. Shell sclerochronology and stable isotopes of the bivalve *Anomalocardia flexuosa* (Linnaeus, 1767) from southern Brazil: implications for environmental and archaeological studies. Palaeogeography, Palaeoclimatology, Palaeoecology. 484, 7–21.

Cook, P.K., Dufour, E., Languille, M.A., Mocuta, C., Réguer, S., Bertrand, L. 2016. Strontium speciation in archaeological otoliths. Journal of Analytical Atomic Spectrometry. 31(3), 700–711.

Coplen, T.B., 1996, New guidelines for reporting of the stable hydrogen, carbon, and oxygen isotope ratio data. Geochimica et Cosmochimica Acta. 60(17), 3359–3360.

Dalai, T.K., Krishnaswami, S., Sarin, M.M., 2002. Barium in the Yamuna River System in the Himalaya: sources, fluxes, and its behavior during weathering and transport.

Geochemistry, Geophysics, Geosystems. 3(12), 1–23.

Dansgaard, W., 1954, The O18-abundance in fresh water, Geochimica et Cosmochimica Acta. 6(5-6), 241–260

Dansgaard, W., 1964, Stable isotopes in precipitation, Tellus. 16(4), 436–468

Davies, N.M., Gauldie, R.W., Crane, S.A., Thompson, R.K., 1988. Otolith ultrastructure of smooth oreo, *Pseudocyttus maculatus,* and black oreo, *Allocyttus sp*., species. Fish Bulletin. 86(3), 499–515.

Dietzel, M., Gussone, N., Eisenhauer, A., 2004. Co-precipitation of Sr^{2+} and Ba^{2+} with aragonite by membrane diffusion of CO_2 between 10 and 50 °C. Chemical Geology. Elsevier. 203(1–2), 139–151.

Dinçer, T. 1968. The Use of oxygen 18 and deuterium concentrations in the water balance of lakes. Water Resources Research. 4(6), 1289–1306.

Diouf, K., Panfili, J., Labonne, M., Aliaume, C., Tomás, J., Do Chi, T., 2006. Effects of salinity on strontium:calcium ratios in the otoliths of the West African black-chinned tilapia *Sarotherodon melanotheron* in a hypersaline estuary. Environmental Biology of Fishes. 77(1), 9–20.

Disspain, M. 2009. Using archaeological otoliths to determine palaeoenvironmental change and Ngarrindjeri resource use in the Coorong and Lower Murray, South Australia. Unpublished honours thesis, Flinders University, Adelaide.

Disspain, M., Wallis, L.A., Gillanders, B.M., 2011. Developing baseline data to understand environmental change: a geochemical study of archaeological otoliths from the Coorong, South Australia. Journal of Archaeological science. 38(8), 1842–1857.

Disspain, M.C., Ulm, S., Izzo, C., Gillanders, B.M., 2016. Do fish remains provide reliable palaeoenvironmental records? An examination of the effects of cooking on the morphology and chemistry of fish otoliths, vertebrae and scales. Journal of Archaeological Science. 74, 45–59.

Dorval, E., Jones, C.M., Hannigan, R., Montfrans, J.V., 2007. Relating otolith chemistry to surface water chemistry in a coastal plain estuary. Canadian Journal of Fisheries and Aquatic Sciences, 64(3) 411–424.

Dorval, E., Piner, K., Robertson, L., Reiss, C.S., Javor, B., Vetter, R., 2011. Temperature record in the oxygen stable isotopes of Pacific sardine otoliths: Experimental vs. wild stocks from the Southern California Bight. Journal of Experimental Marine Biology and Ecology. 397(2), 136–143.

Doubleday, Z.A., Izzo, C., Woodcock, S.H., Gillanders, B.M., 2013. Relative contribution of water and diet to otolith chemistry in freshwater fish. Aquatic Biology. 18(3), 271–280.

Dufour, V., Pierre, C., Rancher, J., 1998. Stable isotopes in fish otoliths discriminate between lagoonal and oceanic residents of Taiaro Atoll (Tuamotu Archipelago, French Polynesia). Coral Reefs. 17(1), 23–28.

Ebner, B.C., Scholz, O., Gawne, B., 2009. Golden perch *Macquaria ambigua* are flexible spawners in the Darling River, Australia. New Zealand Journal of Marine and Freshwater Research. 43(2), 571–578.

Edmonds, J. S. and Fletcher, W. J. 1997. Stock discrimination of pilchards *Sardinops sagax* by stable isotope ratio anlaysis of otolith carbonate. Marine Ecology Progress Series. 152, 241–247.

Edwards, T. W. D. 2004. Use of water isotope tracers in high latitude hydrology and paleohydrology. In: P, S. J., Pienitz, R., Douglas, M. S. V., (Eds.) Long-term environmental change in Arctic and Antarctic lakes. Springer, Dordecht. 187–207.

Eggins, S.M., Kinsley, L.P.J., Shelley, J.M.G., 1998. Deposition and element fractionation processes during atmospheric pressure laser sampling for analysis by ICP-MS. Applied Surface

Science. 127, 278–286.

Elsdon, T. S. and Gillanders, B. M. 2002. Interactive effects of temperature and salinity on otolith chemistry: challenges for determining environmental histories of fish. Canadian Journal of Fisheries and Aquatic Sciences 59(11), 1796–1808.

Elsdon, T. S. and Gillanders, B. M. 2003. Reconstructing migratory patterns of fish based on environmental influences on otolith chemistry. Reviews in Fish Biology and Fisheries. 13(3), 217–235.

Elsdon, T. S. and Gillanders, B. M. 2004. Fish otolith chemistry influenced by exposure to multiple environmental variables. Journal of experimental marine biology and ecology. 313(2), 269–284.

Elsdon, T. S. and Gillanders, B. M. 2005a. Consistency of patterns between laboratory experiments and field collected fish in otolith chemistry: an example and applications for salinity reconstructions. Marine and Freshwater Research. 56(5), 609–617.

Elsdon, T. S. and Gillanders, B. M. 2005b. Alternative life-history patterns of estuarine fish: barium in otoliths elucidates freshwater residency. Canadian Journal of Fisheries and Aquatic Sciences. 62(5), 1143–1152.

Epstein, S., Buchsbaum, R., Lowenstam, H., Urey, H.C. 1951. Carbonate-water isotopic temperature scale. Geological Society of America Bulletin, 62(4), 417–426.

Epstein, S., Buchsbaum, R., Lowenstam, H.A., Urey, H.C., 1953. Revised carbonate-water isotopic temperature scale. Geological Society of America Bulletin. 64(11), 1315–1326.

Epstein, S and Mayeda, T., 1953, Variation of O^{18} content of waters from natural sources, Geochimica et Cosmochimica Acta. 4, 213–224.

Fablet, R., Pecquerie, L., De Pontual, H., Høie, H., Millner, R., Mosegaard, H., Kooijman, S.A., 2011. Shedding light on fish otolith biomineralization using a bioenergetic approach. PLoS ONE. 6(11), 1–7.

Farrell, J. and Campana, S. E. 1996. Regulation of calcium and strontium deposition on the otoliths of juvenile tilapia, *Oreochromis niloticus*. Comparative Biochemistry and Physiology Part A: Physiology. 115(2), 103–110.

Faulks, L.K., Gilligan, D.M., Beheregaray, L.B., 2010. Islands of water in a sea of dry land: hydrological regime predicts genetic diversity and dispersal in a widespread fish from Australia's arid zone, the golden perch (*Macquaria ambigua*). Molecular ecology. 19(21), 4723–4737.

Faure, G. and Mensing, T. M. 2005. Isotopes Principles and Applications. Wiley, Hoboken

Fitzsimmons, K.E., Stern, N. and Murray-Wallace, C.V., 2014. Depositional history and archaeology of the central Lake Mungo lunette, Willandra Lakes, southeast Australia. Journal of Archaeological Science. 41, 349–364.

Fitzsimmons, K.E., Stern, N., Murray-Wallace, C.V., Truscott, W., Pop, C., 2015. The Mungo mega-lake event, semi-arid Australia: non-linear descent into the last ice age, implications for human behaviour. PLoS ONE. 10(6), 1–19.

Fontes, J. C. and Gonfiantini, R., 1967, Comportement isotopique au cours de l'evaporation de deux bassins sahariens. Earth and Planetary Science Letters. 3, 258–266.

Fowler, A.J., Campana, S.E., Thorrold, S.R., Jones, C.M., 1995. Experimental assessment of the effect of temperature and salinity on elemental composition of otoliths using laser ablation ICPMS. Canadian Journal of Fisheries and Aquatic Sciences. 52(7), 1431–1441.

Francis, R. I. C. C. and Campana, S. E. 2004. Inferring age from otolith measurements: a review and a new approach. Canadian Journal of Fisheries and Aquatic Sciences. 61(7), 1269–1284.

Fraser, R.A., Grün, R., Privat, K., Gagan, M.K., 2008. Stable-isotope microprofiling of wombat tooth

enamel records seasonal changes in vegetation and environmental conditions in eastern Australia. Palaeogeography, Palaeoclimatology, Palaeoecology. 269(1–2), 66–77.

Fricke, H.C., O'Neil, J.R., Lynnerup, N., 1995, SPECIAL REPORT: Oxygen isotope composition of human tooth enamel from medieval Greenland: linking climate and society. Geology. 23(10), 869–872.

Friedman, I. and O 'Neil, J. R. 1977. Compilation of stable isotope fractionation factors of geochemical interest. In: Fleischer, M. (Ed.) Data of Geochemistry Sixth Edition. US Government Printing Office KK1-KK12.

Froehlich, K.F.O., Gonfiantini, R. and Rozanski, K., 2005. Isotopes in lake studies: A historical Perspective. In: Aggarwal P.K., Gat J.R., Froehlich K.F. (Eds.) Isotopes in the water cycle. Springer, Dordrechtin, 139–150.

Gaetani, G. A. and Cohen, A. L. 2006. Element partitioning during precipitation of aragonite from seawater: a framework for understanding paleoproxies. Geochimica et Cosmochimica Acta. 70(18), 4617–4634.

Gaillardet, J., Viers, J., Dupré, B., 2003. Trace elements in river waters. Treatise on geochemistry, Volume 5. 225–272.

Gat, J. R. and Levy, Y. 1978. Isotope Hydrology of Inland Sabkhas in the Bardawil Area, Sinai. Limnology and Oceanography. 23(5), 841–850.

Gat, J. R. and Gonfiantini, R. 1981. Stable isotope hydrology: deuterium and oxygen-18 in the water cycle. IAEA (International Atomic Energy Agency) Technical report, 210, Vienna

Gat, J. R. 1995. Stable Isotopes of fresh and saline lakes. In: Lerman A., Imboden D.M., Gat J.R. (Eds.) Physics and Chemistry of Lakes. Springer, Berlin, Heidelberg139–163.

Gauldie, R. W. and Nelson, D. G. A. 1990. Otolith growth in fishes. Comparative Biochemical Physiology. Part A: Physiology, 97(2), 119–135.

Ghosh, P., Eiler, J., Campana, S.E., Feeney, R.F., 2007. Calibration of the carbonate 'clumped isotope' paleothermometer for otoliths. Geochimica et Cosmochimica Acta. 71(11), 2736–2744.

Gibson-Reinemer, D.K., Johnson, B.M., Martinez, P.J., Winkelman, D.L., Koenig, A.E., Woodhead, J.D., 2009. Elemental signatures in otoliths of hatchery rainbow trout (*Oncorhynchus mykiss*): distinctiveness and utility for detecting origins and movement. Canadian Journal of Fisheries and Aquatic Sciences. 66(4), 513–524.

Gibson, J. J. 2002. Short-term evaporation and water budget comparisons in shallow Arctic lakes using non-steady isotope mass balance. Journal of Hydrology. 264(1-4), 242–261.

Gibson, J.J., Birks, S.J., Yi, Y., 2016. Stable isotope mass balance of lakes: A contemporary perspective. Quaternary Science Reviews. 131, 316–328.

Goldstein, S. J. and Jacobsen, S. B. 1987. The Nd and Sr isotopic systematics of river-water dissolved material: Implications for the sources of Nd and Sr in seawater. Chemical Geology: Isotope Geoscience section. 66(3–4), 245–272.

Gonfiantini, R. 1986. Environmental isotopes in lake studies. In: Fritz, P., Fontes, J.C., (Eds.), Handbook of environmental isotope geochemistry. Volume 2. The Terrestrial Environment B, Elsevier, Amsterdam, 113–168.

Gonneea, M.E., Cohen, A.L., DeCarlo, T.M., Charette, M.A., 2017. Relationship between water and aragonite barium concentrations in aquaria reared juvenile corals. Geochimica et Cosmochimica Acta. 209, 123–134.

Grammer, G.L., Morrongiello, J.R., Izzo, C., Hawthorne, P.J., Middleton, J.F., Gillanders, B.M., 2017. Coupling biogeochemical tracers with fish growth reveals physiological and environmental controls on otolith chemistry. Ecological Monographs. 87(3), 487–507.

Guiguer, K.R.R.A., Drimmie, R., Power, M., 2003. Validating methods for measuring $\delta^{18}O$ and $\delta^{13}C$ in

otoliths from freshwater fish. Rapid Communications in Mass Spectrometry, 17(5), 463–471.

Hamer, P.A., Jenkins, G.P., Gillanders, B.M., 2003. Otolith chemistry of juvenile snapper *Pagrus auratus* in Victorian waters: natural chemical tags and their temporal variation. Marine Ecology Progress Series. 263, 261–273.

Hamer, P.A., Jenkins, G.P., Coutin, P., 2006. Barium variation in *Pagrus auratus* (Sparidae) otoliths: a potential indicator of migration between an embayment and ocean waters in south-eastern Australia. Estuarine, Coastal and Shelf Science. 68(3–4), 686–702.

Hanson, N.N., Wurster, C.M., Todd, C.D., 2010. Comparison of secondary ion mass spectrometry and micromilling/continuous flow isotope ratio mass spectrometry techniques used to acquire intra-otolith $\delta^{18}O$ values of wild Atlantic salmon (*Salmo salar*) . Rapid Communications in Mass Spectrometry. 24(17), 2491–2498.

Harris, J. H. and Rowland, S. J. 1996. Family Percichthyidae: Australian freshwater cods and basses. In: McDowall, R. M. (Eds.) Freshwater fishes of South-eastern Australia. Second edition. Sydney: Reed Books. 150–163.

Hays, P.D. and Grossman, E.L., 1991. Oxygen isotopes in meteoric calcite cements as indicators of continental paleoclimate. Geology, 19(5), 441–444.

Higham, T. F. G. and Horn, P. L. 2000. Seasonal dating using fish otoliths: results from the shag river site, New Zealand. Journal of Archaeological science. 27(5), 439–448.

Hill, T.M., Spero, H.J., Guilderson, T., LaVigne, M., Clague, D., Macalello, S., Jang, N., 2011. Temperature and vital effect controls on bamboo coral (Isididae) isotope geochemistry: A test of the 'lines method'. Geochemistry, Geophysics, Geosystems. 12(4), 1–15.

Høie, H., Folkvord, A., Otterlei, E., 2003. Effect of somatic and otolith growth rate on stable isotopic composition of early juvenile cod (*Gadus morhua*) otoliths. Journal of Experimental Marine Biology and Ecology. 289(1), 41–58.

Høie, H., Otterlei, E., Folkvord, A., 2004. Temperature-dependent fractionation of stable oxygen isotopes in otoliths of juvenile cod (*Gadus morhua* L.*).* ICES Journal of Marine Science. 61(2), 243–251.

Høie, H. and Folkvord, A. 2006. Estimating the timing of growth rings in Atlantic cod otoliths using stable oxygen isotopes. Journal of Fish Biology. 68(3), 826–837.

Holdaway, S.J., Fanning, P.C., Rhodes, E.J., Marx, S.K., Floyd, B., Douglass, M.J., 2010. Human response to palaeoenvironmental change and the question of temporal scale. Palaeogeogrphy, Palaeoclimatology, Palaeoecology. 292(1-2), 192–200.

Hughes, C.E., Stone, D.J.M., Gibson, J.J., Sadek, M., Cendón, D., Hankin, S., Hollins, S., Morrison, T., 2012. Stable water isotope investigation of the Barwon-Darling river system, Australia. In: IAEA, (International Atomic Energy Agency), (Ed.) Monitoring Isotopes in Rivers: Creation of the Global Network of Isotopes in Rivers (GNIR): Results of a coordinated research project 2002-2006. Vienna. 97–110.

Humphries, P., King, A.J., Koehn, J.D., 1999. Fish , flows and flood plains : links between freshwater fishes and their environment in the Murray-Darling River system , Australia. Environmental biology of fishes, 56(1-2), 129–151.

Ickert, R.B., Hiess, J., Williams, I.S., Holden, P., Ireland, T.R., Lanc, P., Schram, N., Foster, J.J., Clement, S.W., 2008. Determining high precision, in situ, oxygen isotope ratios with a SHRIMP II: Analyses of MPI-DING silicate-glass reference materials and zircon from contrasting granites. Chemical Geology. 257(1–2), 114–128.

Ireland, T.R., Clement, S., Compston, W., Foster, J.J., Holden, P., Jenkins, B., Lanc, P., Schram, N., Williams, I. S., 2008. Development of SHRIMP. Australian Journal of Earth Sciences. 55(6–7), 937–954.

Izzo, C., Doubleday, Z.A., Schultz, A.G., Woodcock, S.H., Gillanders, B.M., 2015. Contribution of water chemistry and fish condition to otolith chemistry: Comparisons across salinity environments. Journal of Fish Biology. 86(6), 1680–1698.

Jenke, J. 2002. A guide to good otolith cutting, Fisheries Research Report No. 141, Department of Fisheries, Government of Western Australia, 1–21.

Jones, R.N., McMahon, T.A., Bowler, J.M., 2001. Modelling historical lake levels and recent climate change at three closed lakes, Western Victoria, Australia (c.1840–1990). Journal of Hydrology. 246(1–4), 159–180.

Jones, M.D., Leng, M.J., Roberts, C.N., Türkeş, M., Moyeed, R., 2005. A coupled calibration and modelling approach to the understanding of dry-land lake oxygen isotope records. Journal of Paleolimnology. 34(3), 391–411.

Kalish, J. M. 1989. Otolith microchemistry: validation of the effects of physiology, age and environment on otolith composition. Journal of Experimental Marine Biology and Ecology. 132(3), 151–178.

Kalish, J. M. 1991. Oxygen and carbon stable isotopes in the otoliths of wild and laboratory-reared Australian salmon (*Arripis trutta*). Marine Biology. 110(1), 37–47.

Kalish, J. M. 1992. Formation of a stress-induced chemical check in fish otoliths. Journal of Experimental Marine Biology and Ecology. 162(2), 265–277.

Kefous, K. 1977. We have a fish with ears, and wonder if it is valuable. Unpublished honours thesis, Australian National University, Canberra.

Kemp, J. 2004. Flood channel morphology of a quiet river, the Lachlan downstream from Cowra, southeastern Australia. Geomorphology. 60(1–2), 171–190.

Kemp, J. and Rhodes, E. J. 2010. Episodic fluvial activity of inland rivers in southeastern Australia: Palaeochannel systems and terraces of the Lachlan River. Quaternary Science Reviews. 29(5–6), 732–752.

Kemp, J., Pietsch, T., Gontz, A., Olley, J., 2017. Lacustrine-fluvial interactions in Australia's Riverine Plains. Quaternary Science Reviews. 166, 352–362.

Kendall, C. and Coplen, T. B. 2001. Distribution of oxygen-18 and deuterium in river waters across the United States. Hydrological Processes, 15(7), 1363–1393.

Kennett, D. J. and Voorhies, B. 1996. Oxygen isotopic analysis of archaeological shells to detect seasonal use of wetlands on the southern Pacific Coast of Mexico. Journal of Archaeological Science. 23(5), 689–704.

Kim, S.T. and O'Neil, J.R., 1997. Equilibrium and nonequilibrium oxygen isotope effects in synthetic carbonates. Geochimica et Cosmochimica Acta. 61(16), 3461–3475.

Kim, S.T., O'Neil, J.R., Hillaire-Marcel, C., Mucci, A., 2007. Oxygen isotope fractionation between synthetic aragonite and water: Influence of temperature and Mg^{2+} concentration. Geochimica et Cosmochimica Acta. 71(19), 4704–4715.

King, A.J., Tonkin, Z., Mahoney, J., 2009. Environmental flow enhances native fish spawning and recruitment in the Murray River, Australia. River Research and Applications. 15(10), 1205–1218

Knudson, K.J., 2009, Oxygen isotope analysis in a land of environmental extremes: the complexities of isotopic work in the Andes, International Journal of Osteoarchaeology. 19(2), 171–191.

Koch, P. L., 1998, Isotopic reconstruction of past continental environments, Annual Review of Earth and Planetary Sciences. 26(1), 573–613

Koehn, J. and O'Connor, W. G. 1990. Biological information for management of native freshwater fish in Victoria. Government Printer, Melbourne, 1–165.

Koster, W.M., Dawson, D.R., Liu, C., Moloney, P.D., Crook, D.A., Thomson, J.R., 2017. Influence of streamflow on spawning-related movements of golden perch *Macquaria ambigua* in south-eastern Australia. Journal of Fish Biology. 90(1), 93–108.

Kraus, R. T. and Secor, D. H. 2004. Incorporation of strontium into otoliths of an estuarine fish. Journal of Experimental Marine Biology and Ecology. 302(1), 85–106.

Langdon, J. S. 1987. Active osmoregulation in the Australian Bass, *Macquaria novemaculeata* (Steindachner), and the golden perch, *Macquaria ambigua* (Richardson) (Percichthyidae). Marine and Freshwater Research. 38(6), 771–776.

Leclerc, A. J. and Labeyrie, L. 1987. Temperature dependence of the oxygen isotopic fractionation between diatom silica and water. Earth and Planetary Science Letters. 84(1), 69–74.

Lee, G. F.,. and Wilson, W., 1969. Use of chemical composition of freshwater clamshells as indicators of paleohydrologic conditions. Ecology. 50(6), 990–997.

Lintermans, M. 2007. Fishes of the Murray-Darling Basin: an introductory guide. Murray-Darling Basin Commission, Canberra, Australia.

Llewellyn, L. C. and MacDonald, M. C. 1980. Family Percichthyidae. Australian freshwater basses and cods. In: McDowel, R. M., (Ed.), Freshwater fishes of South-eastern Australia. 142–149.

Long, K., 2012, 'An ear to the ground': Fish otolith geochemistry, environmental conditions and human occupation at Lake Mungo. Unpublished honours thesis, Australian National University, Canberra

Long, K., Stern, N., Williams, I.S., Kinsley, L., Wood, R., Sporcic, K., Smith, T., Fallon, S., Kokkonen, H., Moffat, I., Grün, R., 2014. Fish otolith geochemistry, environmental conditions and human occupation at Lake Mungo, Australia. Quaternary Science Reviews. 88, 82–95.

Long, K., Wood, R., Williams, I.S., Kalish, J., Shawcross, W., Stern, N. and Grün, R., 2018. Fish otolith microchemistry: snapshots of lake conditions during early human occupation of Lake Mungo, Australia. Quaternary International. 463, 29–43.

Longerich, H. P. et al. 1996. Laser ablation inductively coupled plasma mass spectrometric transient signal data acquisition and analyte concentration calculation. Journal of Analytical Atomic Spectrometry. 11, 899–904.

Lowe, M.R., DeVries, D.R., Wright, R.A., Ludsin, S.A., Fryer, B.J., 2009. Coastal largemouth bass (*Micropterus salmoides*) movement in response to changing salinity. Canadian Journal of Fisheries and Aquatic Sciences. 66(12), 2174–2188.

Macdonald, J. I. and Crook, D. A. 2010. Variability in Sr: Ca and Ba: Ca ratios in water and fish otoliths across an estuarine salinity gradient. Marine Ecology Progress Series. 413, 147–161.

Mallen-Cooper, M. and Stuart, I. G. 2003. Age, growth and non-flood recruitment of two potamodromous fishes in a large semi-arid/temperate river system. River Research and Applications. 19(7), 697–719.

Martin, J.-M. and Whitfield, M. 1983. The Significance of the River Input of Chemical Elements to the Ocean. In: Wong C.S., Boyle E., Bruland K.W., Burton J.D., Goldberg E.D., (Eds.) Trace Metals in Sea Water. NATO Conference Series (IV Marine Sciences), vol 9. Springer, Boston, MA 265–296.

Martin, G.B., Thorrold, S.R., Jones, C.M., 2004. Temperature and salinity effects on strontium incorporation in otoliths of larval spot (*Leiostomus xanthurus*). Canadian Journal of Fisheries and Aquatic Sciences. 61(1), 34–42.

Martin, G. B. and Wuenschel, M. J. 2006. Effect of temperature and salinity on otolith element incorporation in juvenile gray snapper *Lutjanus griseus*. Marine Ecology Progress Series. 324, 229–239.

Martin, J., Bareille, G., Berail, S., Pecheyran, C., Daverat, F., Bru, N., Tabouret, H., Donard, O., 2013.

Spatial and temporal variations in otolith chemistry and relationships with water chemistry: a useful tool to distinguish Atlantic salmon *Salmo salar parr* from different natal streams. Journal of fish biology. 82(5), 1556–1581.

Matta, M.E., Orland, I.J., Ushikubo, T., Helser, T.E., Black, B.A., Valley, J.W., 2013. Otolith oxygen isotopes measured by high-precision secondary ion mass spectrometry reflect life history of a yellowfin sole (*Limanda aspera*). Rapid communications in mass spectrometry. 27(6), 691–699.

McCulloch, M., Cappo, M., Aumend, J., Müller, W., 2005. Tracing the life history of individual barramundi using laser ablation MC-ICP-MS Sr-isotopic and Sr/Ba ratios in otoliths. Marine and Freshwater Research. 56(5), 637–644.

McLaren, S., Wallace, M.W., Gallagher, S.J., Miranda, J.A., Holdgate, G.R., Gow, L.J., Snowball, I., Sandgren, P., 2011. Palaeogeographic, climatic and tectonic change in southeastern Australia: The Late Neogene evolution of the Murray Basin. Quaternary Science Reviews. 30(9-10), 1086–1111.

Meredith, K. T., Hollins, S.E., Hughes, C.E., Cendón, D.I., Hankin, S., Stone, D.J.M., 2009. Temporal variation in stable isotopes (^{18}O and ^{2}H) and major ion concentrations within the Darling River between Bourke and Wilcannia due to variable flows, saline groundwater influx and evaporation. Journal of Hydrology. 378(3–4), 313–324.

Meredith, K. T, Hollins, S.E, Hughes, C.E., Cendón, D.I, Stone, D.J.M., 2013. The influence of groundwater/surface water exchange on stable water isotopic signatures along the Darling River, NSW, Australia. In Ribeiro, L., Stigter, T., Chambel, A., Condesso de Melo, M., Monteiro, J., Medeiros, A. (Eds.) Groundwater and ecosystems. London: CRC Press. 57–68.

Meredith, K.T., Hollins, S.E., Hughes, C.E., Cendón, D.I., Chisari, R., Griffiths, A., Crawford, J., 2015. Evaporation and concentration gradients created by episodic river recharge in a semi-arid zone aquifer: Insights from Cl-, $\delta^{18}O$, $\delta^{2}H$, and ^{3}H. Journal of Hydrology. 529, 1070–1078.

Miller, J. A. 2009. The effects of temperature and water concentration on the otolith incorporation of barium and manganese in black rockfish *Sebastes melanops*. Journal of Fish Biology. 75(1), 39–60.

Miller, J. A. 2011. Effects of water temperature and barium concentration on otolith composition along a salinity gradient: Implications for migratory reconstructions. Journal of Experimental Marine Biology and Ecology. 405(1–2), 42–52.

Millner, R.S., Pilling, G.M., McCully, S.R., Høie, H., 2011. Changes in the timing of otolith zone formation in North Sea cod from otolith records: An early indicator of climate-induced temperature stress? Marine Biology. 158(1), 21–30.

Milton, D. A. and Chenery, S. R. 1998. The effect of otolith storage methods on the concentrations of elements detected by laser-ablation ICPMS. Journal of Fish Biology. 53(4), 785–794.

Milton, D. A. and Chenery, S. R. 2001. Sources and uptake of trace metals in otoliths of juvenile barramundi (*Lates calcarifer*). Journal of Experimental Marine Biology and Ecology. 264(1), 47–65.

Mohseni, O., Stefan, H.G., Erickson, T.R., 1998. A nonlinear regression model for weekay stream temperatures. Water Resources Research, 34(10), 2685–2692.

Mohseni, O., Erickson, T.R., Stefan, H.G., 1999. Sensitivity of stream temperatures in the United States to air temperatures projected under a global warming scenario, Water Resources Research 35(12), 3723–3733.

Mommsen, T.P., Vijayan, M.M., Moon, T.W., 1999. Cortisol in teleosts:dynamics, mechanisms of action, and metabolic regulation. Reviews in Fish Biology and Fisheries. 9(3), 211–268.

Morales-nin, B. 1987. Ultrastructure of the organic and inorganic constituents of the otoliths of the sea bass. In: Summerfelt, R.C., Hall, G.E. (Eds.), Age and Growth of Fish. Iowa State

University Press, Ames. 331–343.

Morales-Nin, B. 2000. Review of the growth regulation processes of otolith daily increment formation. Fisheries Research. 46(1-3), 53–67.

Morrongiello, J.R., Crook, D.A., King, A.J., Ramsey, D.S., Brown, P., 2011. Impacts of drought and predicted effeects of climate change on fish growth in temperate Australian Lakes. Global Change Biology. 17(2), 745–755.

Mosegaard, H., Svedäng, H., Taberman, K., 1988. Uncoupling of somatic and otolith growth rates in arctic char (*Salvelinus alpinus*) as an effect of differences in temperature response. Canadian Journal of Fisheries and Aquatic Sciences. 45(9), 1514–1524.

Mugiya, Y. and Uchimura, T. 1989. Otolith resorption induced by anaerobic stress in the goldfish, *Carassius auratus*. Journal of Fish Biology. 35(6), 813–818.

Munro, A.R., Gillanders, B.M., Elsdon, T.S., Crook, D.A., Sanger, A.C., 2008. Enriched stable isotope marking of juvenile golden perch (*Macquaria ambigua*) otoliths. Canadian Journal of Fisheries and Aquatic Sciences. 65(2), 276–285.

Murray Darling Basin Authority. 2018. Ecological needs of low flows in the Barwon-Darling. Murray-Darling Basin Authority Technical Report, Canberra.

Neat, F.C., Wright, P.J., Fryer, R.J., 2008. Temperature effects on otolith pattern formation in Atlantic cod *Gadus morhua*. Journal of Fish Biology. 73(10), 2527–2541.

Newman, S.J., Pember, M.B., Rome, B.M., Mitsopoulos, G.E.A., Skepper, C.L., Allsop, Q., Saunders, T., Ballagh, A.C., Van Herwerden, L., Garrett, R.N., Gribble, N.A., 2011. Stock structure of blue threadfin Eleutheronema tetradactylum across northern Australia as inferred from stable isotopes in sagittal otolith carbonate. Fisheries Management and Ecology. 18(3), 246–257.

Nolf, D. 1985. Handbook of Paleoichthyology. Vol. 10. Otolithi piscium. Fischer, Stuttgart, NY. 1–141

O'Neil, J.R., Clayton, R.N., Mayed, T.K., 1969, Oxygen isotope fractionation in divalent metal carbonates. The Journal of Chemical Physics. 51(12), 5547–5558.

O'Connor, J.P., O'Mahony, D.J., O'Mahony, J.M., 2005. Movements of *Macquaria ambigua* , in the Murray River , south-eastern Australia. Journal of Fish Biology. 66(2), 392–403.

Page, K., Dare-Edwards, A., Nanson, G., Price, D., 1994. Late Quaternary evolution of Lake Urana, New South Wales, Australia. Journal of Quaternary Science. 9(1), 47–57.

Page, K.J., Kemp, J., Nanson, G.C., 2009. Late Quaternary evolution of riverine plain paleochannels, southeastern Australia. Australian Journal of Earth Sciences. 56(S1), S19–S33.

Pangle, K.L., Ludsin, S.A., Fryer, B.J., 2010. Otolith microchemistry as a stock identification tool for freshwater fishes: testing its limits in Lake Erie. Canadian Journal of Fisheries and Aquatic Sciences. 67(9), 1475–1489.

Pannella, G. 1971. Fish otoliths: daily growth layers and periodical patterns. Science. 173, 1124–1127.

Patterson, W.P., Smith, G.R., Lohmann, K.C., 1993. Continental paleothermometry and seasonality using the isotopic composition of aragonitic otoliths of freshwater fishes. In: Swart, P.K., Lohmann, K. C., Mckenzie, J., Savin, S.,(Eds.) Climate Change in Continental Isotopic Records, Geophysical Monograph Series. 78, 191–202.

Patterson, W.P., 1999. Oldest isotopically characterized fish otoliths provide insight to Jurassic continental climate of Europe. Geology. 27(3), 199-202.

Payan, P., De Pontual, H., Bœuf, G., Mayer-Gostan, N., 2004. Endolymph Chemistry and otolith growth in fish. Comptes Rendus Palevol 3(6-7). 535–547.

de Pontual, H., Groison, A.L., Piñeiro, C., Bertignac, M., 2006. Evidence of underestimation of European hake growth in the Bay of Biscay, and its relationship with bias in the agreed

method of age estimation. ICES Journal of Marine Science. 63, 1674–1681.

Prendergast, A. L. and Schöne, B. R. 2017. Oxygen isotopes from limpet shells: Implications for palaeothermometry and seasonal shellfish foraging studies in the Mediterranean. Palaeogeography, Palaeoclimatology, Palaeoecology. 484, 33–47

Prichard, J. 2005. Linking fish growth and climate across modern space and evolutionary time. Unpublished PhD thesis, Australian National University, Canberra.

Radtke, R. L. 1989. Strontium-calcium concentration ratios in fish otoliths as environmental indicators. Comparative Biochemical Physiology. 92A(2), 189–193.

Radtke, R.L., Lenz, P., Showers, W., Moksness, E., 1996. Environmental information stored in otoliths: insights from stable isotopes. Marine Biology. 127(1), 161–170.

Railsback, B. L., 2006, Some fundamentals of mineralogy and geochemistry: oxygen isotope composition of calcite as a function of temperature and water composition, www.gly.uga.edu/railsback/FundamentalsIndex.html

Reynolds, L. F. 1983. Migration patterns of five fish species in the Murray-Darling River system. Australian Journal of Marine and Freshwater Research. 34(6), 857–871.

Rohling, E. J. 2013. Quantitative assessment of glacial fluctuations in the level of Lake Lisan, Dead Sea rift. Quaternary Science Reviews. 70, 63–72.

Rohling, E. J. 2016. Of lakes and fields: a framework for reconciling palaeoclimatic drought inferences with archaeological impacts. Journal of Archaeological Science. 73, 17–24.

Rondeau, B., Cossa, D., Gagnon, P., Pham, T.T., Surette, C., 2005. Hydrological and biogeochemical dynamics of the minor and trace elements in the St. Lawrence River. Applied Geochemistry. 20(7), 1391–1408.

Rowell, K. et al. 2008. Fish without water : Validation and application of δ 18 O in Totoaba macdonaldi otoliths, Peces sin agua : Validación y aplicación de δ 18 O en los otolitos de Totoaba macdonaldi. Ciencias marinas 34, 55–68.

Sako, A., MacLeod, K.G., O'Reilly, C.M., 2007. Stable oxygen and carbon isotopic compositions of *Lates stappersii* otoliths from Lake Tanganyika, East Africa. Journal of Great Lakes Research. 33(4), 806–815.

Santschi, P. H. 1988. Factors controlling the biogeochemical cycles of trace-elements in fresh and coastal marine waters as revealed by artificial radioisotopes. Limnology and Oceanography. 33(4), 848–866.

Secor, D.H., Dean, J.M., Laban, E.H., 1992. Otolith removal and preparation for microstructural examination. Otolith microstructure examination and analysis. Canadian special publication of fisheries and aquatic sciences. 117, 19–57.

Secor, D.H., Henderson-Arzapalo, A., Piccoli, P.M., 1995. Can otolith microchemistry chart patterns of migration and habitat utilization in anadromous fishes? Journal of Experimental Marine Biology and Ecology. 192(1), 15–33.

Secor, D. H. and Rooker, J. R. 2000. Is otolith strontium a useful scalar of life cycles in estuarine fishes? Fisheries Research. 46(1–3), 359–371.

Shackleton, N.J., 1974. Attainment of isotopic equilibrium between ocean water and the benthonic foraminifera genus Uvigerina: isotopic changes in the ocean during the last glacial. Les méthodes quantitatives d'étude des variations du climat au cours du Pleistocène, Gif-sur-Yvette, Colloque international du CNRS 219, 203–210

Shaw, T.J., Moore, W.S., Kloepfer, J., Sochaski, M.A., 1998. The flux of barium to the coastal waters of the southeastern USA: The importance of submarine groundwater discharge. Geochimica et Cosmochimica Acta. 62(18), 3047–3054.

Shiller, A. M. 1997. Dissolved trace elements in the Mississippi River: Seasonal, interannual, and

decadal variability. Geochimica et Cosmochimica Acta. 61(20), 4321–4330.

Sinclair, D. J. and McCulloch, M. T. 2004. Corals record low mobile barium concentrations in the Burdekin River during the 1974 flood: Evidence for limited Ba supply to rivers? Palaeogeography, Palaeoclimatology, Palaeoecology. 214(1–2), 155–174.

Skougstad, M. W. and Albert, H. C. 1963. Occurrence and distribution of strontium in natural water. Water Supply Paper, United States Government Printing Office, 1496, 55–97

Smith, J.E., Schwarcz, H.P., Risk, M.J., McConnaughey, T.A., Keller, N., 2000. Paleotemperatures from Deep-Sea Corals : Overcoming ' Vital Effects '. Palaios. 15(1), 25–32.

Somerville, A.D., Froehle, A.W., Schoeninger, M.J., 2018. Environmental influences on rabbit and hare bone isotope abundances: Implications for paleoenvironmental research. Palaeogeography, Palaeoclimatology, Palaeoecology. 497, 91–104.

Stefan, H. G. and Preud'homme, E. B. 1993. Stream temperature estimation from air temperature. Journal of the American Water Resources Association. 29(1), 27–45.

Steinman, B.A. and Abbott, M.B., 2013. Isotopic and hydrologic responses of small, closed lakes to climate variability: Comparison of measured and modeled lake level and sediment core oxygen isotope records. Geochimica et Cosmochimica Acta. 105, 342–359.

Stephenson, A. E. 1986. Lake Bungunnia - A Plio-Pleistocene megalake in southern Australia. Palaeogeography, Palaeoclimatology, Palaeoecology. 57(2–4), 137–156.

Stern, N., Tumney, J., Fitzsimmons, K.E., Kajewski, P., 2013. Strategies for investigating human responses to changes in landscape and climate at Lake Mungo in the Willandra Lakes, southeast Australia. In: Frankel, D., Webb, J., and Lawrence, S. (Eds.) Archaeology in Environment and Technology: Intersections and Transformations. London: Routledge. 31–50.

Stern, N. 2015. 13 . The Archaeology of the Willandra its empirical structure and narrative potential. In: McGrath, A. and Jebb, M. A. (Eds.) Long History, Deep Time: Deepening Histories of Place. Canberra: ANU Press. 221–240.

Stuart, I. G. 2006. Validation of otoliths for determining age of golden perch, a long-lived freshwater fish of Australia. North American Journal of Fisheries Management. 26(1), 52–55.

Sturrock, A.M., Hunter, E., Milton, J.A., Johnson, R.C., Waring, C.P., Trueman, C.N., 2015. Quantifying physiological influences on otolith microchemistry. Methods in Ecology and Evolution. 6(7), 806–816.

Tabouret, H., Lord, C., Bareille, G., Pécheyran, C., Monti, D., Keith, P., 2011. Otolith microchemistry in *Sicydium punctatum*: indices of environmental condition changes after recruitment. Aquatic Living Resources. 24(4), 369–378.

Thorrold, S.R., Campana, S.E., Jones, C.M., Swart, P.K., 1997. Factors determining $\delta^{13}C$ and also $\delta^{18}O$ fractionation in aragonitic otoliths of marine fish. Geochimica et Cosmochimica Acta. 61(14), 2909–2919.

Townsend, D.W., Radtke, R.L., Corwin, S., Libby, D.A., 1992. Strontium:calcium ratios in juvenile Atlantic herring *Clupea harengus* L. otoliths as a function of water temperature. Journal of Experimental Marine Biology and Ecology. 160(1), 131–140.

Twaddle, R.W., Wurster, C.M., Bird, M.I., Ulm, S., 2017. Complexities in the palaeoenvironmental and archaeological interpretation of isotopic analyses of the Mud Shell *Geloina erosa* (Lightfoot, 1786). Journal of Archaeological Science: Reports. 12, 613–624.

Tzeng, W.N., 1996. Effects of salinity and ontogenetic movements on strontium:calcium ratios in the otoliths of the Japanese eel, *Anguilla japonica* Temminck and Schlegel. Journal of Experimental Marine Biology and Ecology. 199(1), 111–122.

van Vliet, M.T.H., Ludwig, F., Zwolsman, J.J.G., Weedon, G.P., Kabat, P.,2011. Global river

temperatures and sensitivity to atmospheric warming and changes in river flow. Water Resources Research. 47(2).

de Vries, M.C., Gillanders, B.M., Elsdon, T.S., 2005. Facilitation of barium uptake into fish otoliths: Influence of strontium concentration and salinity. Geochimica et Cosmochimica Acta. 69(16), 4061–4072.

Waite, A.J., and Swart, P.K, 2015, The inversion of aragonite to calcite during the sampling of skeletal archives: implications for proxy interpretation. Rapid Communication in Mass Spectrometry, 29(10), 955–964

Walther, B. D. and Thorrold, S. R. 2006. Water, not food, contributes the majority of strontium and barium deposited in the otoliths of a marine fish. Marine Ecology Progress Series. 311, 125– 130.

Walther, B. D. and Thorrold, S. R. 2009. Inter-annual variability in isotope and elemental ratios recorded in otoliths of an anadromous fish. Journal of Geochemical Exploration. 102(3), 181–186.

Walther, B.D., Kingsford, M.J., O'Callaghan, M.D., McCulloch, M.T., 2010. Interactive effects of ontogeny, food ration and temperature on elemental incorporation in otoliths of a coral reef fish. Environmental Biology of Fishes. 89(3-4), 441–451.

Wang, T., Surge, D., Walker, K.J., 2011. Isotopic evidence for climate change during the Vandal Minimum from *Ariopsis felis* otoliths and *Mercenaria campechiensis* shells, southwest Florida, USA. The Holocene. 21(7), 1081–1091.

Webb, B.W., Clack, P.D., Walling, D.E., 2003. Water-air temperature relationships in a Devon river system and the role of flow. Hydrological Processes. 17(15), 3069–3084.

Webb, B.W., Hannah, D.M., Moore, R.D., Brown, L.E., Nobilis, F., 2008. Recent advances in stream and river temperature research. Hydrological Processes: An International Journal, 22(7), 902–918.

Webb, S.D., Woodcock, S.H., Gillanders, B.M., 2012. Sources of otolith barium and strontium in estuarine fish and the influence of salinity and temperature. Marine Ecology Progress Series. 453, 189–199.

Weidman, C. R. and Millner, R. 2000. High-resolution stable isotope records from North Atlantic cod. Fisheries Research. 46(1–3), 327–342.

Wells, B.K., Rieman, B.E., Clayton, J.L., Horan, D.L., Jones, C.M., 2003. Relationships between water, otolith, and scale chemistries of westslope cutthroat trout from the Coeur d'Alene River, Idaho: the potential application of hard-part chemistry to describe movements in freshwater. Transactions of the American Fisheries Society. 132(3), 409–424.

West, C.F., Wischniowski, S., Johnston, C., 2012. Pacific cod (*Gadus macrocephalus*) as a paleothermometer: otolith oxygen isotope reconstruction. Journal of Archaeological Science. 39(10), 3277–3283.

White, C., Longstaffe, F.J., Law, K.R., 2004. Exploring the effects of environment, physiology and diet on oxygen isotope ratios in ancient Nubian bones and teeth. Journal of Archaeological Science. 31(2), 233–250.

Willmes, M., Bataille, C.P., James, H.F., Moffat, I., McMorrow, L., Kinsley, L., Armstrong, R.A., Eggins, S., Grün, R., 2018. Mapping of bioavailable strontium isotope ratios in France for archaeological provenance studies. Applied Geochemistry. 90, 75–86.

Woodcock, S.H., Gillanders, B.M., Munro, A.R., McGovern, F., Crook, D.A., Sanger, A.C., 2011. Using enriched stable isotopes of barium and magnesium to batch mark otoliths of larval golden perch (*Macquaria ambigua,* Richardson). Ecology of Freshwater Fish. 20(1), 157–165.

Woodcock, S. H. and Walther, B. D. 2014. Concentration-dependent mixing models predict values of diet-derived stable isotope ratios in fish otoliths. Journal of Experimental Marine

Biology and Ecology. 454, 63–69.

Wright, P. J. 1991. The influence of metabolic rate on otolith increment width in Atlantic salmon parr, *Salmo salar* L. Journal of Fish Biology. 38(6), 929–933.

Wright, P.J., Panfili, J., Morales-Lín, B., Greffen, A.J., Pontual, H., Troadec, H., 2002. Otoliths. in Panfili, J., de Pontual, H., Troadec, H., Wright, p.J., (Eds.) Manual of Fish Sclerochronology. Brest: France: Ifremer-IRD coedition. 31–58.

Wurster, C.M., Patterson, W.P., Cheatham, M.M., 1999. Advances in micromilling techniques: a new apparatus for acquiring high-resolution oxygen and carbon stable isotope values and major/minor elemental ratios from accretionary carbonate. Computers & Geosciences. 25(10), 1159–1166.

Wurster, C. M. and Patterson, W. P. 2001. Seasonal variation in stable oxygen and carbon isotope values recovered from modern lacustrine freshwater molluscs: paleoclimatological implications for sub-weekly temperature records. Journal of Paleolimnology, 26(2), 205–218.

Wurster, C.M., Patterson, W.P., Stewart, D.J., Bowlby, J.N., Stewart, T.J., 2005. Thermal histories, stress, and metabolic rates of chinook salmon (*Oncorhynchus tshawytscha*) in Lake Ontario: evidence from intra-otolith stable isotope analyses. Canadian Journal of Fisheries and Aquatic Sciences, 62(3), 700–713.

Ye, Q., Cheshire, K., Fleer, D., 2008. Recruitment of golden perch and selected large-bodied fish species following the weir pool manipulation in the River Murray, South Australia. SARDI Aquatic Sciences, Adelaide, pp 33, SARDI Aquatic Sciences Publication Number: F2008/000606-1.

Zhisheng, A., Bowler, J.M., Opdyke, N.D., Macumber, P.G., Firman, J.B.,1986. Palaeomagnetic stratigraphy of Lake Bungunnia: Plio-Pleistocene precursor for aridity in the Murray Basin, southeastern Australia. Palaeography, Palaeoclimatology, Palaeoecology. 54, 219–239.

Zimmerman, C. E. 2005. Relationship of otolith strontium-to-calcium ratios and salinity : experimental validation for juvenile salmonids. Canadian Journal of Fisheries and Aquatic Sciences, 62(1), 88–97.

9. Appendix

9.1 Full results from DI-MS $\delta^{18}O$ analysis of powdered otoliths samples

Run ID	Row	Line	Position	Type of sample	Identifier 1	Weight (microg)	1 Cycle Int Samp 44	1 Cycle Int Ref 44	d 13C/12C Mean	d 13C/12C Std Dev	d 18O/16O Mean	d 18O/16O Std Dev	Corrected δ13C/12C V-PDB	Corrected δ18O/16O V-PDB
20150825_Long.xls	25	1	14	Standard	ANU M2	41	4539.643885	4607.296138	2.832	0.009	-9.474	0.019	2.831320987	-7.49177124
20150825_Long.xls	26	2	14	Standard	ANU M2	56	6144.277069	6297.58237	2.817	0.003	-9.384	0.023	2.816346117	-7.402580744
20150825_Long.xls	27	1	15	Standard	NBS 19	40	4163.477559	4323.841507	1.958	0.012	-4.127	0.018	1.958785257	-2.19286476
20150825_Long.xls	28	2	15	Standard	NBS 19	40	3768.786323	3763.060211	0.797	0.014	-7.473	0.015	0.799730357	-5.508769208
20150825_Long.xls	29	1	16	Standard	NBS 18	57	6188.418691	6288.604687	-4.952	0.007	-24.993	0.019	-4.939637965	-22.8711858
20150825_Long.xls	30	2	16	Standard	NBS 18	56	5803.791556	5937.063359	-5.039	0.011	-25.159	0.037	-5.026492208	-23.03569272
20150825_Long.xls	32	2	17	Otolith	3424-1	42	3386.704362	3479.239574	-10.383	0.02	-8.65	0.043	-10.36153905	-6.675182697
20150825_Long.xls	33	1	18	Otolith	3419-1	33	3802.502376	3934.719991	-9.964	0.009	-8.526	0.013	-9.943241031	-6.552298013
20150825_Long.xls	34	2	18	Otolith	3419-2	28	2071.467613	2148.542868	-10.069	0.015	-8.398	0.022	-10.04806512	-6.425449307
20150825_Long.xls	35	1	19	Otolith	3430	60	4295.30272	4305.747517	-10.546	0.004	-8.258	0.019	-10.52426597	-6.286708536
20150825_Long.xls	36	2	19	Standard	NBS 19	44	3699.657183	3713.623315	1.918	0.013	-4.164	0.005	1.918852271	-2.229531964
20150825_Long.xls	37	1	20	Standard	NBS 19	50	4147.367179	4129.921044	1.969	0.014	-4.089	0.018	1.969766828	-2.155206551
20150825_Long.xls	38	2	20	Standard	NBS 19	43	3736.241442	3749.425558	1.96	0.012	-4.107	0.013	1.960781906	-2.17304465
20150825_Long.xls	39	1	21	Standard	NBS 19	48	4905.598006	4984.030326	1.941	0.011	-4.184	0.015	1.941813738	-2.249352075

9.2 LA-ICPMS analytical parameters for each session

Session title	Otoliths analysed
KL7th May_1	N3430, N3419, N3424, LH130, LH129, LH2, LH1, DSM 12-2, DSM 12-3, DSM 12-4, DSM 12-12
KL7th May_2	A4/3/1, A7/8/1, B7/9/1, A7/9-10/1, A5/10/1, B8/11/1, B8/12/1, B5/13/1, B4/14/1, B4/15/1, B4/20, N3433, N3422, N3425, N3428

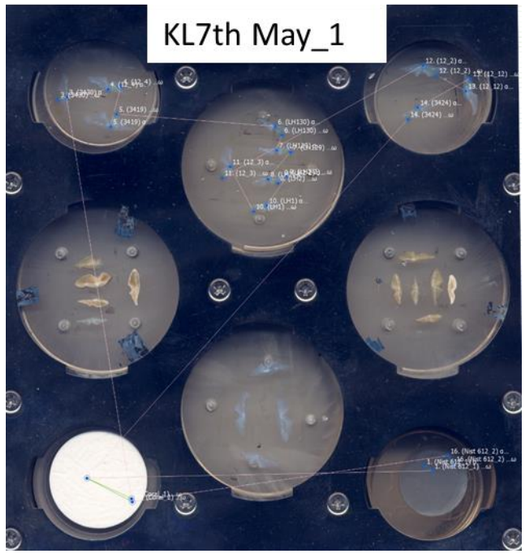

Number of masses measured	12											
List of masses	11	24	31	43	55	86	88	89	137	138	232	238
Reference Mass	43	appears at position	4	in mass list								
Number of Time Slices	7627											
Analysis Time (seconds)	4005.51											

	Ranges on Sheet "Intensity_Data"	Start Time (seconds)	End Time (seconds)	Time Range (rounded)
1st Background Range	$A$56:$A$209	21.01	101.36	21 : 101
2nd Background Range	$A$7448:$A$7612	3903.12	3989.22	3903 : 3989
1st Standard Range	$A$249:$A$331	122.36	165.43	122 : 165
2nd Standard Range	$A$7305:$A$7385	3828.02	3870.03	3828 : 3870
Sample Start	$A$608	310.91		311
Sample End	$A$7007		3671.53	3672

Standard used for calibration NIST 612

Mass Number	11	24	31	43	55	86	88	89	137	138	232	238
Average Background Counts	214.4984326	360.1097179	7389.874608	20.84639498	9590.044	56.89655	0.548589	7.680251	12.93103	12.30408	15.83072	15.59561
2 sigma Std Deviation	193.3589145	192.8932693	940.2790766	43.63534909	1128.618	74.06249	7.336475	27.45686	38.81653	36.74346	39.66128	39.13962

Note: These values are for information only. Linear regression lines, based on the selected ranges, are used for background subtraction.

Mass Ratio	11 / 43	24 / 43	31 / 43	43 / 43	55 / 43	86 / 43	88 / 43	89 / 43	137 / 43	138 / 43	232 / 43	238 / 43
% Drift between std ranges	-2.502377541	4.035562731	3.509680576	0	1.660763	0.823742	0.607685	3.23383	-0.50476	-0.32688	-1.57312	-2.72153

(End of 2nd range relative to start of 1st range)

Concentration in Sample of Reference Element (ppm)	400000

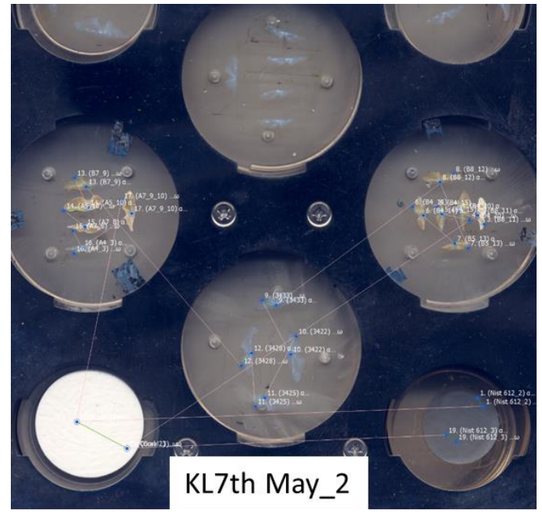

Number of masses measured\	12												
List of masses	11	24	31	43	55	86	88	89	137	138	232	238	
Reference Mass	43	appears at position	4	in mass list									
Number of Time Slices	9714												
Analysis Time (seconds)	5101.51												

	Ranges on Sheet "Intensity_Data"	Start Time (seconds)	End Time (seconds)	Time Range (rounded)
1st Background Range	$A$67:$A$248	26.77	121.81	27 : 122
2nd Background Range	$A$9411:$A$9690	4933.98	5080.5	4934 : 5080
1st Standard Range	$A$322:$A$397	160.69	200.07	161 : 200
2nd Standard Range	$A$9260:$A$9356	4854.68	4905.1	4855 : 4905
Sample Start	$A$679	348.17		348
Sample End	$A$8987		4711.31	4711

Standard used for calibration NIST 612

Mass Number	11	24	31	43	55	86	88	89	137	138	232	238
Average Background Counts	150.8658009	317.8030303	7482.608225	22.4025974	10394.27	59.95671	0.378788	7.900433	10.01082	12.17532	15.42208	15.9632
2 sigma Std Deviation	135.7362403	183.5524377	945.544997	44.24670699	1358.493	75.77219	6.114392	30.70586	35.38753	35.57874	40.54859	40.37744

Note: These values are for information only. Linear regression lines, based on the selected ranges, are used for background subtraction.

Mass Ratio	11 / 43	24 / 43	31 / 43	43 / 43	55 / 43	86 / 43	88 / 43	89 / 43	137 / 43	138 / 43	232 / 43	238 / 43
% Drift between std ranges	-5.623118944	0.574201852	-1.891279792	0	-0.22685	3.573978	-1.1506	-3.33552	-1.31504	-1.11645	-4.17589	-1.41915

(End of 2nd range relative to start of 1st range)

Concentration in Sample of Reference Element (ppm)	400000